TRACING HYDRAULIC FRACTURING FLUIDS AND FORMATION BRINES USING BORON, RADIUM, AND STRONTIUM ISOTOPES

by

Nathaniel R Warner

Department of Earth and Ocean Sciences
Duke University

Date:_____

Approved:

_____
Avner Vengosh, Supervisor

_____
Paul A Baker

_____
Gary S Dwyer

_____
Thomas D Bullen

_____
Robert B Jackson

Dissertation submitted in partial fulfillment of
the requirements for the degree of Doctor
of Philosophy in the Department of
Earth and Ocean Sciences in the Graduate School
of Duke University

2013

ABSTRACT

TRACING HYDRAULIC FRACTURING FLUIDS AND FORMATION BRINES USING

BORON, RADIUM, AND STRONTIUM ISOTOPES

by

Nathaniel R Warner

Department of Earth and Ocean Sciences
Duke University

Date:_____

Approved:

_____
Avner Vengosh, Supervisor

_____
Paul A Baker

_____
Gary S Dwyer

_____
Thomas D Bullen

_____
Robert B Jackson

An abstract of a dissertation submitted in partial
fulfillment of the requirements for the degree
of Doctor of Philosophy, in the Department of
Earth and Ocean Sciences in the Graduate School of
Duke University

2013

Abstract

Production of oil and gas from unconventional natural gas reservoirs such as impermeable organic-rich shale formations was made possible through the use of horizontal drilling and high volume slick water hydraulic fracturing (HVHF). This combination of technologies has changed the energy landscape in the Unites States and possibly provided a vast new energy source from multiple sedimentary basins in the United States (Kargbo et al., 2010; Kerr, 2010) (Figure 1). HVHF requires large volumes of water (~5 million gallons/well) (Lutz et al., 2013) injected under high pressure to stimulate methane release from the fracture systems in the shale formations. The process is conducted within low-permeability formations, which include organic-rich shale rocks that are often the source rock for overlying conventional oil and gas reservoirs but do not easily transport gas to the well bore without stimulation. Once the permeability of the target formation is increased to a level that oil and gas can be recovered, pressure is released and 20-30% of the fluid that was injected flows back up to the surface through the well (Lutz et al., 2013). The remaining 70% stays underground, either lost to adjacent formations or imbed within the formation itself.

While HVHF operations rapidly expanded in many shale plays (e.g., Marcellus, Fayetteville), the possible negative environmental impacts remained un-quantified but a debated topic (Howarth et al., 2011). This dissertation focuses on quantification and

evaluation of several water resources for evidence of contamination from HVHF. My hypotheses are: (1) HVHF have distinctive chemical and isotopic fingerprints that are different from other potential contamination sources; and (2) these fingerprints could be identified in aquifers and surface water systems.

I tested these hypotheses in two shallow drinking water aquifers overlying current unconventional gas development, northeastern Pennsylvania and north-central Arkansas, and one area of surface water disposal in western Pennsylvania. I used specific geochemical (Br, Cl, SO_4, Na, Ca, Mg, Ba, Sr, B, and Li) and isotopic ($^{87}Sr/^{86}Sr$, $^{2}H/H$, $^{18}O/^{16}O$, $\delta^{11}B$, and $^{228}Ra/^{226}Ra$) tracers to characterize the target-formation brines and delineate possible contamination. The combined geochemical fingerprint distinguished hydraulic fracturing fluids and brines from other types of contamination that could influence water quality (e.g., road salt, sewage, acid mine drainage).

In Pennsylvania (Chapter 1), geochemical and isotopic data shows no direct evidence of contamination in shallow drinking-water aquifers associated with natural gas extraction of the Marcellus Formation. The data instead demonstrated that brine with the same geochemical (Br/Cl, Sr/Cl, and Ba/Cl) and isotopic fingerprint ($^{87}Sr/^{86}Sr$) of the Marcellus brine was likely naturally present in the shallow formations prior to the most recent oil and gas development. The data indicates that there may be areas in northeastern Pennsylvania that may be at increased risk of contamination from HVHF because of the presence of natural pathways that connect the shallow drinking water

aquifers with deeper formations. This Chapter was published in *Proceedings of the National Academy of Sciences* in July 2012.

A very different result was observed in Arkansas (Chapter 2). While the shallow groundwater data indicated that there was no direct evidence of contamination, there was also no indication of hydrodynamic connections between the deeper formation brine and the shallow aquifers. Indeed $^{87}Sr/^{86}Sr$, $\delta^{11}B$, ^{18}O, and ^{2}H values exclude Fayetteville Formation water as a source of salinity in shallow aquifers in the study area. The combined studies indicate that site and basin-specific studies of groundwater quality are necessary in order to evaluate the potential for contamination from HVHF. The Chapter was published in *Applied Geochemistry* in May 2013.

Surface water disposal of hydraulic fracturing fluids and brines (Chapter 3) clearly impacted western Pennsylvania sediment and water quality. Sediments in the stream at the point of effluent discharge from a treatment facility indicate radium activities 200 times higher than any background values. The $^{228}Ra/^{226}Ra$ ratios in the sediments also indicate that the source of contamination is likely the recent treatment and disposal of Marcellus brine. Impacts were also observed farther downstream. The concentrations of bromide and chloride in the effluent were so high that an increase in the concentrations measured in the stream was elevated almost two kilometers downstream. Chapter 3 was submitted to *Environmental Science and Technology* in May 2013.

Overall, this thesis aims to establish inorganic geochemical and isotopic tools for identification of hydraulic fracturing fluids in the environment and assess their possible impact on both surface and groundwater resources.

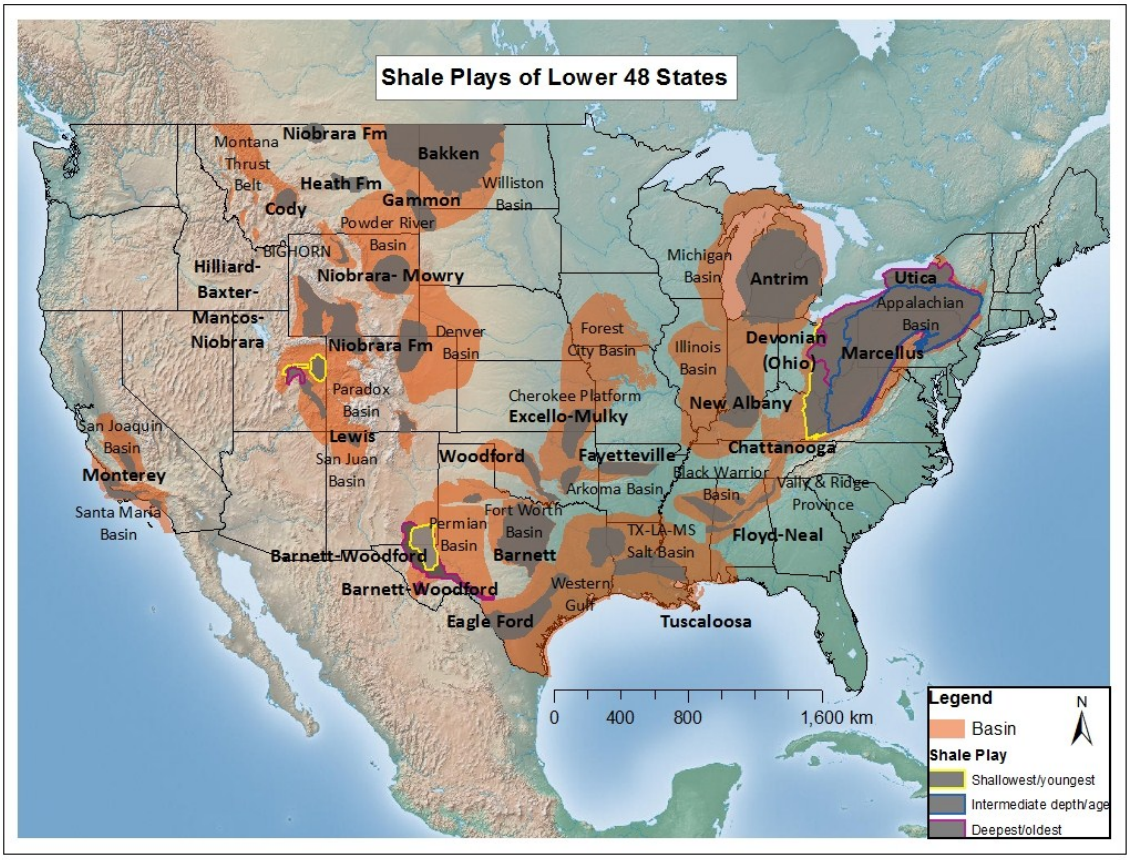

Figure 1: Unconventional shale plays of the contiguous United States. Adapted from USEIA (2011).

Dedication

To my wife Casey and my parents who have all supported my passion for science and education.

Contents

List of Tables

List of Figures

Acknowledgements

Funding for these studies was provided by the Nicholas School of the Environment and the Center on Global Change at Duke University and by funding to the Nicholas School from Fred and Alice Stanback. Field sampling activities in Arkansas were funded by Shirley Community Development Corporation and Faulkner County, Arkansas. Surface water sampling activities were funded in part by the Park Foundation. Studies of shallow drinking water quality would not be possible without the support of numerous homeowners and community organizers. I also need to acknowledge numerous coauthors without whom the manuscripts would not have been possible; Chapter 1: Tom Darrah, Alissa White, Kaiguang Zhao, Robert Jackson, Adrian Down and Avner Vengosh; Chapter 2: Tim Kresse, Phil Hays, Adrian Down, Avner Vengosh, and Robert Jackson; Chapter 3: Kyle Ferrar, Cidney Christie, Avner Vengosh, and Robert Jackson. Reviewers for Chapter 1: Tom Bullen, Gary Dwyer, Flip Froelich, Terry Engelder, Karl Turekian, and two anonymous reviewers provided valuable and critical comments that greatly improved the manuscript. Reviewers for Chapter 2: Two anonymous reviewers.

1. Geochemical evidence for possible natural migration of Marcellus Formation brine to shallow aquifers in Pennsylvania

1.1 Introduction

The extraction of natural gas resources from the Marcellus Shale in the Appalachian Basin of the northeastern United States (Kargbo et al., 2010; Kerr, 2010) has increased awareness of potential contamination in shallow aquifers routinely used for drinking water. The current debate surrounding the safety of shale gas extraction (Howarth et al., 2011) has focused on stray gas migration to shallow groundwater (Osborn et al., 2011a) and the atmosphere (Jiang et al., 2011), as well as the potential for contamination from toxic substances in hydraulic fracturing fluid and/or produced brines during drilling, transport, and disposal (Dresel and Rose, 2010; Gregory et al., 2011; Hayes, 2009; Rowan et al., 2011).

The potential for shallow groundwater contamination caused by natural gas drilling is often dismissed because of the large vertical separation between the shallow drinking water wells and shale gas formations and the relatively narrow zone (up to 300 meters) of seismic activity reported during the deep hydraulic fracturing of gas wells (Fisher, 2010; Veil, 2011). Recent findings in northeastern Pennsylvania (NE PA) demonstrated that shallow water wells in close proximity to natural gas wells (i.e. <1km) yielded, on average, higher concentrations of methane ethane and propane with a heavy carbon isotopic signature (i.e. more thermally mature). By comparison, water wells

farther away from natural gas development had lower combustible gas concentrations and a isotopic signature consistent with a mixture between thermogenic and biogenic components (Osborn et al., 2011a). In contrast, when inorganic water geochemistry from active drilling areas was compared to non-active wells and historical background values, no statistically significant differences were observed (5). Increasing reports of changes in water quality have nevertheless been blamed on the accelerated rate of shale gas development.

The study area in NE PA consists of six counties (Figure 2) that lie within the Appalachian Plateaus physiographic province in the structurally and tectonically complex transition between the highly deformed Valley and Ridge Province and the less deformed Appalachian Plateau (Faill, 1985; Vengosh, 2003).

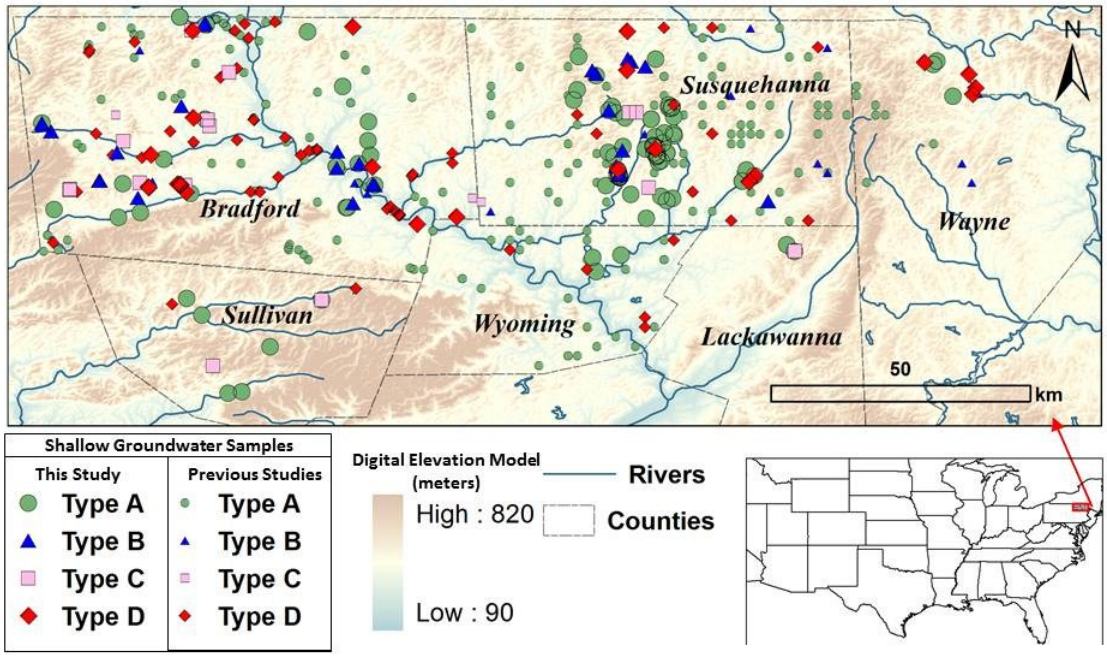

Figure 2: Digital elevation model (DEM) map of northeastern PA. Shaded brown areas indicate higher elevations and green shaded areas indicate lower elevations (valleys). The distribution of shallow (<90m) groundwater samples from this study and previous studies (Taylor, 1984; Williams et al., 1998) are labeled based on water type. Two low salinity (Cl<20 mg/L) water types dominated by Ca-HCO3 (type A=green circles) or Na-HCO3 (type B=blue triangles) were the most common, and two higher salinity (Cl>20 mg/L) water types were also observed: Br/Cl<0.001 (type C=pink squares) and brine-type groundwater Br/Cl>0.001 (type D=red diamonds). Type D groundwater samples appear associated with valleys (Table 1) and are sourced from conservative mixing between a brine and fresh meteoric water. The digital elevation model (DEM) data were obtained from NASA' Shuttle Radar Topography Mission http://srtm.usgs.gov/ .

The geologic setting and shallow aquifer characteristics are described and mapped in greater detail in multiple sources (Alexander, 2005; Geyer, 1982 ; Lohman, 1957, 1973; Osborn et al., 2011a; Taylor, 1984; Williams et al., 1998). The study area contains a surficial cover composed of a mix of unconsolidated glacial till, outwash, alluvium and

deltaic sediments, and post glacial deposits (the Alluvium aquifer) that are thicker in the valleys (Geyer, 1982 ; Taylor, 1984; Williams et al., 1998) (Figure 3).

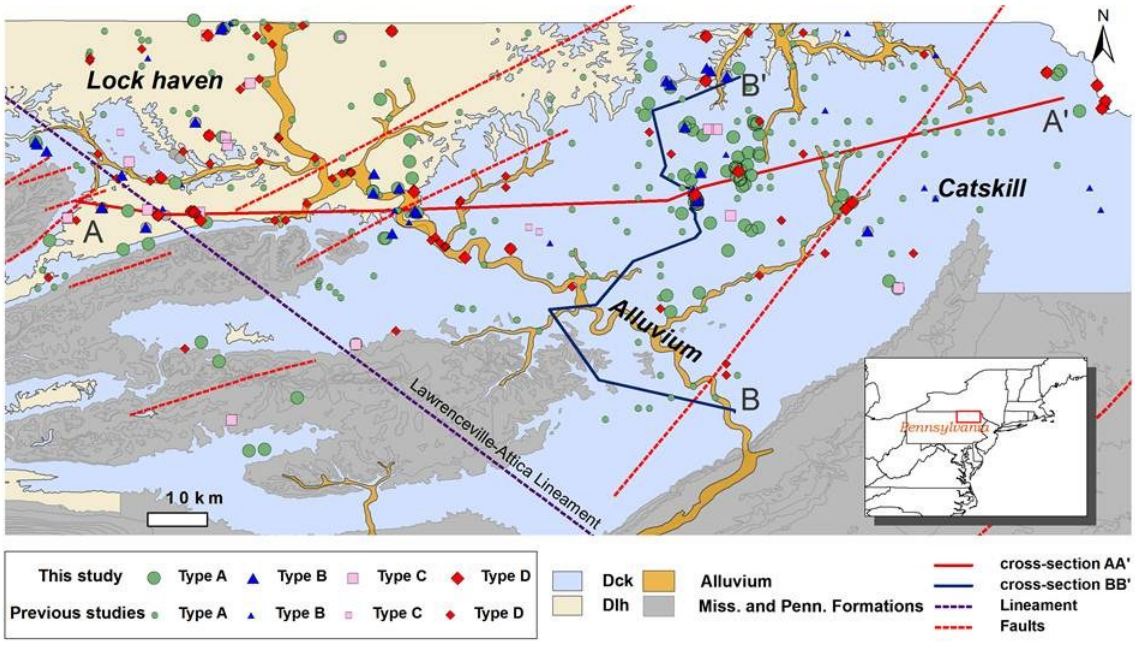

Figure 3: Geologic map of the study area with the three major aquifers Alluvium, Catskill (Dck), and Lock Haven (Dhl) and samples collected during this study. Other formations of Mississippian and Pennsylvanian are shown in gray. Cross section lines are approximated based on (Osborn et al., 2011a) and (Molofsky et al., 2011).

These sediments are underlain by Upper Devonian through Pennsylvanian age sedimentary sequences that are gently folded and dip shallowly (1-3°) to the east and south (Figure 3). The gentle folding creates alternating exposure of synclines and anticlines at the surface that are offset surface expressions of deeper deformation.

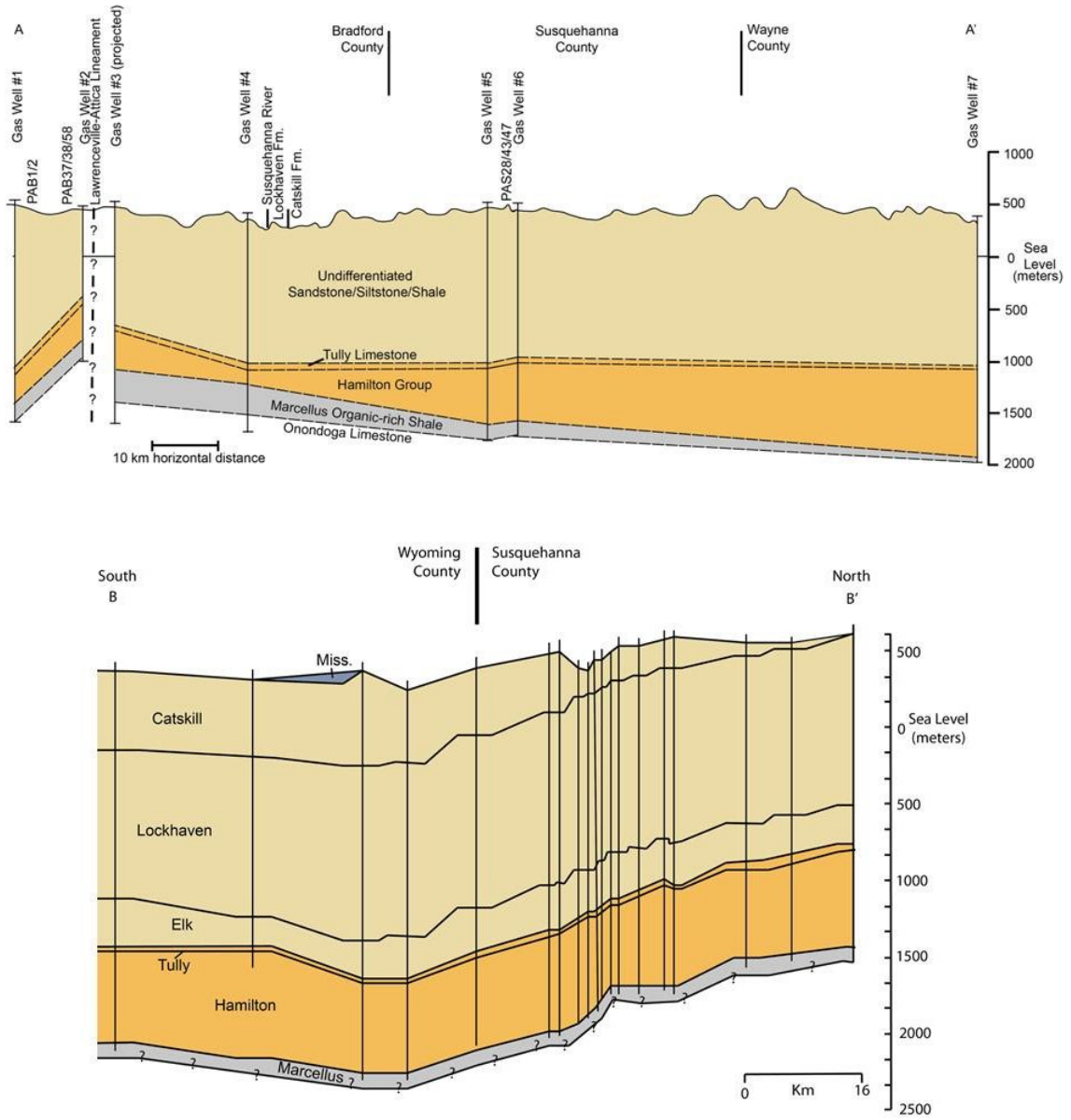

Figure 4: Generalized cross sections adapted from (Osborn et al., 2011a) and (Molofsky et al., 2011) that display the relative vertical separation between the shallow aquifers (Alluvium, Catskill, and Lock Haven) and underlying formations. Note that the alluvium aquifer is not depicted, nor was it included in the source for the well logs (Geological Sample Co., Farmington, NM); however, it is present and is thicker in valleys than uplands. The vertical separation between the water wells and

the Marcellus Formation ranges between 800-2000 m with the minimum found at the apex of the anticlinal hinge displayed in S2b. Note that these low amplitude anticline-syncline features are common in this region of the Appalachian plateau.

The two major bedrock aquifers in the study area are the Upper Devonian Catskill and the underlying Lock Haven Formations (Lohman, 1957,1973; Taylor, 1984;Williams et al., 1998). The average depth of drinking water wells in our study is between 60 to 90 m (Table 1). The underlying geological formations, including the Marcellus Shale (at a depth of 1,200-2,500 m below the surface), are presented in Figures 4a, 4b, and 5.

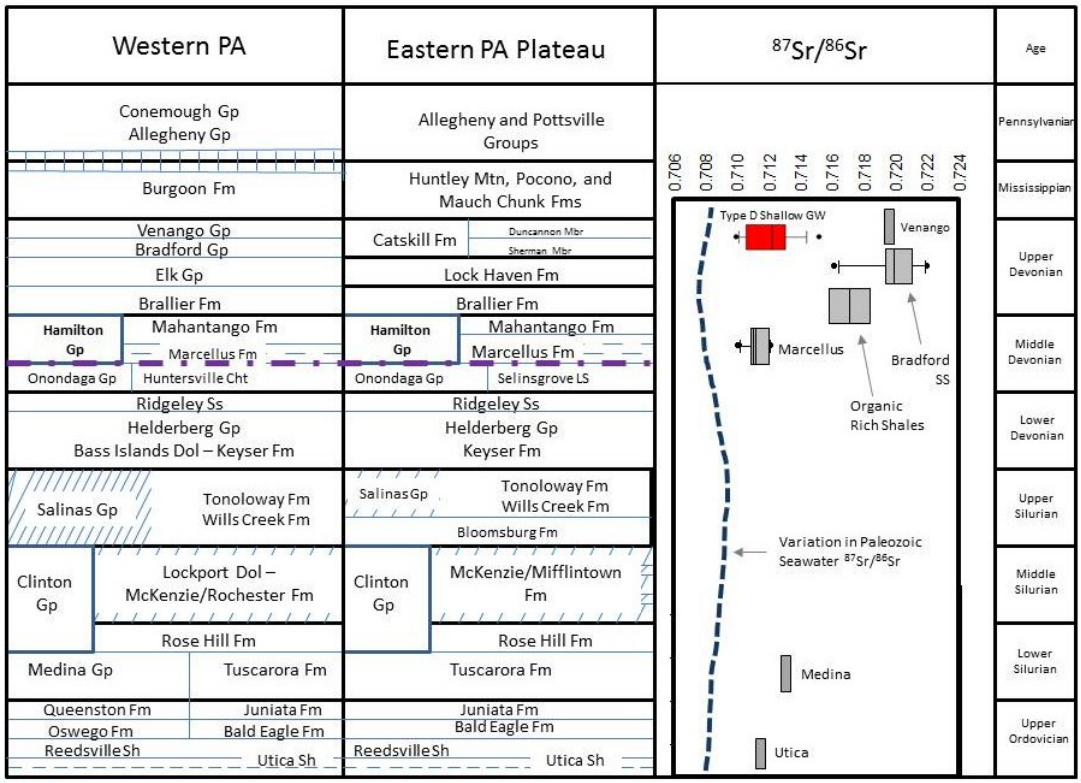

Figure 5: Generalized stratigraphic section in the subsurface of western PA and Eastern plateau, PA, adapted from (Lohman, 1957, 1973; Taylor, 1984; Williams et al., 1998). Variations of $^{87}Sr/^{86}Sr$ ratios in Appalachian Brine and type-D groundwater samples all show enrichment compared to the Paleozoic secular seawater curve (dashed grey line) (Denison et al., 1998). Note the overlap in values of type-D shallow ground water with reported $^{87}Sr/^{86}Sr$ values in Marcellus brines or older formations (Chapman et al., 2012; Osborn et al., submitted 2011; Osborn and McIntosh, 2010) but little/no overlap with reported values for the Upper Devonian brines in stratigraphically equivalent formations (Table 2) (Chapman et al., 2012; Osborn et al., 2012).

In this study, we analyze the geochemistry of 109 newly-collected water samples and 49 wells from our previous study (Osborn et al., 2011a) from the three principal aquifers, Alluvium (n=11), Catskill (n=102), and Lock Haven (n=45), categorizing these waters into four types based on their salinity and chemical constituents (Figures 2 and

3). We combine these data with 268 previously-published data for wells in the Alluvium (n=57), Catskill (n=147), and Lock Haven (n=64) aquifers (Taylor, 1984; Williams et al., 1998) for a total of 426 shallow groundwater samples. We analyzed major and trace element geochemistry and a broad spectrum of isotopic tracers ($\delta^{18}O$, $\delta^{2}H$, $^{87}Sr/^{86}Sr$, $^{228}Ra/^{226}Ra$), in shallow ground water and compared these to published (Dresel and Rose, 2010; Chapman et al., 2012; Osborn and McIntosh, 2010) and new data of 83 samples from underlying brines in deeper formations from the region (Table 2) to examine the possibility of fluid migration between the hydrocarbon producing Marcellus Formation and shallow aquifers in NE PA. We hypothesize that integration of these geochemical tracers could delineate possible mixing between the Appalachian brines and shallow groundwater.

1.2 Methods

Drinking water wells were purged until pH, electrical conductance, and temperature were stabilized. Samples were collected prior to any treatment systems and filtered/ preserved following USGS protocols (Kumar and Martinez, 1982). All major element and isotopic chemistry analyses were conducted at Duke University. Major anions were determined by ion chromatography (IC), major cations by direct current plasma optical emission spectrometry (DCP-OES), and trace-metals by VG PlasmaQuad-3 inductively coupled plasma mass-spectrometer (ICP-MS). Alkalinity was determined in duplicate by titration with HCl to pH 4.5. Stable isotopes were determined by

continuous flow isotope ratio mass spectrometry, using a ThermoFinnigan TCEA and Delta+XL mass spectrometer at the Duke Environmental Isotope Laboratory (DEVIL). Analytical precisions for $\delta^{18}O$ and $\delta^{2}H$ were estimated as +/- 0.1‰ and +/- 1.5‰, respectively. Radium isotope analyses (^{226}Ra and ^{228}Ra) were measured at the Laboratory for Environmental Analysis of RadioNuclides (LEARN) using a Durridge RAD7 radon-in-air monitor (^{226}Ra) and Canberra DSA2000BEGe gamma detector (^{228}Ra) following methods described in (Williams et al., 2001) and (Vinson et al., 2009b). Strontium isotopes were analyzed by thermal ionization mass spectrometer (TIMS) on a ThermoFisher Triton. The mean $^{87}Sr/^{86}Sr$ of the SRM-987 standard was 0.710266 +/- 0.000005 (SD).

For strontium isotopes measurements, water samples were prepared by total desiccation of sample aliquot containing approximately 2-4 ug of Sr. The dried sample was then digested in 3 N ultra-pure HNO_3 acid and extracted using Teflon micro columns containing Eichrom Sr resin. The extracted Sr was then dried again before digestion with TaCl solution and loaded onto Re filaments for a final drydown.

The derived distance-to-valley and distance-to-gas well distances represent planimetric lengths from sampling locations to either nearest gas wells or valley centerlines and do not account for the direction or extent of horizontal drilling in the subsurface. Distances to valley centerline were either automatically determined with respect to the national stream network (i.e., Distance to Valley –National Stream

Network) or manually measured in reference to the digital elevation model (DEM) layer (i.e., Distance to Valley Manual Calculation) valley centers in northeastern PA.

Statistical analysis was performed using SPSS v.17.0 statistical software. Before each statistical comparison, the normality was verified using a 1-sample Kolmogorov-Smirnov test. Parameters that did not achieve normality were transformed using log transformation and verified for normality. Statistical summaries of elemental concentrations and isotopic composition including mean and median are shown for each water type (i.e. A, B, C, D) in Table 4. In order to simultaneously test whether several means are equal (e.g. whether type D [Cl], Br/Cl, $^{87}Sr/^{86}Sr$ are significantly different than the types A-C and the variance observed in the suite of samples), we performed a post-hoc one-way analysis of variance (ANOVA) for each of the water types (Table 4). We compare the historical (Taylor, 1984; Williams et al., 1998) and current dataset (2010-2011), using an independent 2-way t-test of log transformed data (and verified with non-parametric 2-sample independent Mann-Whitney U test) similar to methods shown previously (e.g. Darrah et al., 2009).

1.3 Geological Setting

In the northern Appalachian Basin, sedimentary deposition is relatively continuous throughout the Paleozoic era, although several unconformities erase sequence records regionally (e.g. The Tri-States unconformity removes Lower Devonian

strata in western New York, while complete sequences are found in central New York and northeastern PA) (Brett et al., 1996). The sedimentary column represents periods of deposition, burial, lithification, uplift and subsequent erosion that form relatively simple sets of horizontal strata (~ 1-3 degree dip to the south and east) derived from various depositional environments (ranging from proposed deep- to mid- basin black shale to terrestrial red beds) within the Plateau region (northeastern and western PA and most of NY) (Brett et al., 2011; Brett et al., 1996; Lash and Engelder, 2011; Straeten et al., 2011). The monocline, including the entire Appalachian sedimentary sequence is bound on the north by the Precambrian Canadian Shield and Adirondack uplift (N-NE), on the west by the Algonquin and Findlay arches, and on the south and east by the Appalachian fold belt (i.e. Valley and Ridge Province) (Jenden et al., 1993; Milici and W. de Witt, 1988). Bedrock thickness ranges within the basin from ~920 meters along the southern shore of Lake Ontario in the north (northern NY) to ~7600 meters along the Appalachian structural front in the south. Erosion has beveled the monocline flat, allowing for elongate, east-west trending outcrop belts of strata across the majority of the Appalachian Plateau physiographic province. The stratigraphic names and continuity of specific stratigraphic sequences change regionally. As a result, we present a simplified stratigraphic reconstruction in Figure 5 showing the stratigraphy from western and eastern PA (Brett and Baird, 1996; Brett et al., 2011; Brett et al., 1996; Lash and Engelder, 2011; Straeten et al., 2011; Straeten et al., 1994). The study area constitutes a transition

from the Valley and Ridge to the Plateau province, and includes sequential low amplitude anticline/syncline structures, numerous thrust faults, lineaments, joints, and natural fractures (Alexander, 2005; Engelder et al., 2009; Jacobi, 2002; Lash and Engelder, 2009; Pohn, 2000; Trenton et al., 2006) (Figure 3).

The Appalachian Basin sedimentary sequence is underlain by Precambrian crystalline basement rocks of the (Grenville province) Canadian Shield (Brett et al., 1996). The Appalachian Basin consists primarily of sedimentary sequences of Ordovician to Pennsylvanian age that are derived from the Taconic (~450Ma), Acadian (~410-380Ma), and Alleghanian (~330-250Ma) orogenic events (Jenden et al., 1993; Rast, 1989). Exposed at its northern extent near Lake Ontario is the Upper Ordovician-Lower Silurian contact (Cherokee unconformity). Younger deposits (Upper Silurian, Devonian, and Mississippian) occur in successive outcrop belts to the south towards the Appalachian structural front (Brett et al., 1996; Lash and Engelder, 2011; Straeten et al., 2011). While erosion has removed any post-Pennsylvanian deposition within western-central New York and the majority of our study area within northeastern PA (exceptions noted in Figure 3).

The Middle Ordovician Trenton/Black River Group consists of interbedded limestones and shales overlain by the calcareous and organic-rich Utica Shale derived primarily by sediment offloading from the Taconic orogeny ~420Ma (Brett et al., 1996; Lavoie, 1994; Lehmann et al., 1995). The lower most Silurian age strata is the fine-

grained Tuscarora Formation sandstones, which is overlain by the middle Silurian Clinton Group with locally inter-bedded limestone, dolostone, sandstone, and shale (Figures 3 and 5). The Upper Silurian is characterized by the transition from the Silurian Lockport Dolomite/McKenzie argillaceous limestone to the Bloomsburg red sandstone and evaporitic Salina Group in the plateau region of the Appalachian Basin (Brett et al., 1996; Ryder et al., 1996; Ryder, 1998). The Salina Group consists of interbedded shales, dolomites, and primarily salt deposits that acts as the decollement to younger stratigraphic units (Frey, 1973; Scanlin and Engelder, 2003). As a result, structural folds and faults above the decollement (i.e. Devonian and younger stratigraphic units) bear no resemblance in deformation style to those present beneath the Salina Group (Faill, 1985; Faill and Nickelsen, 1999; Frey, 1973; Scanlin and Engelder, 2003). The transition from Upper Silurian to Lower Devonian is comprised of the Helderberg Group (layered dolomites and limestones often lost in western NY) and Tri-States Group consisting of the Oriskany Sandstone and Onondaga and Selinsgrove Limestones, which lies directly beneath the Hamilton Group (Baird and Staeten, 1999; Straeten et al., 2011; Straeten et al., 1994). The Hamilton Group is an eastward to southeastward thickening wedge of marine sediments that includes the Marcellus Formation.

The Marcellus Formation is an organic-rich, hydrocarbon producing, siliciclastic-rich black shale present beneath much of Pennsylvania, New York, and the northeastern US. The Marcellus Formation constitutes the stratigraphically lowest subgroup of the

Middle Devonian Hamilton Group (Baird and Staeten, 1999; Brett et al., 2011; Straeten et al., 2011; Straeten et al., 1994) and was deposited in the foreland basin of the Acadian Orogeny (~385-375 Ma). The Marcellus Formation includes two distinct calcareous and iron-rich black shale members; i.e. the Union Springs (lower) and Mount Marion/Oatka Creek (upper)) interrupted by the Cherry Valley limestone (Baird and Staeten, 1999; Brett et al., 2011; Lash and Engelder, 2009; Straeten et al., 2011; Straeten et al., 1994). By comparison to the Valley and Ridge province or the region in close proximity to the Appalachian Structural Front, the plateau portion of the Marcellus Formation is significantly less deformed (e.g.Faill and Nickelsen, 1999; Faill, 1997a, b).

Like the Marcellus, the upper part of the Devonian sequence is deposited from material sourced from the Acadian orogeny. Above the Marcellus, the Hamilton Group consists of the Mahantango grey shale, locally interbedded by limestones and the Tulley limestone. The Upper Devonian consists of thick synorogenic sequences of grey shales (i.e. the Brallier Formation), beneath the Lock Haven Formation sandstone and Catskill Formation clastic deltaic red sandstones deposited in foreland basin of the Acadian Orogeny. The latter two sequences, the Lock Haven and Catskill Formations, constitute the two primary aquifer lithologies in northeastern PA along with the overlying glacial and sedimentary alluvium, which is thicker in valleys than the uplands. Deformation of Devonian lithologies (i.e. the Hamilton Group including the Marcellus Formation) and the Upper Devonian (Lock Haven and Catskill aquifers)) began during the onset of the

Alleghanian orogeny in the latest (330-250Ma) in the Carboniferous Age. In the plateau physiographic province, deformation is accommodated by a combination of layer parallel shortening, folding that lead to the gentle anticline/syncline sequences, and low angle thrust faulting structures observable in northeastern PA (Davis and Engelder, 1985; Engelder, 1979; Engelder and Engelder, 1977; Engelder and Geiser, 1980; Engelder and Whitaker, 2006; Evans, 1995; Gray and Mitra, 1999; Lash et al., 2004; Lash and Engelder, 2009; Scanlin and Engelder, 2003). The initiation of deformation during the Alleghanian orogeny also likely led to the onset of catagenesis for the Marcellus Formation and the joint sets observed in the Upper Devonian sedimentary rocks (Engelder and Whitaker, 2006). The majority of stratigraphic sequences above the Catskill Formation are eroded in our study area and therefore only briefly discussed. More complete reviews of Carboniferous Age deposition (Mississippian and Pennsylvanian) are available elsewhere (e.g. Faill and Nickelsen, 1999;Faill, 1997a,b).

1.4 Results and Discussion

The water chemistry data from the Alluvial, Catskill, and Lock Haven shallow aquifers (Table 1) reveal a wide range of solute concentrations, from dilute groundwater with total dissolved solids (TDS) <500 mg/L and Cl < 20 mg/L to highly saline water (e.g., a salt spring, with TDS of 7,800 mg/L and Cl ~ 4,000). Based on these characteristics, we divide the water samples into four types of ground water (Figure 1). Two groundwater types (A and B; n=118 of 158 samples from this and our previous

study (5)) are characterized by low salinity and high Na/Cl and Br/Cl ratios (Table 1). The two elevated salinity (Cl>20 mg/L) water types (C and D) were divided based on their Br/Cl ratios. Type (C) (n=13 of 158) has a distinctive low (<0.001) Br/Cl ratio (Figure 6) and higher NO_3^- concentrations that we attribute to salinization from domestic sources such as wastewater and/or road salt that have typically low Br/Cl ratios (28, 29). The fourth subset of shallow groundwater (type D) (n=27 of 158) was identified with a relatively high Br/Cl ratio (>0.001) and low Na/Cl ratio (Na/Cl<5) with a statistically significant difference in water chemistry from types A-C (Table 3).

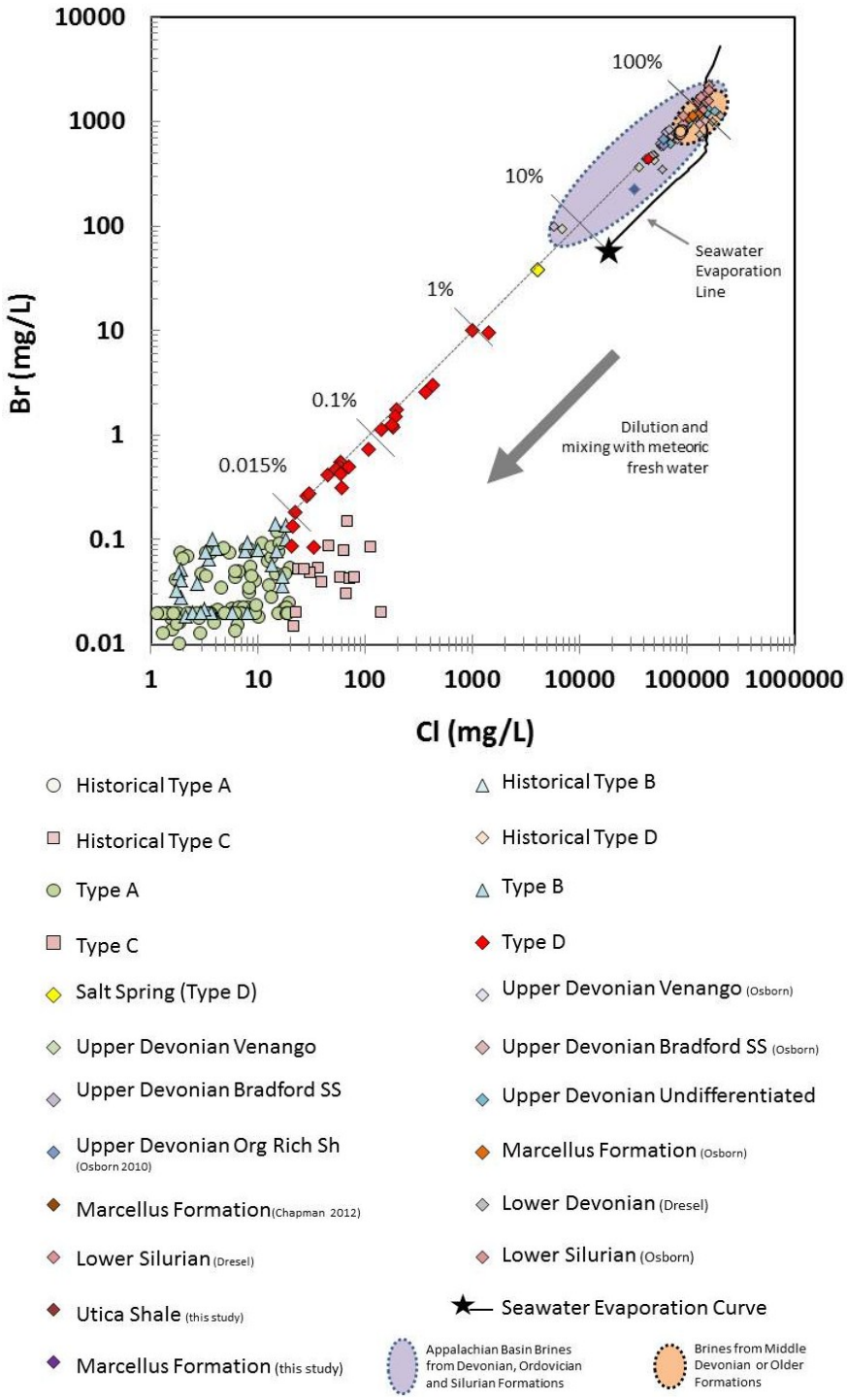

Figure 6: Bromide versus chloride concentrations (log-log scale) in shallow groundwater in NE PA and Appalachian brines from this and previous studies

(Taylor, 1984; Williams et al., 1998). The linear relationship (type D r2=0.99, p=1.94x10^{-24}; all type A-D samples r2=0.88) between the conservative elements Br and Cl demonstrates that the majority of the higher salinity samples of type D are derived from dilution of Appalachian Brine that originated from evaporated seawater. Even with a large dilution of the original brine, the geochemical signature of type-D waters are still discernable in shallow groundwater from other high salinity (Cl> 20 mg/L) groundwater with low Br/Cl ratios (type C). Type C water likely originated from shallow sources such as septic systems or road deicing. Seawater evaporation line is from (McAfferty, 1987).

A geochemical analysis of published data (268 samples) collected in the 1980s (Taylor, 1984; Williams et al., 1998) revealed similar shallow salinized groundwater with a distinctive higher Cl (>20 mg/L) and low Na/Cl ratio. The saline groundwater mimics Type D water with statistically indistinguishable (p=0.56-0.83) concentrations of major cations and anions (Figure 7a and 7b).

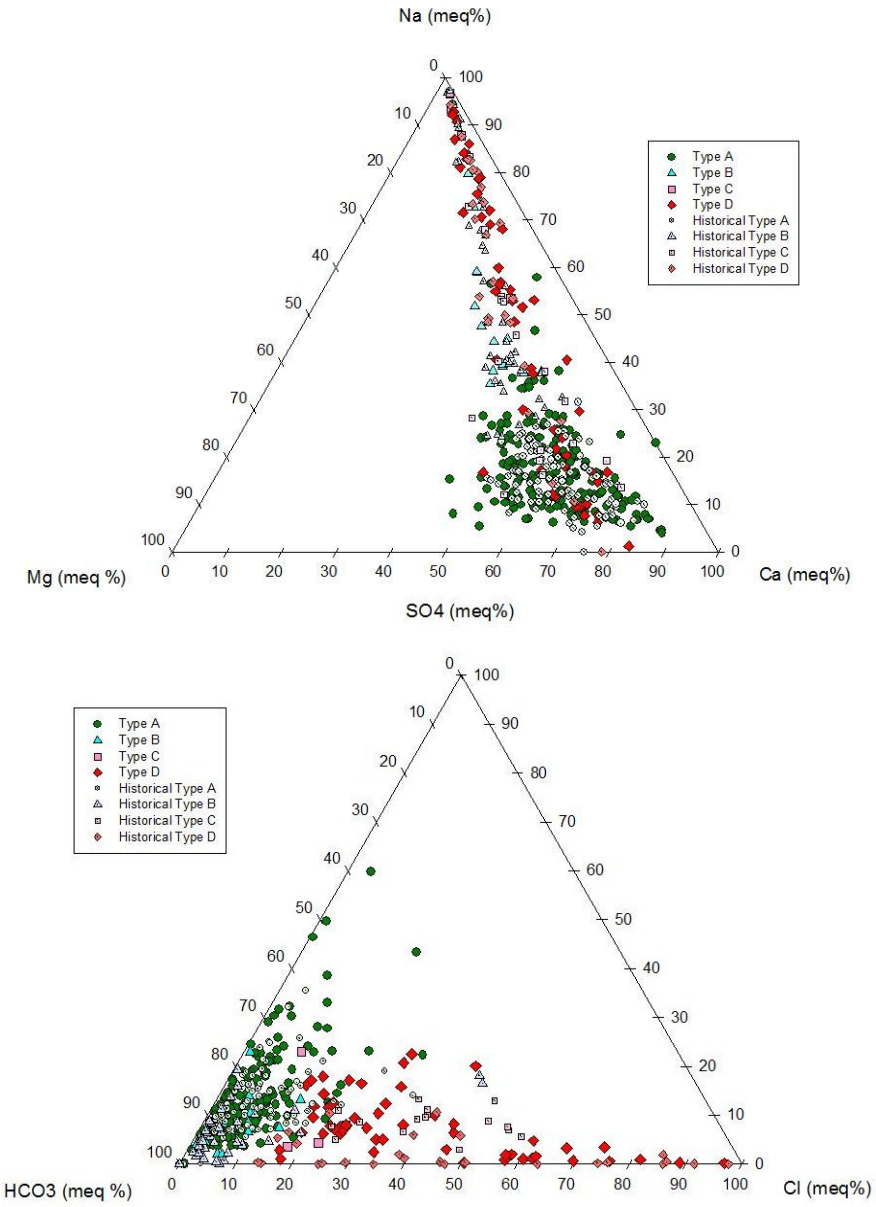

Figure 7: Ternary diagrams that display the relative percent of the major cations (A) and anions (B) in shallow groundwater samples from this and previous studies (Taylor, 1984; Williams et al., 1998). The overlap indicates that Na-Ca-Cl type saline water was present prior to the recent shale-gas development in the region and could be from natural mixing.

However, bromide concentrations were not available in the historical data set.

Nonetheless, we designated historical samples with high Cl (>20 mg/L) and low Na/Cl

ratio (Na/Cl<5) as possible type-D (n=56 of 268). The remaining historical samples with Cl concentrations (> 20 mg/L) were designated as type C. All water types (A-D) were statistically indistinguishable from their respective historical types (A-D)(Table 4).

Type D saline waters characterized by a Na-Ca-Cl composition with Na/Cl, Sr/Cl, Ba/Cl, Li/Cl, and Br/Cl ratios similar to brines found in deeper Appalachian formations (e.g., the Marcellus brines) (Dresel and Rose, 2010; Chapman et al., 2012; Osborn and McIntosh, 2010; Osborn et al., 2011a) (Table 2). This suggests mixing of shallow modern water with deep formation brines. Furthermore, the linear correlations observed for Br, Na, Sr, Li, and Ba with chloride (Figures 6 and 8a-8f) demonstrate the relatively conservative and non-reactive behavior of these constituents and that the salinity in these shallow aquifers is most likely derived from mixing of deeper formation brines.

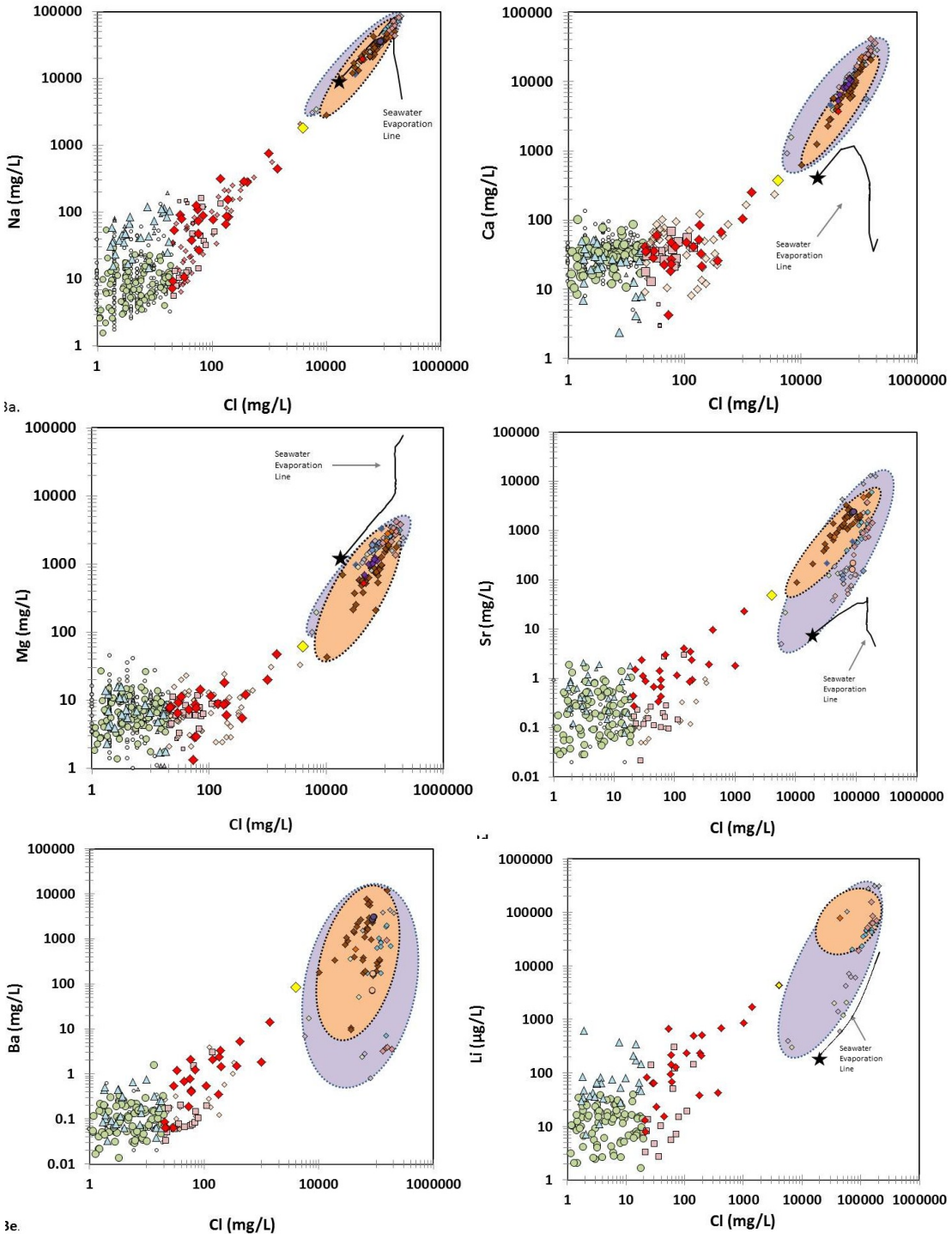

Figure 8: Na, Ca, Mg, Sr, Ba, and Li versus Cl concentrations (log-log scale) in investigated shallow groundwater in NE PA and deep Appalachian basin brines from this and previous studies (Taylor, 1984; Williams et al., 1998). The linear relationship

between the different elements and the conservative Cl demonstrates that the majority of the higher salinity samples of type D are derived from conservative dilution (mixing) of Appalachian brine in NE PA. Type D regression results (r2, p – value) between Cl and Ca (0.89, $2.17x10^{-12}$), Mg (0.83, $2.4x10^{-10}$) Sr (0.92, $4.8x10^{-14}$), Na (0.94, $1.33x10^{-15}$) Ba (0.92, $3.23x10^{-14}$) and Li (0.96, $3.7x10^{-17}$). See Figure 6 legend for symbol description.

The stable isotopes ($\delta^{18}O$ (-8 to -11‰) and $\delta^{2}H$ (-53 to -74‰)) of all shallow groundwater types (A-D) are indistinguishable ($p > 0.231$) and fall along the local meteoric water line (LMWL) (Kendall and Coplen, 2001) (Figure 9).

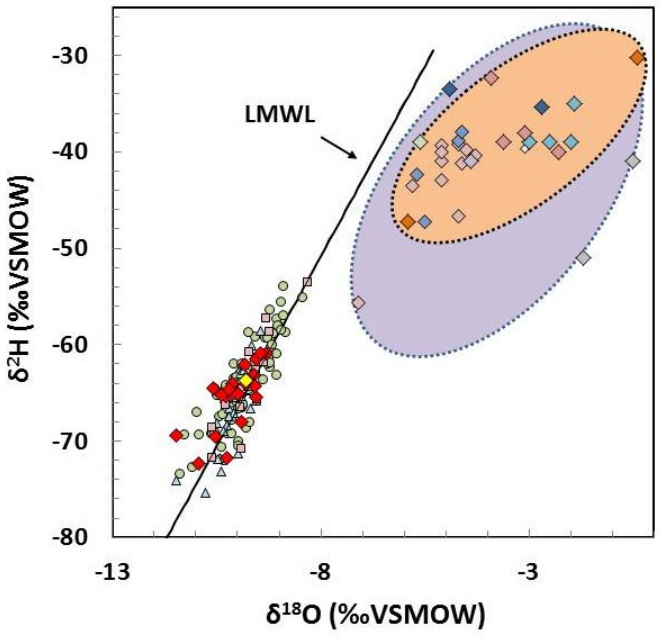

Figure 9: $\delta^{18}O$ versus $\delta^{2}H$ in shallow groundwater from this study and Appalachian brines. The water isotope composition of the shallow groundwater samples, including the Salt Spring, appear indistinguishable from the local meteoric water line (LMWL) (Kendall and Coplen, 2001) and do not show any apparent trends toward the stable isotope ratios of the Appalachian brines (Dresel and Rose, 2010; Osborn and McIntosh, 2010). The data indicate that dilution of the type-D waters likely occurred on modern time scales (<10,000 years). Symbol legend is provided in Figure 6.

The similarity of the stable isotopic compositions to the modern LMWL (Kendall and Coplan, 2001) likely indicate dilution with modern (<10,000 year) meteoric water. Shallow ground water isotopic compositions do not show any positive $\delta^{18}O$ shifts towards the seawater evaporation isotopic signature (i.e. higher $\delta^{18}O$ relative to $\delta^{2}H$) as observed in the Appalachian brines (Figure 9 and Table 2). Because of the large difference in concentrations between the brines and fresh water, very small contributions of brine have a large and measureable effect on the geochemistry and isotopes of dissolved salts (Figure 6), but limited effect on $\delta^{18}O$ and $\delta^{2}H$. Mass-balance calculations indicate that only a brine fraction of higher than ~20% would change the $\delta^{18}O$ and $\delta^{2}H$ of salinized groundwater measurably. Oxygen and hydrogen isotopes are therefore not sensitive tracers for the mixing of the Appalachian brines and shallow groundwater because of the large percentage of the fresh water component in the mixing blend. For example, the salt spring at Salt Springs State Park with the highest salinity among shallow groundwater samples is calculated to contain less than 7% brine.

The discrete areas of type-D water have lower average elevations and closer distances to valley centers but do not correlate with distance to the nearest shale gas wells (Figures 2 and 3, Table 1). The lack of geospatial association with shale-gas wells and the occurrence of this type of saline water prior to shale gas development in the study area (Lohman, 1957, 1973; Taylor, 1984; Williams et al., 1998) (see distribution in Figures 7a and 7b) suggests that it is unlikely that hydraulic fracturing for shale gas

caused this salinization and that it is instead a naturally occurring phenomenon that occurs over longer timescales.

Distinguishing the ultimate source of the salinized water in NE PA requires an evaluation of the geochemical signatures of underlying brines in the Appalachian Basin. The data presented in this study (Table 2, Figures 6 and 8a-8f) and previous studies (Dresel and Rose, 2010; Osborn et al., 2012 ; Osborn and McIntosh, 2010; Osborn et al., 2011a), suggest that the Appalachian brines evolved by evaporation from a common seawater origin, but underwent varying stages of alteration. The first stage of evolution, common to all of the brines, is the evaporation of seawater beyond halite saturation resulting in brines with high Br/Cl and low Na/Cl ratios relative to seawater (Dresel and Rose, 2010). The degree of evaporation that is computed based on the Br/Cl ratio in the Appalachian brines (4-7$\times10^{-3}$; Figure 6) as compared to evaporated sea water curve (McCaffrey et al., 1987) is equivalent to 20-40-fold. The brines then likely underwent dolomitization with carbonate rocks that enriched Ca and depleted Mg in the brine relative to the seawater evaporation curve (Dresel and Rose, 2010) (Figures 8b, 8c) and sulfate reduction. In addition, the composition of each respective hypersaline Ca-Cl Appalachian brine (i.e. Ordovician, Salina, and/or Marcellus), was differentially altered by interactions with the host aquifer rocks, presumably under tectonically-induced thermal conditions (Saunders and Swann, 1990) that resulted in resolvable variations in

Sr/Ca, Ba/Sr, and $^{87}Sr/^{86}Sr$ ratios. The final stage of brine alteration that accounts for the observed brine compositions is dilution (Dresel and Rose, 2010).

The net results of these processes generated large variations in brine salinity (TDS of 10 to 343 g/L), relatively homogeneous elevated Br/Cl ratios (range of $2.4x10^{-3}$ to $7.6x10^{-3}$) and enriched $\delta^{18}O$ (0‰ to -7‰) and $\delta^{2}H$ (-33‰ to -45‰) in all Appalachian brines. The remnant geochemical signatures (i.e. Sr/Ca, Ba/Sr, and $^{87}Sr/^{86}Sr$) of formation specific brine-rock interactions provide the most suitable basis for differentiating the original formation unit that produced brines. The Sr/Ca ratios (0.03-0.10) of the produced waters from Marcellus wells are significantly higher than brines evolved through calcite ($0.4\text{-}1.6x10^{-3}$) or aragonite ($1.5\text{-}2.2x10^{-2}$) dolomitization, but are consistent with equilibrium with other minerals such as gypsum or celestite (Sass and Starinsky, 1979). Similarly, the Ba/Sr (0.07-1.78) ratios range up to values observed for typical upper continental crust (Ba/Sr=1.3-1.7) (Kesler et al., 2012).

New and compiled data presented in Table 2 show distinctive geochemical fingerprints (Sr/Ca, Ba/Sr, Sr/Cl, Ba/Cl, Li/Cl, and $^{87}Sr/^{86}Sr$) among the Appalachian brines in the different formations. We therefore used these variables as independent tracers to differentiate possible brine sources for the shallow Type-D groundwater. Brines from the Marcellus Formation show systematically low (less radiogenic) $^{87}Sr/^{86}Sr$ (~0.710 to 0.712; n=50) and high Sr/Ca (0.11 to 0.17) ratios compared to the more

radiogenic Upper Devonian brines ($^{87}Sr/^{86}Sr$ ratio= 0.71580 to 0.72200; n=12; Figure 10) and low Sr/Ca (0.002 to 0.006; Figure 11).

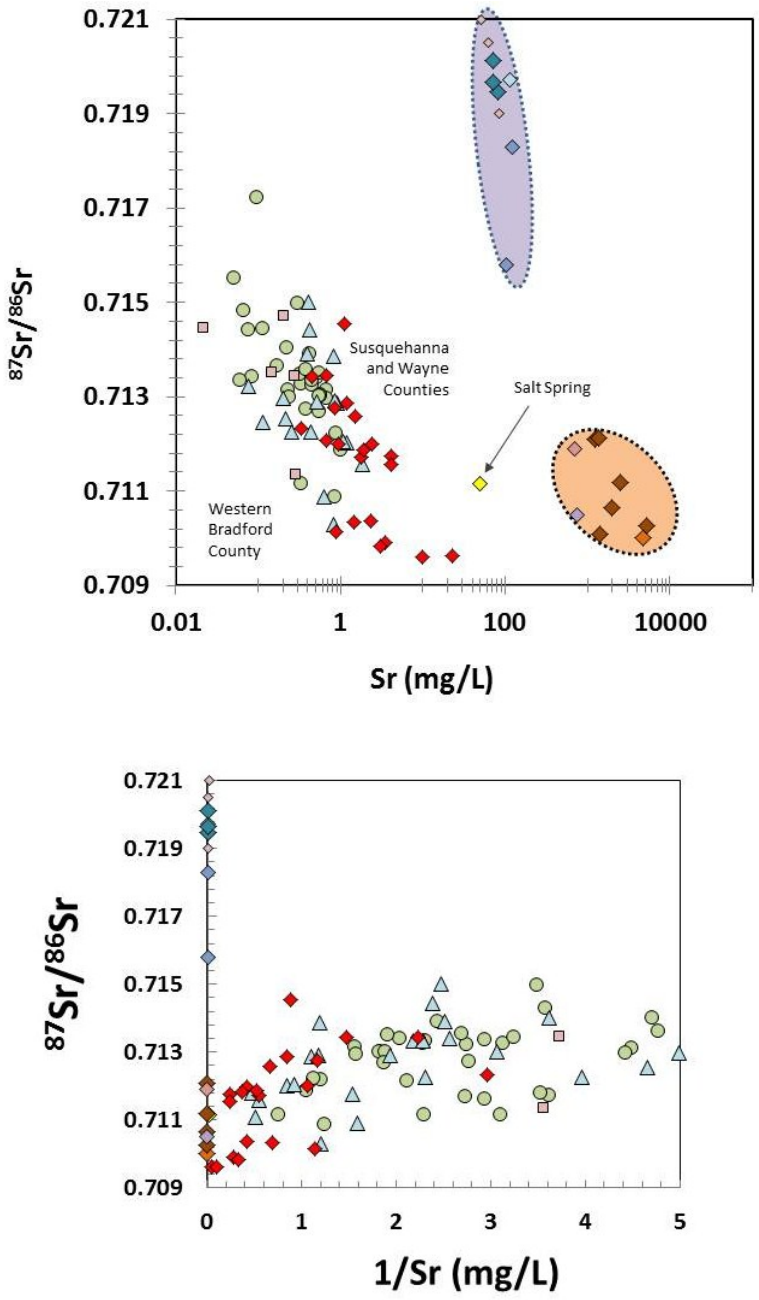

Figure 10a: $^{87}Sr/^{86}Sr$ versus Sr concentrations (log scale) of Appalachian Brines (Chapman et al., 2012; Osborn et al., 2012) and shallow groundwater samples in the

study area. The shallow groundwater samples are divided in the figure based on water types. Increased concentrations of Sr in the shallow aquifers are likely derived from two component mixing: (1) a low salinity, radiogenic $^{87}Sr/^{86}Sr$ sourced from local aquifer reactions; and (2) a high salinity, less radiogenic $^{87}Sr/^{86}Sr$ water consistent with Marcellus Formation brine. The Marcellus Formation $^{87}Sr/^{86}Sr$ appears lower in western Bradford than in Susquehanna and Wayne counties. Other brine sources such as the Upper Devonian formations have a more radiogenic $^{87}Sr/^{86}Sr$ ratio, which does not appear to show any relationship to the salinized shallow groundwater. 10b) $^{87}Sr/^{86}Sr$ versus 1/Sr concentrations (mg/L). Mixing appear as a straight line in the lower graph, demonstrating the apparent mixing of a Marcellus Formation Brine with shallow groundwater. Symbol legend is provided in Figure 6.

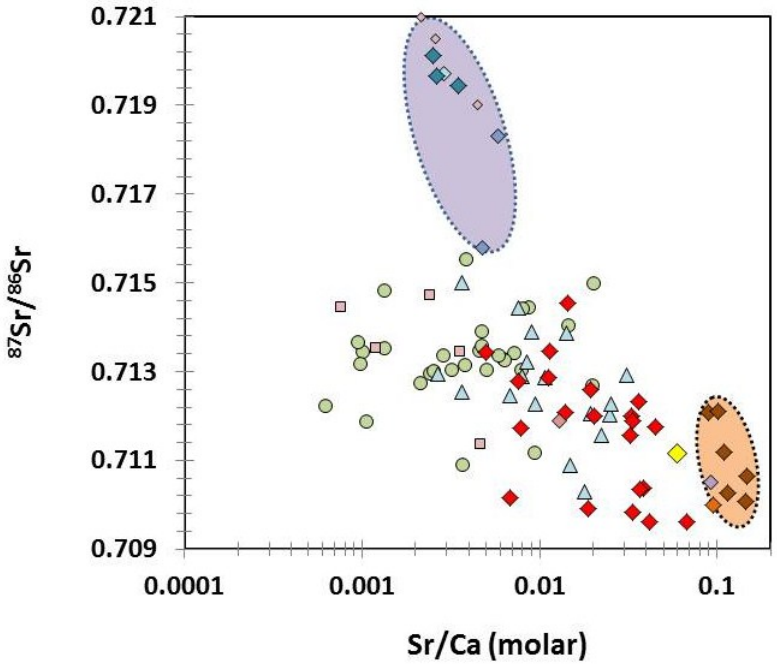

Figure 11. $^{87}Sr/^{86}Sr$ versus Sr/Ca ratios in shallow ground water samples in NE PA and Appalachian brines. The distinctive high Sr/Ca and low $^{87}Sr/^{86}Sr$ fingerprints of the Marcellus Formation brine (Chapman et al., 2012) appear to control the Sr/Ca and $^{87}Sr/^{86}Sr$ variations of the saline groundwater of type D. These values are distinct from the compositions of other Appalachian Brines collected from Upper Devonian formations (Venango, Bradford sandstone, and organic-rich shales). See Figure 6 legend for symbol description.

Because of the relatively high Sr concentration and diagnostic Sr/Ca Ba/Sr, and $^{87}Sr/^{86}Sr$ ratios, this geochemical proxy has the potential to elucidate regional flow paths (16, 17), salinity sources (18, 19), and the specific source of the Appalachian brines (Chapman et al., 2012; Osborn et al., 2012) (Figure 10). The $^{87}Sr/^{86}Sr$ ratios (0.71030-0.71725 ±0.000003 SE) of low-saline groundwater (type A and B) vary widely in the shallow aquifers, but the overwhelming majority are distinctly different from values of produced water brines from both Upper Devonian (0.71580-0.72200) (Osborn et al., 2012); Table 2) and Middle Devonian Marcellus Formation (0.71000-0.71210; Figure 10) (Chapman et al., 2012). Conversely, the type D shallow groundwater data show both a linear correlation between Sr and Cl (i.e., conservative behavior of Sr; Figure 8d) and a decrease of $^{87}Sr/^{86}Sr$ from 0.71533 to 0.70962 with increasing Sr concentrations and salinity, confirming that the resulting salinity is derived from mixing with Marcellus Formation brine (Figure 10). Our data also display a strong association between $^{87}Sr/^{86}Sr$ and Sr/Ca ratios (Figure 11), a relationship suggested as a sensitive indicator of Marcellus brines because of the unique combination of low $^{87}Sr/^{86}Sr$ ratios and high Sr/Ca ratios reported for brines from the Marcellus Formation (Chapman et al., 2012).

While the saline waters in the eastern portion of the study area follow the expected Sr-isotope mixing trend hypothesized from new and published data on produced water from the Marcellus Formation (Figure 10), the saline waters from the western portion of our study area show systematic mixing with an end-member of a

slightly lower $^{87}Sr/^{86}Sr$ ratio (0.70962). This lower ratio could reflect provenance variations within the formation (e.g. lower siliclastic detrital component away from the Acadian clastic source) in the region (Chapman et al., 2012). In sum, while the high Br/Cl ratio in type D saline groundwater reflects mixing with underlying Appalachian brines from a common evaporated seawater origin, the $^{87}Sr/^{86}Sr$ ratios indicate mixing with brines with lower $^{87}Sr/^{86}Sr$ fingerprints of ~0.7096-0.7110 that cannot be accounted for by Upper Devonian formations but similar to the underlying Marcellus Formation brines.

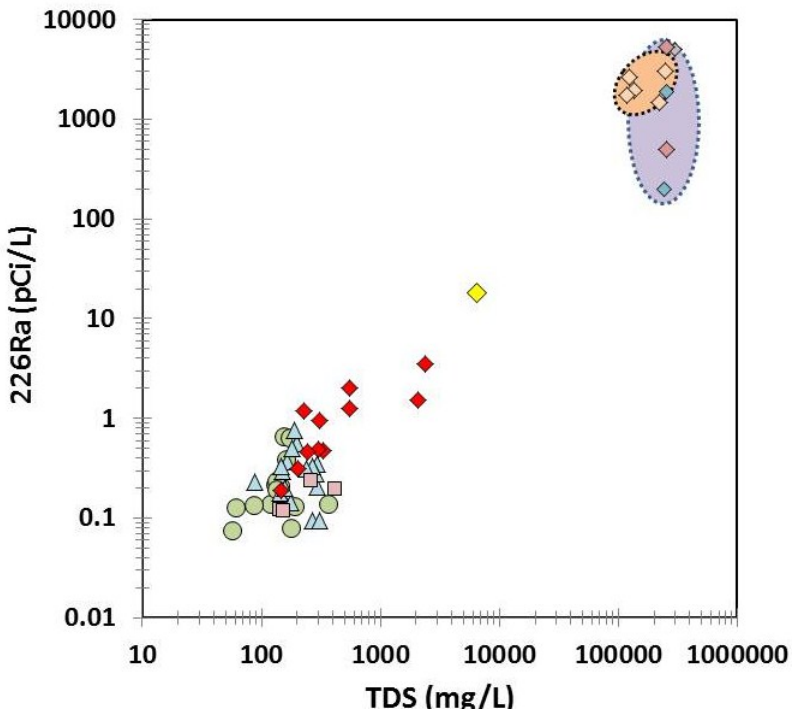

Figure 12: ^{226}Ra activities (pCi/L) versus total dissolved salts (TDS) in shallow groundwater and Marcellus brines (Rowan et al., 2011) from NE PA. The increase of ^{226}Ra with salinity appears consistent with conservative mixing (Type D: r^2=0.93, p=3.39x10^{-7}) with Marcellus Formation brine from the study area. The activities of Ra in most of the shallow aquifer samples are rarely above the EPA guideline (5 pCi/L). See Figure 6 legend for symbol description.

Other features that characterize the produced waters from the Marcellus Formation are the high activities of naturally occurring nuclides of ^{226}Ra and ^{228}Ra and low $^{228}Ra/^{226}Ra$ ratios (Rowan et al., 2011). ^{226}Ra and ^{228}Ra are the disintegration products of ^{238}U and ^{232}Th, respectively, and are generated in groundwater from alpha recoil, desorption from sediments, and dissolution of aquifer material (Rowan et al., 2011; Vinson et al., 2009b). In most of the shallow groundwater we sampled (Table 1), combined Ra activities were low (<20 pCi/L). In contrast, reported activities of Ra in Marcellus brines from the study area were high (1,500 to 3,100 pCi/L) (Figure 12) with low $^{228}Ra/^{226}Ra$ ratios (0.12 to 0.73) (Rowan et al., 2011). The highest Ra activities that we measured were in Type-D waters, and the range (0.07 to 18 pCi/L) is consistent with our calculated mixing range of ~0.01% to 7% based on chloride and bromide mass-balance calculations (Fig. 3), although some interaction such as adsorption with the aquifer rocks (Vinson et al., 2009a) is likely. In addition, the $^{228}Ra/^{226}Ra$ ratio in the salinized groundwater (mean=0.5) is higher than that of the majority of the Marcellus produced waters from the study area (mean=0.33; (Rowan et al., 2011); Table 2), indicating that some of the dissolved Ra in the shallow groundwater is likely derived from water-rock interactions and not from conservative mixing. Overall, because of the increase of Ra content (Figure 12) and decrease of $^{228}Ra/^{226}Ra$ with salinity (Table 1) we infer that Ra content in the saline groundwater could be derived from both mixing with the brine and

mobilization of Ra from the aquifer rocks, a geochemical process that is known to be enhanced with increasing salinity (Vinson et al., 2009b).

Methane data from our previous studies (Osborn et al., 2011a, b) can be examined based on the four water types (A-D) we found in this study. The highest average methane concentrations were observed in type-D waters throughout the dataset, followed by type B and A. In locations >1 km away from shale gas drilling sites, only one sample, a type B water, out of total of 41 samples contained elevated methane concentrations (>10 mg/L); one newly sampled type D water from the spring at Salt Springs State Park (Osborn et al., 2011b) also had concentrations >10 mg/L. Within 1 km of a natural gas well, three type A, three type B, and five type D samples had methane concentrations >10 mg/L. In three type D groundwater samples that were located in the lowland valleys >1 km from shale gas drilling sites, methane concentrations were 2 to 4 mg/L for the two previously sampled shallow ground waters and 26 mg/L for the newly sampled salt spring. In contrast, type A groundwater >1 km away from drilling sites had methane concentrations less than 0.01 mg/L in all samples (n=14). This could suggest that methane in type D water >1 km away from drilling sites could be derived from natural seepage (Molofsky et al., 2011), but at concentrations much lower than those observed near drilling (Osborn et al., 2011a).

Cross-formational pathways allowing deeper saline water to migrate into shallower, fresher aquifers have been documented in numerous studies, including

western Texas(Hogan et al., 2007; Mehta et al., 2000a), Michigan Basin (Long et al., 1988; Weaver et al., 1995), Jordan Rift Valley (Farber et al., 2004), Appalachian Basin (Saunders and Swann, 1990), and Alberta, Canada (Eltschlager et al., 2001). In the Michigan Basin, upward migration of saline fluid into the overlying glacial (Long et al., 1988; Weaver et al., 1995) sediments was interpreted to reflect isostatic rebound following the retreat of glaciers, leading to fracture intensification and increased permeability (Weaver et al., 1995). The dynamics and rate of this brine migration was suggested to be of a recent geological time scale (Mehta et al., 2000b). Alternatively, vertical migration of over-pressured hydrocarbons has been proposed for the Appalachian Basin in response to tectonic deformation and catagenesis (i.e. natural gas induced fracturing) during the Alleghenian Orogeny (Engelder, 2009; Lash and Blood, 2007; Lash and Engelder, 2009). This deformation resulted in joints that cut across formations (J_2) in Middle and Upper Devonian formations (Engelder, 2009). In addition, the lithostatic and isostatic rebound following glacial retreat significantly increased fracture intensification and permeability in the Upper Devonian aquifers within our study area.

We hypothesize that regions with the combination of deep high hydrodynamic pressure and enhanced natural flowpaths (i.e., fracture zones) (Engelder, 2009; Jacobi, 2002; Llewellyn, 2011) could induce steep hydraulic gradients and allow the flow of deeper fluids to zones of lower hydrodynamic pressure (Harrison, 1983, 1985). The higher frequency of the saline type D water occurrence in valleys (Table 1) is consistent

with hydrogeological modeling of regional discharge to lower hydrodynamic pressure in the valleys with greater connectivity to the deep subsurface (Harrison, 1983, 1985; Tóth, 1970).

The possibility of drilling and hydraulic fracturing causing rapid flow of brine to shallow groundwater in lower hydrodynamic pressure zones is unlikely but still unknown. By contrast, the time scale for fugitive gas contamination of shallow aquifers can be decoupled from natural brine movement, specifically when gas concentrations exceed solubility (~30cc/kg) and forms mobile free phase gases (i.e. bubbles). In western PA, on the Appalachian Plateau, contamination of shallow aquifers has been described as leakage of highly pressurized gas through the over-pressurized annulus of gas wells and into the overlying freshwater aquifers via fractures and faults (Harrison, 1983, 1985). The faults are often connected to local and regional discharge areas (i.e., valleys) where the methane contamination is observed (Harrison, 1983). Buoyant flow of methane gas bubbles through these fractures is far more rapid than head-driven flow of dense brine, occurring on time scales of less than a year (Etiope and Klusman, 2002).

This study shows that some areas of elevated salinity with type D composition in NE PA were present prior to shale-gas development and most likely are unrelated to the most recent shale gas drilling. However, the coincidence of elevated salinity in shallow groundwater with a geochemical signature similar to produced water from the Marcellus Formation suggest that these areas could be at a greater risk of contamination

from shale-gas development because of a pre-existing network of cross-formational pathways that has enhanced hydraulic connectivity to deeper geological formations (Harrison, 1983). Future research should focus on systematically monitoring these areas to test potential mechanisms of enhanced hydraulic connectivity to deeper formations, confirm the brine source, and determine the timescales for possible brine migration.

2. Geochemical and isotopic variations in shallow groundwater in areas of Fayetteville Shale development, north-central Arkansas

2.1 Introduction

The combined technological development of horizontal drilling and hydraulic fracturing has enabled the extraction of hydrocarbons from unconventional sources, such as organic-rich shales, and is reshaping the energy landscape of the United States (Kargbo et al., 2010; Kerr, 2010). Unconventional natural gas currently supplies ~20% of US domestic gas production and is projected to provide ~50% by 2035 (USEIA, 2010). Therefore, ensuring that unconventional natural gas resource development results in the minimal possible negative environmental impacts is vital, not only for domestic production within the U.S., but also for establishing guidance for worldwide development of shale gas resources. Recent work in the Marcellus Shale basin demonstrated a relation between methane levels in shallow groundwater and proximity of drinking water wells to shale-gas drilling sites in northeastern Pennsylvania,

suggesting contamination of shallow groundwater by stray gas (Osborn et al., 2011a). In addition, previous study has shown evidence for natural pathways from deep formations to shallow aquifers in northeastern Pennsylvania that may allow leakage of gas or brine, and might pose a potential threat to groundwater in areas of shale gas extraction (USGS, 2013). While previous studies have focused on the Pennsylvania and New York portion of the northern Appalachian Basin, many other shale-gas basins currently are being developed that have not been examined for potential effects on water quality. One of the critical aspects of potential contamination of shallow aquifers in areas with shale-gas development is the hydraulic connectivity between shale and other deep formations and overlying shallow drinking water aquifers. Here we investigate the quality and geochemistry of shallow groundwater directly overlying the Fayetteville Shale (FS) in north-central Arkansas. The Fayetteville Shale is an unconventional natural gas reservoir with an estimated total production of 906 billion cubic meters (EIA, 2011), where approximately 4,000 shale-gas wells have been drilled since 2004. This value includes vertical wells and also more recently horizontal shale-gas wells.

In this study, we analyzed water samples from 127 shallow domestic wells in the Hale, Bloyd, and Atoka formations in north-central Arkansas and six flowback/produced water samples from the underlying FS in an attempt to identify possible groundwater contamination. Five of the produced water samples were collected within 21 days of fracturing (i.e., defined as flowback water) and a single sample was

collected at about a year following hydraulic fracturing (i.e., defined as produced water). We analyzed the concentrations of major anions (Cl, SO_4, NO_3, Br, and dissolved inorganic carbon [DIC]), cations (Na, Ca, Mg, and Sr), trace elements (Li and B), and a smaller subset of samples for dissolved CH_4 and selected isotopic tracers ($\delta^{11}B$, $^{87}Sr/^{86}Sr$, $\delta^{2}H$, $\delta^{18}O$, $\delta^{13}C_{DIC}$, and $\delta^{13}C_{CH4}$). Using multiple geochemical and isotopic tracers together with their geospatial distribution provides a multidimensional approach to examine potential groundwater contamination in areas of shale gas development. We hypothesize that shallow groundwater could be contaminated by stray gas migration associated with poorly cemented gas wells, similar to the observations of previous studies (Osborn et al., 2011a). Shallow drinking water may also be contaminated with deeper saline fluids at the same time as the migration of stray gas associated with drilling. A third possibility would be natural migration and connectivity between the shallow drinking water and deep formations with higher salinity formation waters through faults or other more permeable pathways(Warner et al., 2012). This study is to our knowledge the first to report such a comprehensive geochemical evaluation of possible shallow groundwater contamination outside the Marcellus Shale basin (Osborn et al., 2011a; USGS, 2013).

2.2 Geologic Setting

The study area is located within the currently active development area for the FS in north-central Arkansas with the majority of samples collected in Van Buren County and the northern part of Faulkner County (Figure 13).

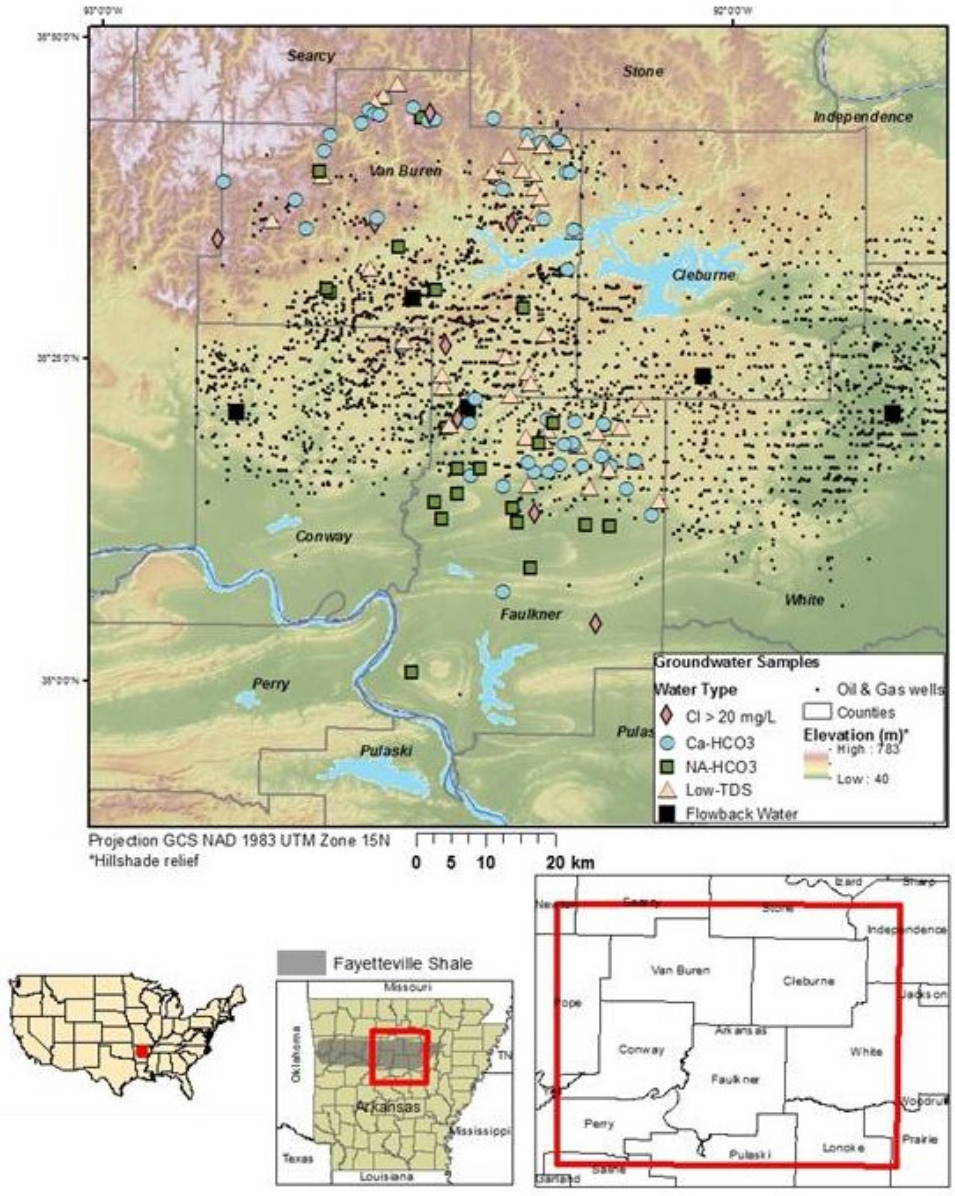

Figure 13: Study site location in north-central Arkansas. Unconventional shale-gas wells completed into the Fayetteville Shale are shown in black. Shallow groundwater samples were cataloged based on major element chemistry into four water categories: low-TDS (beige triangles), Ca-HCO_3 (blue circles), Na-HCO_3 (green squares), and Cl>20 mg/L (red diamonds).

The area is characterized by a rugged and mountainous landscape to the north and rolling hills to the south, spanning the southern area of the Ozark Mountains, to the northern Arkansas River valley (Imes and Emmett, 1994). The bedrock in the study area comprises the Pennsylvanian-age Hale, Bloyd, and Atoka formations, which are composed of shale with interbedded minor occurrences of relatively permeable sandstone, limestone, and coal (Cordova, 1963) (Figure 14).

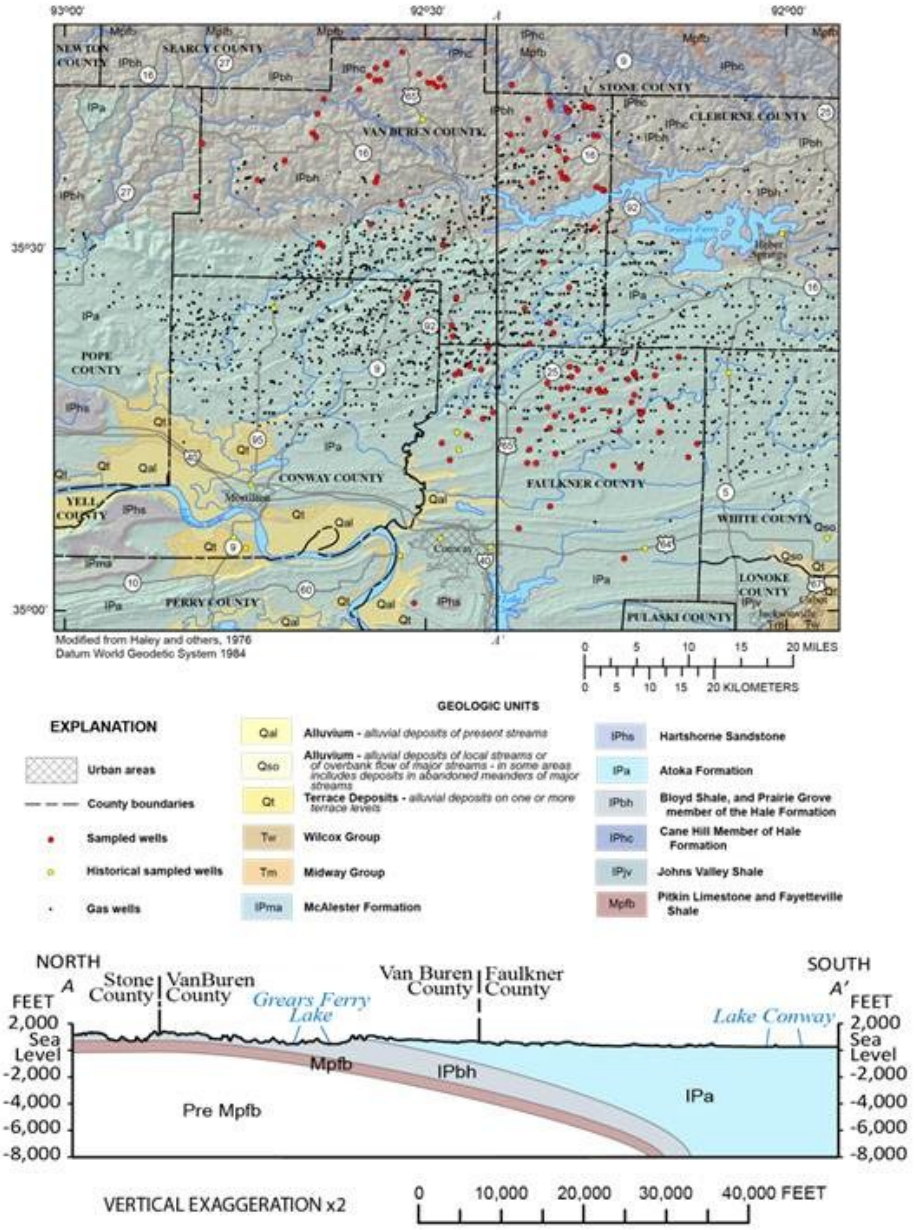

Figure 14: Map of sample location and bedrock geology in the study area of north-central Arkansas. The majority of samples were collected from the Atoka (southern area) and Hale Formations (northern area). North-to-south geological cross-section in the study area (A-A′ line is shown). Geological units gently dip to the south with the Atoka formation outcropping in the southern portion of the study area. The underlying Fayetteville shale shoals to the north.

The shale portion of the Atoka underlies the lowlands because its lack of resistance to weathering (Cordova, 1963) thin beds of coal are present throughout but limestone is only present in the north of the study area (Cordova, 1963). The Mississippian-age Fayetteville Shale is the target formation during drilling and lies approximately 500-2,100 meters below the ground surface (mgbs), with the southern portion of the study area being the deepest. These formations are part of the Western Interior Confining System with groundwater flow restricted to the weathered and fractured upper 100 m of bedrock (Imes and Emmett, 1994). No one formation within this confining system, even where representing a source of local water supply, forms a distinct aquifer regionally, and the regional designation as a confining unit indicates that on a regional scale these formations impede the vertical flow of water and confine the underlying aquifers. Domestic wells in the area typically provide limited groundwater yields (Imes and Emmett, 1994). The average reported drinking water well depth is 26 m and minimum and maximum of 7.8 m and 120 m, respectively. Wells drilled deeper than 100 m revealed much more compacted and less permeable section of the formations (Imes and Emmett, 1994).

The underlying Fayetteville Shale production zone is ~ 17 to 180 m thick and 500 m to 2,100 mbgs. The Fayetteville Shale production zone occupies an area of approximately 6,500 km^2; the area of groundwater samples for this study covered approximately 1/3 of the area of the production zone. The density of shale-gas drilling

varied widely across the study area. For our sample set of drinking water the total number of unconventional shale-gas wells within 1 km ranged from zero natural gas wells to over 14 natural gas wells within 1 km and represents an area of moderate to intense unconventional shale-gas development, similar to other areas of extensive shale gas developments, such as NE Pennsylvania (Osborn et al., 2011a). Importantly the Fayetteville Shale is the first oil and gas development in this study area, and we did not find records that indicated the presence of historical conventional wells, which may provide possible conduits for vertical migration of stray gas and/or hydraulic fracturing fluids. Saline water unsuitable for human consumption was identified between 150 to 600 mbgs but generally is 300 mbgs in the study area (Imes and Emmett, 1994).

The exposed and shallow subsurface geologic formations serving as local aquifers for Van Buren and Faulkner Counties are a series of dominantly sandstone and shale units of the Hale, Bloyd, and Atoka Formations (Figure 14). Subsurface geology, particularly with respect to lateral facies within the Fayetteville Shale, was poorly defined prior to development of gas and most of the detailed stratigraphic and reservoir analysis were held as proprietary by a few companies.

The Fayetteville Shale is a black, fissile, concretionary shale, which contains pyrite and silica replacement fossils in some intervals. The Fayetteville Shale formation dips from north to south (Figure 14). The highly organic-rich facies within the Fayetteville Shale is present in the middle and lower part of the formation. Vitrinite

reflectance falls within 1.93 to 5.09 percent, which corresponds to the dry gas window (Imes and Emmett, 1994).

The Hale Formation is made up of two members; the lower is the Cane Hill Member, which is typically composed of silty shale interbedded with siltstone and thin-bedded, fine-grained sandstone. The upper is the Prairie Grove Member, which is composed of thin to massive limey sandstone. The Hale Formation thickness is up to 90 m (Imes and Emmett, 1994). The Cane Hill Member of the Hale Formation is exposed in the extreme northern part of Van Buren County (Figure 14).

The Bloyd Formation in northwestern Arkansas is formally divided into five members, two of which are limestone members absent in the study area. The lower two thirds of the Bloyd Formation consists dominantly of very thin- to thinly-bedded sandstone with shale interbeds. The upper Bloyd is dominantly a shale with interbedded sandstone that is commonly calcareous; the sandstone units can reach a thickness of up to 24 m (Imes and Emmett, 1994). Total thickness for the Bloyd can exceed 120 m in the study area. Exposures of the Bloyd Formation are found in northern Van Buren County (Figure 14).

The Atoka Formation in the study area consists of a sequence of thick shales that are interbedded with typically thin-bedded, very-fine grained sandstone. The Atoka Formation is unconformable with the underlying Bloyd Formation with a thickness of

up to 7,500 m in the Ouachita Mountains (Imes and Emmett, 1994). The Atoka Formation is exposed throughout the southern portion of the study area (Figure 14).

2.3 Materials and Methods

All shallow groundwater samples from homes were collected by USGS personnel in July and November 2011. Methods for collection of field parameters (pH, temperature, and specific conductance) and water sampling followed standard USGS protocols (Wilde, 2006) and included purging water wells until field parameters stabilized, followed by 0.45 micron water filtering on site for water samples collected for trace and major ion analyses. Dissolved gas sample collection followed Isotech Laboratories, Inc. methods (Isotech Laboratories, Inc., 2012). Samples of FS water were collected from production wells (flowback or produced waters) by Arkansas Oil and Gas Commission personnel.. Samples were labeled flowback waters if collected within 3 weeks of hydraulic fracturing (5 total samples) and produced water if collected more than 3 weeks after fracturing (1 sample; ~ 50 weeks following fracturing). All water samples were preserved on ice and shipped to Duke University (Durham, North Carolina, USA), where they were refrigerated until analysis.

Samples for major cations, anions, trace metals and selected isotopes (oxygen, hydrogen, boron, strontium, and carbon-DIC) were analyzed at Duke University. Isotech Laboratories performed dissolved gas analysis for concentrations of methane and higher-chain hydrocarbons on twenty samples using chromatographic separation

followed by combustion and dual-inlet isotope ratio mass spectrometry to measure $\delta^{13}C_{CH4}$.

Dissolved methane concentrations and $\delta^{13}C\text{-}CH_4$ were determined by cavity ring-down spectroscopy (CRDS)(Busch and Busch, 1997) on an additional 31 samples at the Duke Environmental stable Isotope Laboratory (DEVIL) using a Picarro G2112i. Dissolved methane concentrations were calculated using a head-space equilibration method (Kampbell and Vandegrift, 1998). Headspace equilibrations and extractions and concentration calculations were performed by a modification of the method of Kampbell and Vandegrift (1998). For each 1L sample bottle, 100 mL of headspace was generated by displacing water with zero air (methane-free air) injected with gastight syringes equipped with luer-lock valves. Bottles were shaken at 300 rpm for 30 minutes to equilibrate headspace with dissolved methane. The equilibrated headspace was then extracted with gastight syringes while compensating volume with deionized water from plastic syringes. The extracted headspace was then injected into tedlar bags (Environmental Supply, Durham, NC) equipped with septum valves and introduced into the Picarro model G2112-i CRDS (Picarro, Inc, Santa Clara, CA). In some cases, dilution into a second tedlar bag with zero-air was required to keep the measured concentration in the optimal range for the instrument. Concentrations were corrected for volumetric and Henry's Law effects using the equations reported in (Kampbell and Vandegrift, 1998). Calculated detection limits of dissolved methane were 0.002 mg/L

water. Reporting limits for reliable $\delta^{13}C\text{-}CH_4$ were 0.1 mg/L, consistent with Isotech Laboratories (Illinois, USA) reporting values. Concentrations and $\delta^{13}C$ values were also corrected for instrument calibrations using known methane standards from Airgas (Durham, NC) and Isometric Instruments (Victoria, BC).

To confirm the accuracy of the CRDS results, a set of 49 field duplicate groundwater samples was collected analyzed at Isotech. These groundwater samples were collected from North Carolina, New York, Pennsylvania, and Arkansas in order to span a wider range of both concentrations (<0.002 mg/L through values well above saturation ~100 mg/L) and carbon isotope values (-30‰ through -75‰). The comparison of the field duplicates using these two independent methods showed good correlation for concentration (r^2=0.90; Figure 15a) and excellent agreement for $\delta^{13}C_{CH4}$ (r^2=0.95; Figure 15b). Relative standard deviation of dissolved methane concentrations determined by CRDS on field duplicates was 9.8%. Standard deviation of $\delta^{13}C$ measurements determined by CRDS for 8 field duplicate samples ranged from a minimum of 0.07‰ to a maximum of 1.0‰ with a mean 0.55‰, resulting in a relative standard deviation of 1.7%.

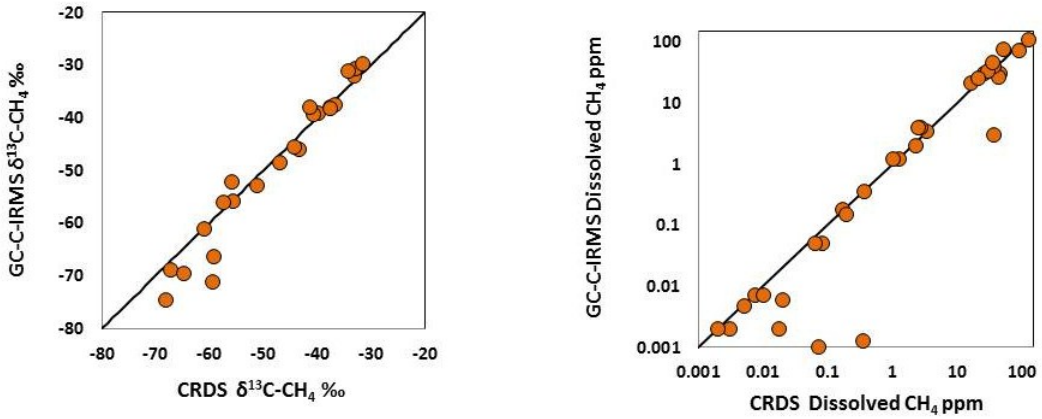

Figure 15: Comparison of results for duplicate samples submitted to a private laboratory (Isotech) to those performed using a cavity-ring-spectroscopy (CRDS) analyzer at Duke University for both dissolved methane concentrations and $\delta^{13}C\text{-}CH_4$. Dissolved methane concentrations from the two independent methods showed a good correlation ($r^2=0.90$, $p<1x10^{-15}$) with some variability at higher concentrations. The comparison of the $\delta^{13}C\text{-}CH_4$ values obtained from the two analytical techniques showed a strong correlation ($r^2=0.95$, $p<1x10^{-15}$). The CRDS methodology showed some bias at lower $\delta^{13}C\text{-}CH_4$ compared to the private laboratory. Note that this comparison includes samples from other study areas to cover a wide range of concentrations and $\delta^{13}C\text{-}CH_4$ values.

Major anions were determined by ion chromatography, major cations by direct current plasma optical emission spectrometry (DCP-OES), and trace-metals by VG PlasmaQuad-3 inductively coupled plasma mass-spectrometer (ICP-MS). Four replicate samples showed good reproducibility for both major and trace element concentrations (Online Supplement). Strontium and boron isotopes were analyzed by thermal ionization mass spectrometer (TIMS) on a ThermoFisher Triton at the TIMS lab in Duke University. The average $^{87}Sr/^{86}Sr$ of the SRM-987 standard measured during this study was 0.710266 +/-0.000005 (SD). The average $^{11}B/^{10}B$ of NIST SRM-951 during this study was 4.0055 +/- 0.0015. The long-term standard deviation of $\delta^{11}B$ in the standard and

seawater replicate measurements was 0.5‰. DIC concentrations were determined in duplicate by titration with HCl to pH 4.5. Values of $\delta^{18}O$ and $\delta^{2}H$ were determined by thermochemical elemental analysis/continuous flow isotope ratio mass spectrometry (TCEA-CFIRMS), using a ThermoFinnigan TCEA and Delta+XL mass spectrometer at the Duke Environmental Isotope Laboratory (DEVIL). $\delta^{18}O$ and $\delta^{2}H$ values were normalized to V-SMOW and V-SLAP. The carbon isotope ratio of dissolved inorganic carbon was analyzed by acid digestion on a ThermoFinnigan (Bremen, Germany) GasBench II feeding a ThermoFinnigan Delta+XL Isotope Ratio Mass Spectrometer (IRMS) in the DEVIL lab. Several mL (volume depending on DIC concentration) of each sample were injected into 11 mL septum vials that had each been pre-dosed with 150 micro-liter (uL) phosphoric acid and pre-flushed 10 minutes with helium at 50 mL/min to remove air background. Raw $\delta^{13}C$ of resulting CO_2 was normalized vs Vienna Pee Dee Belemnite (VPDB) using NBS19, IAEA CO-8 standards, and an internal $CaCO_3$ standard.

Natural gas well locations were obtained from the Arkansas Oil and Gas Commission database. Arkansas Oil and Gas Commission also provided ^{228}Ra and ^{226}Ra values. Historical water data were gathered from the USGS National Water Information System (NWIS) data base for the six counties that comprise the bulk of permitted and active gas production wells: Cleburne, Conway, Faulkner, Independence, Van Buren, and White Counties (Figure 14). The data set includes 43 groundwater samples collected near the study area prior to shale-gas development 1948 and 1983.

2.4 Results and Discussion

2.4.1 Geochemical characterization of the shallow groundwater

We divided the 127 shallow groundwater samples into four major water categories (Figure 13 and Online Supplement). The first category was low-TDS (<100 mg/L) and generally low-pH (pH<6.6; n=54) water. The second was a Ca-HCO_3 water (n=40), with moderate TDS (100>TDS<200 mg/L). The third was a Na-HCO_3 water with a wider range of TDS (100>TDS<415 mg/L; n=24). The fourth group was classified as Ca-Na-HCO_3 water type with the highest TDS (200>TDS<487 mg/L) and slightly elevated Cl (>20 mg/L) and Br/Cl molar ratios> $1x10^{-3}$ (n=9). The fourth group was identified because the elevated Cl and Br/Cl could potentially indicate contamination from the underlying saline formation water (see description below).

The carbon isotope ratio of dissolved inorganic carbon ($\delta^{13}C_{DIC}$; n= 81 samples) ranged from -22‰ to -10‰ (Online Supplement). The low-TDS and Ca-HCO_3 water types had lower DIC concentrations but all water types had similar $\delta^{13}C_{DIC}$, while most water samples fell within a narrower and lower range of -20‰ to -17‰. In the Na-HCO_3 groundwater we observed a positive correlation between DIC concentrations and $\delta^{13}C_{DIC}$ values (r^2=0.49, $p<0.05$; Figure 16).

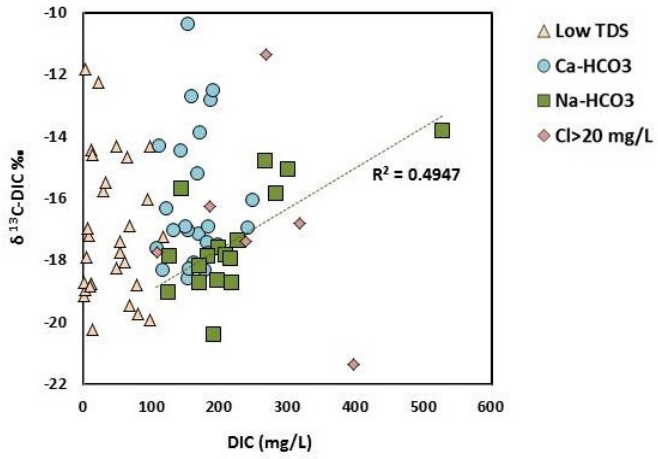

Figure 16: δ^{13}C-DIC (‰) and DIC (mg/L) in shallow groundwater samples. The average δ^{13}C-DIC (-17‰ to -20‰) in the bulk groundwater indicates the majority of DIC is derived from weathering of silicate minerals that would approach -22‰. Methanogens in some of the Na-HCO_3 waters would generate DIC with elevated residual δ^{13}C-DIC (green arrow).

The strontium isotope ratios ($^{87}Sr/^{86}Sr$) vary from 0.7097 to 0.7166 (Figure 17a). Most of the Ca-HCO_3 waters have slightly lower $^{87}Sr/^{86}Sr$ (mean =0.71259; n=12) relative to the Na-HCO_3 waters (mean =0.71543; n=13). Boron isotope ratios ($\textcircled{o}^{11}B$) show a wide range from 4‰ to 33‰, with a general increase of $\textcircled{o}^{11}B$ with boron content (Figure 17b) with no systematic distinction between the water types ($p>0.05$).

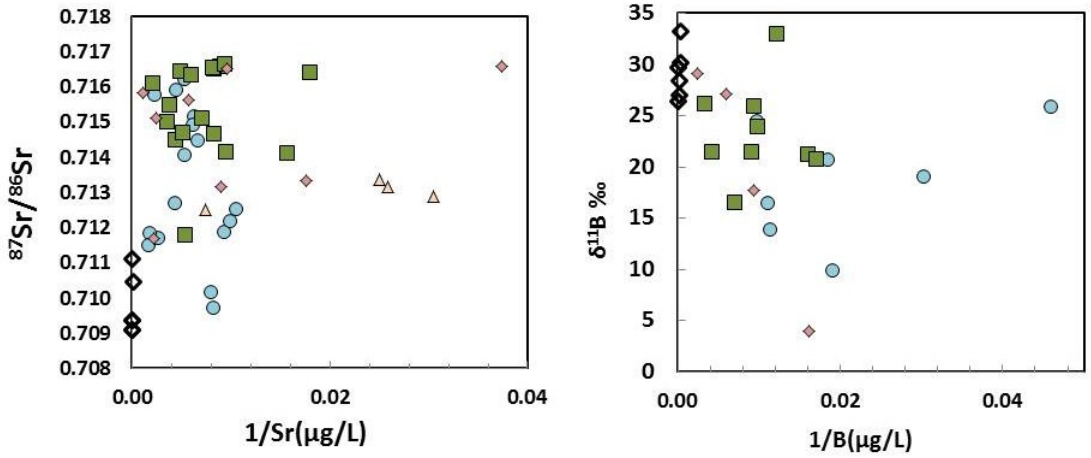

Figure 17: $^{87}Sr/^{86}Sr$ versus 1/Sr concentration (µg/L) and $\delta^{11}B$‰ versus 1/ Boron concentration (µg/L). Mixing relationships would appear as straight lines in both graphs, however the lack of strong linear strontium and boron isotopic variations exclude possible mixing between the Fayetteville Shale water and the shallow groundwater. Instead the isotopic variations appear to be controlled by weathering and water-rock interactions. Note that Cl> 20mg/L samples with less than 60 ug/L boron were not able to be analyzed for $\delta^{11}B$‰ because of inadequate sample volume.

The stable isotope composition of all water types did not show any distinctions ($p>0.05$) related to the water composition (Online Supplement) and $\delta^{18}O$ and $\delta^{2}H$ variations are consistent with the Local Meteoric Water Line (LMWL) (Kendall and Coplan, 2001) of modern precipitation in the region. This similarly suggests a common meteoric origin, and also indicates that all of the geochemical modifications presented below were induced from water-rock interactions along groundwater flowpath in the shallow aquifers.

Historical groundwater quality data from in or near the study area from the NWIS data base (Figure 14) includes 43 samples collected prior to shale-gas development between 1948 and 1983 (Online Supplement). Although collected from the

same formations, the majority of historical samples were collected to the east and only three sampling sites overlap with our study area (Figure 14) and therefore a complete statistical comparison to historical data was not possible. However, the reported chemical composition of the water samples collected prior to shale gas development in the area is consistent with the Ca-HCO_3 and Na-HCO_3 water types, with a predominance of Na-HCO_3 water type in the Atoka formation (Figure 14) as reported in previous studies (Cordova, 1963; Imes and Emmett, 1994). Likewise, the range of concentrations in this study fell within the minimum and maximum reported values in the NWIS (Online Supplement).

2.4.2 Methane sources in shallow groundwater

Dissolved methane concentration and carbon isotope ratios of methane ($\delta^{13}C_{CH4}$) were analyzed in 51 of the 127 water samples from wells collected for this study (Online Supplement). Methane was detected (>0.002 mg/L) in 63% of wells (32 of the 51), but only six wells had concentrations >0.5 mg CH_4/L, with a single sample point (28.5 mg/L) above the potential recommended action level 10 mg/L in the United States (Eltschlager et al., 2001) (Figure 18).

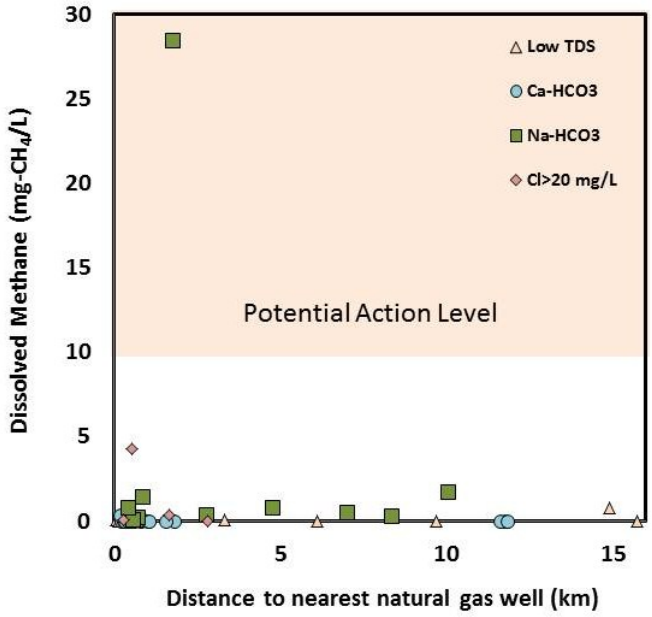

Figure 18: Dissolved methane concentrations (mg/L) in domestic wells plotted versus distance of the domestic wells to nearest natural gas well. Only one of 51 wells analyzed contained methane at concentrations above the potential action level set by the Department of Interior (10 mg/L). There is no statistically significant difference in dissolved methane concentrations from wells collected within 1 km of a gas well and those collected >1 km from a well. The highest dissolved methane concentrations were detected in Na-HCO_3 water.

Dissolved methane concentrations were not higher closer to shale gas wells (Online Supplement and Figure 18), nor was any statistical difference (student t-test) apparent between concentrations in groundwater of 32 wells collected within 1 km of shale-gas production and 19 wells >1km away from gas wells ($p > 0.1$; Online Supplement).

The $\delta^{13}C_{CH4}$ ranged from -42.3‰ to -74.7‰ (Figure 19), but the range in $\delta^{13}C_{CH4}$ in the six samples with concentrations greater than 0.5 mg/L was systematically ($p<0.01$) lower (-57.6‰ to -74.7‰), which provides evidence for a more biogenic origin of the

dissolved gas (i.e., <-55‰) (Coleman et al., 1981). The $\delta^{13}C_{CH4}$ of 13 out of 14 samples did not overlap the reported values (Zumberge et al., 2012) for Fayetteville Shale production gas (Figure 19).

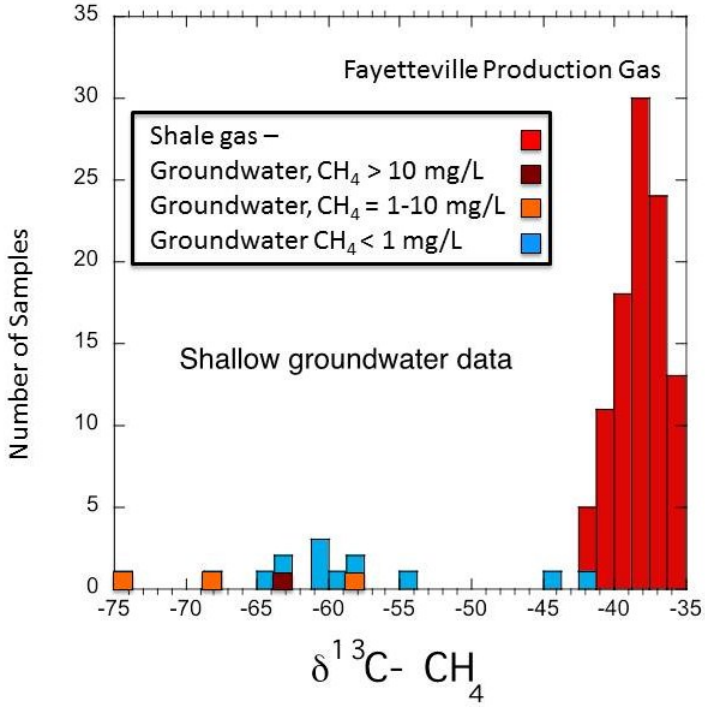

Figure 19: $\delta^{13}C$-CH_4 (‰) values of dissolved methane plotted in comparison to published values for Fayetteville Shale produced gas $\delta^{13}C$-CH_4 (‰)(Zumberge et al., 2012). Concentrations of the dissolved methane in shallow groundwater are indicated by color. The majority of samples, including all of those at higher CH_4 concentrations plot at lower $\delta^{13}C$-CH_4 values indicating that shallow biogenic origin likely contribute to the formation of methane. The lone sample that overlaps with Fayetteville Shale values may represent migration of stray production gas, but at very low concentrations.

The only one sample with a $\delta^{13}C_{CH4}$ value (-42.3‰) that approaches the values reported for shale gas well had low methane content (0.15 mg/L). Samples with trace (<0.5 mg/L) methane concentrations and $\delta^{13}C_{CH4}$ values between -42 and -60‰ could

reflect either flux of deep-source thermogenic gas (Schoell, 1980) or a mixture of biogenic and thermogenic gas. The sample with the highest $\delta^{13}C_{CH4}$ value (-42.3‰) had low chloride concentration (2 mg/L). The combined low chloride and methane rules out possible contamination from underlying fluids (gas and water) (see discussion below). Further evidence for a biogenic origin of methane in the shallow groundwater is provided by the lack of detectable higher chain hydrocarbons (C_2<0.0005 mol%) in the 20 samples analyzed at the commercial laboratory (C_2+ was detected in only 1 of 20 samples analyzed). The single detection of a higher chain hydrocarbon (C_2=0.0277 mol%) was in a sample with a higher C_1/C_2+ ratio= (C_1/C_2=730) consistent within the expected biogenic range (~1,000) (Boschetti et al.; Coleman et al., 1981; Ferrar et al., 2013) or biogenic mixed with a small portion of thermogenic gas (Online Supplement). The distribution of dissolved methane concentrations and $\delta^{13}C_{CH4}$ values (Figure 20a) suggest a local, shallow origin of dissolved methane unrelated to shale-gas extraction in the vast majority of

samples.

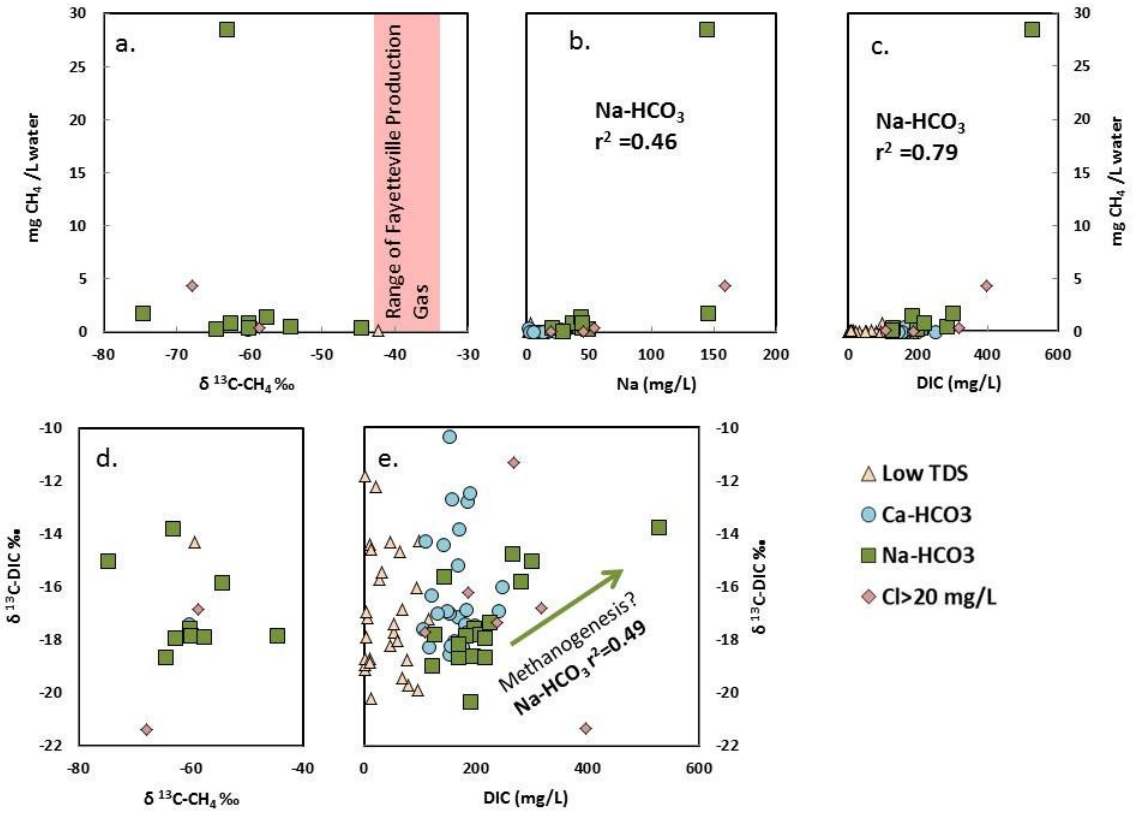

Figure 20: Dissolved methane (mg/L) versus δ^{13}C-CH_4 (‰)(8a), Na (mg/L)(8b) δ^{13}C-DIC (‰)(8c), and DIC (mg/L) (8d), in shallow groundwater samples. The correlations observed between methane and Na (r^2=0.46) and DIC (r^2=0.79) indicate that the highest methane is found in Na-HCO_3 groundwater. At the higher DIC and CH_4 concentrations the depleted δ^{13}C-CH_4 indicates that methanogens [19] likely contribute to the formation of methane. δ^{13}C-DIC versus δ^{13}C-CH_4(‰)(8e) and DIC (mg/L)(8f) in shallow groundwater. The average δ^{13}C-DIC (-17‰ to -20‰) in the bulk groundwater indicates the majority of DIC is derived from weathering of silicate minerals that would approach -22‰. Methanogens in some of the Na-HCO_3 waters would generate DIC with elevated residual δ^{13}C-DIC (green arrow).

If the methane was sourced from biogenic processes within the shallow aquifers, the ground water chemistry could provide further support for its biogenic origin

(Aravena et al., 1995; NYDEC, 1999). Median dissolved CH_4 concentrations were highest in the Na-HCO_3 water type, with positive correlations to Na and DIC (r^2=0.46 and 0.79, respectively; Figure 20b and 20d). In addition, the positive correlation between DIC concentrations and $\delta^{13}C_{DIC}$ values (r^2=0.49, $p<0.05$; Figure 20f) could suggest that methanogenesis is occurring within the formations, perhaps within the minor coal beds (Imes and Emmett, 1994) under reduced conditions. If the minor concentrations of observed methane were sourced from microbial CO_2 reduction, we would expect generation of $\delta^{13}C_{CH4}$ of -70‰ to -80‰ (LaZerte, 1981; Renner, 2009) parallel to elevated residual $\delta^{13}C_{DIC}$ (e.g., >+10‰) during methane production (Aravena and Wassenaar, 1993; Whiticar et al., 1986). However, in our study the majority of the $\delta^{13}C_{DIC}$ values are significantly lower (-20‰ to -17‰), demonstrating that methanogens are not the main source of DIC in the aquifer. In the low TDS water only trace levels (CH_4<0.8 mg/L) of dissolved methane were recorded (n=9) and only two low-TDS samples had detectable higher $\delta^{13}C_{CH4}$ (-42.3 and -59.6‰). These values could indicate either a minor presence of thermogenic gas in the shallow aquifers (Renner, 2009) or bacterial oxidation (Coleman et al., 1981).

2.4.3 Water-rock interactions and mixing with external fluids

The geochemical variations from low TDS, Ca-HCO_3, and Na-HCO_3 water types infer different modes of water-rock interactions. The low-TDS waters could reflect early stage of groundwater recharge without much mineralization induced from water-rock

interactions, while the Ca-HCO_3 waters suggest dissolution of carbonate minerals in the aquifers. A Na-HCO_3 water type typically (e.g.(NYDEC, 1999) indicates silicate weathering and ion exchange processes (e.g., reverse base-exchange reaction). In the majority of the shallow groundwater samples, regardless of the water type, DIC nearly balances the sum of sodium, calcium, and magnesium concentrations (in equivalent units; Figure 21).

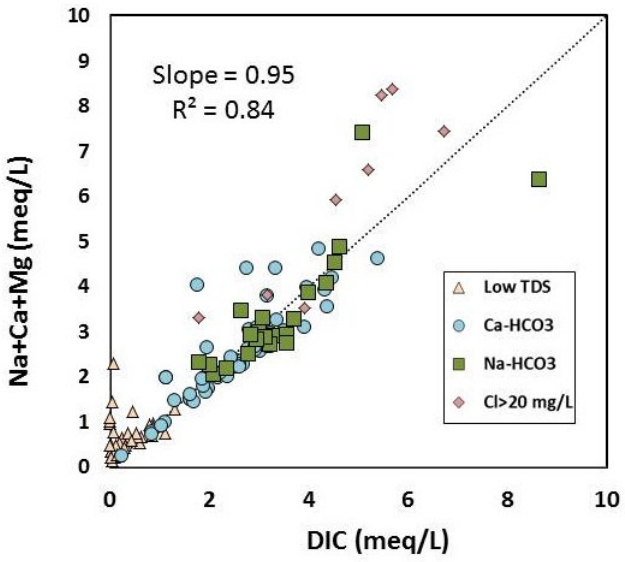

Figure 21: The sum of Na, Ca and Mg (meq/L) versus dissolved inorganic carbon (DIC; meq/L) in shallow groundwater samples. Note that DIC balances the majority of the total cations in shallow groundwater samples across all water types.

DIC could be generated in the shallow aquifers by either weathering of silicate minerals in the shale, dissolution of marine carbonate by carbonic acid produced through oxidation of organic matter, or bacterial sulfate reduction. Silicate weathering would mobilize Na, Ca, Mg, and Sr with a radiogenic $^{87}Sr/^{86}Sr$ signature (Bullen et al.,

1996) and boron with a wide $\delta^{11}B$ range from 0‰, which would characterize structural boron in silicate minerals (Lemarchand and Gaillardet, 2006) to 15-20‰ in "desorbable" boron on marine clay surfaces (Spivack and Edmond, 1987). The $\delta^{13}C_{DIC}$ value would reflect the isotopic fractionation between DIC species and expect to be similar to the composition of the carbonic acid that triggered the silicate weathering (~-22‰). If, instead, dissolution of marine carbonate minerals was occurring, one would expect contributions of Ca, Mg, and Sr with a low $^{87}Sr/^{86}Sr$ (~0.7082) for the Pennsylvanian-age marine formation (Busch and Busch, 1997), and boron with $\delta^{11}B$ of a marine carbonate signature (~20‰) (Vengosh et al., 1991). Dissolution of marine carbonate would generate HCO_3^- with $\delta^{13}C_{DIC}$ ~-11‰, assuming a closed system with equal proportions of marine calcite dissolution ($\delta^{13}C_{DIC}$ ~0‰) and carbonic acid ($\delta^{13}C_{DIC}$ ~-22‰), and that all DIC-bearing species would be in isotopic equilibrium (Bullen et al., 1996). Carbonate dissolution could contribute Ca that would be exchanged with Na from exchange sites on clay minerals, resulting in Na-HCO_3 water. In such a scenario, the Ca concentrations would be inversely correlated with that of Na.

Examining all of these geochemical and isotopic constraints, we clearly show that neither of these two mechanisms (i.e., silicate weathering versus marine carbonate dissolution combined with base-exchange reaction) is explicitly consistent with the geochemical variations measured in the shallow groundwater in this study. For example, in most of the groundwater samples, including those defined as the Na-HCO_3

type, Na is positively correlated with Ca, indicating contribution of both elements that would reflect silicate weathering. In contrast, the most DIC-rich (Figure 22a) waters show an inverse relationship between Na and Ca (Figure 22b) that typically mimics reverse base-exchange reactions.

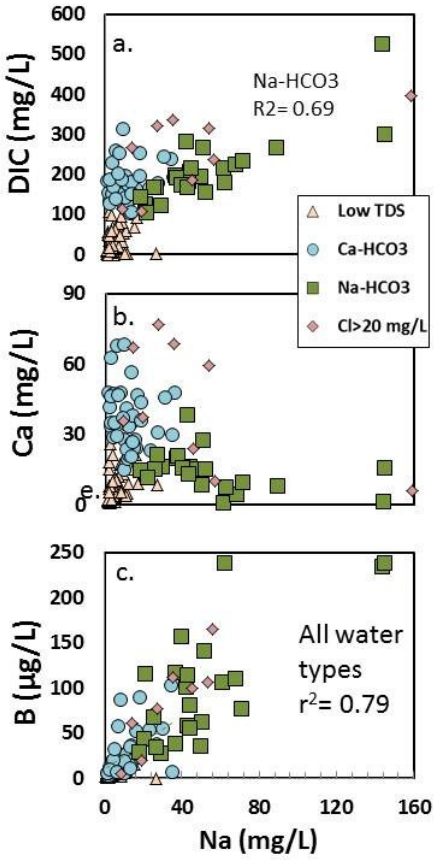

Figure 22: The DIC, Ca and boron concentrations versus Na in shallow groundwater samples.

Likewise, all of the water types show a positive correlation (r^2=0.79) between Na and boron (Figure 22c), a combination that could reflect mobilization from exchangeable sites on clay minerals. The most DIC-rich waters have a lower Ca/Na ratio and lower Na

relative to B (Figure 22c), inferring a different source. The $\delta^{11}B$ of the Na-HCO_3 waters (range of 16.5‰ to 33‰; Figure 17b) are also consistent with boron sourced from exchangeable sites on marine clay minerals.

In contrast, relatively low $\delta^{13}C_{DIC}$ (-20‰ to -17‰) (Online Supplement) and radiogenic $^{87}Sr/^{86}Sr$ ratios (0.7097 to 0.7166) (Figure 17a) in the majority of the studied groundwater rule out the possibility that marine carbonate dissolution is the major process that controls the generation of Ca-HCO_3 water. Nonetheless, given the shale in the study area is carbonate-rich (Imes and Emmett, 1994), carbonate dissolution likely contributes Ca and HCO_3, in which Ca would be exchanged with Na to generate Na-HCO_3 water. Reverse base-exchange reaction would remove Ca and Sr, and thus the uptake of Sr is not expected to modify its original isotopic ratio (i.e., $^{87}Sr/^{86}Sr$ ratio of the Pennsylvanian-age marine carbonate). One possible explanation for the high $^{87}Sr/^{86}Sr$ ratio is that the carbonate in the shale was diagenetically-modified from bacterial sulfate reduction process with modified fluids containing radiogenic $^{87}Sr/^{86}Sr$ and depleted $\delta^{13}C_{DIC}$ relative to the original composition of the marine carbonates. Given that the groundwater has a radiogenic $^{87}Sr/^{86}Sr$ ratio (0.7097 to 0.7166) that is similar to the composition of the local shale formations (Kresse and Hays, 2009), we conclude that the water chemistry was controlled by *both* silicate minerals weathering and dissolution by diagenically modified carbonate cement followed by ion-exchange reactions. Further study is needed to characterize the composition of the carbonate cement and delineate

the specific mechanism that has caused evolution of the groundwater into Na-HCO_3 composition.

The fourth shallow groundwater type, the higher-chloride waters, shows a high correlation between Cl and Br (r^2=0.89; Figure 23a) with a high Br/Cl ratio (>$1x10^{-3}$) that is similar to the elevated Br/Cl in the FS brine (see below). This geochemical composition could be interpreted as mixing of shallow groundwater with underlying formation water, similar to the salinization phenomena observed in NE Pennsylvania (USGS, 2013). However, the variations of other dissolved constituents such as boron and strontium are not correlated with chloride (Figure 23f-23h), and their isotopic ratios, including $^{87}Sr/^{86}Sr$ (Figure 17a), $\delta^{13}C_{DIC}$ (Figure 16), and the majority of $\delta^{11}B$ (Figure 17b) are distinctly different from expected mixing relations with the FS brines (Online Supplement). This infers that the composition of the groundwater with (Cl> 20mg/L) was modified by weathering and water-rock interaction and our ability to delineate the exact saline end-member that generated the saline groundwater is limited.

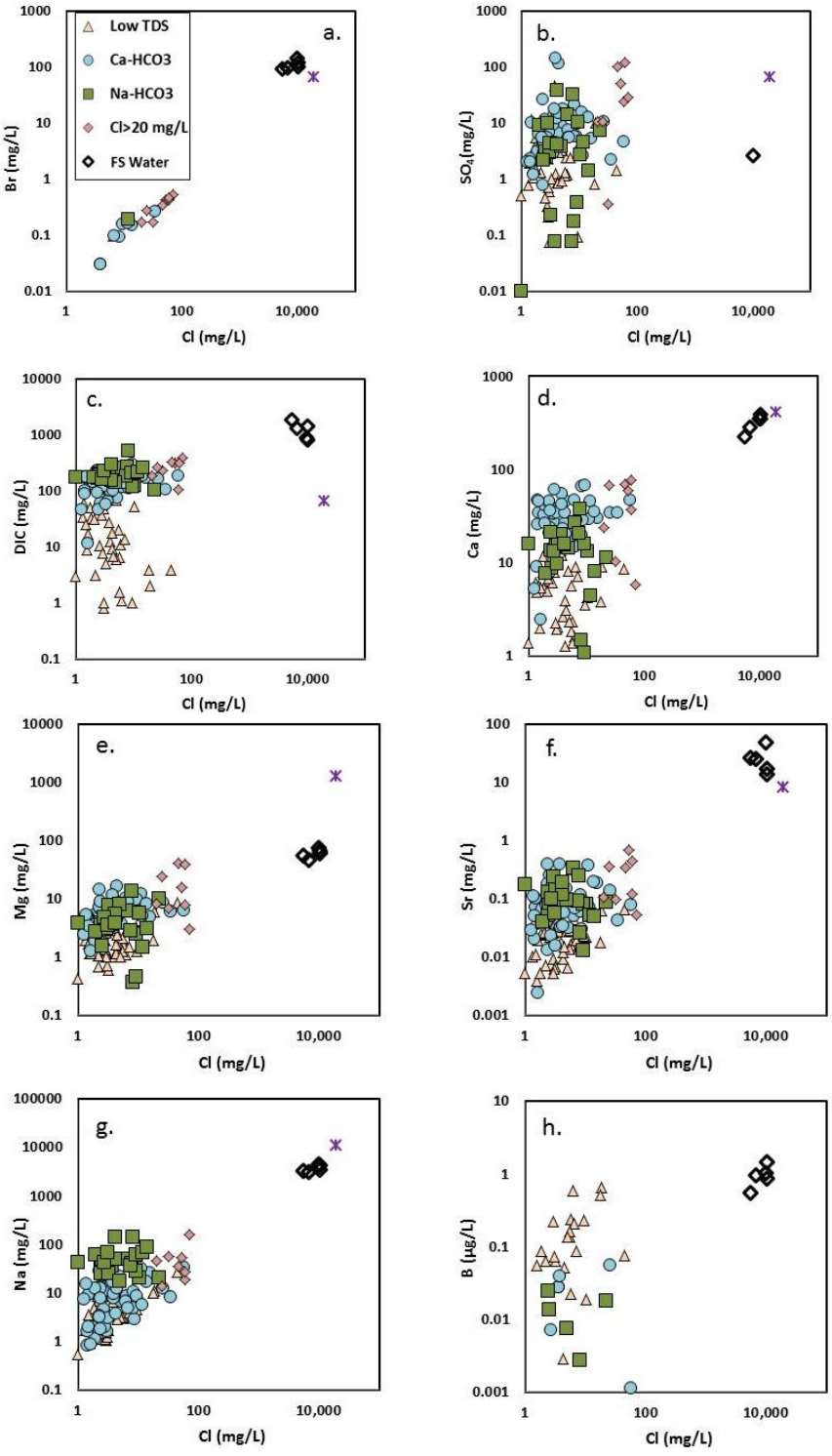
a.
Low TDS
Ca-HCO3
Na-HCO3
Cl>20 mg/L
FS Water
Br (mg/L)
Cl (mg/L)
b.
SO4 (mg/L)
c.
DIC (mg/L)
d.
Ca (mg/L)
e.
Mg (mg/L)
f.
Sr (mg/L)
g.
Na (mg/L)
h.
B (µg/L)
1
100
10,000

Figure 23: The variations of major elements as normalized to chloride contents in shallow groundwater and the FS saline water. The composition of the FS water infers modified seawater through evaporation and halite precipitation (high Br/Cl ratio), water-rock interactions (enrichment of Na, Sr, Mg, and Ca relative to the expected evaporated seawater curve), followed by dilution with meteoric water. Note that there is no apparent relationship between concentrations of constituents in shallow groundwater and the deeper FS waters. Variations of DIC (mg/L), chloride (mg/L), Ca and Na in Fayetteville Shale (FS) flowback and produced waters. The negative correlation between Cl and DIC indicates that dilution is the main factor for the high DIC in the formation water. The positive correlation of Na/Cl and Ca/Cl with DIC concentration indicates that Na, Ca, and DIC within the FS are likely sourced from carbonate dissolution combined with base-exchange reactions that have modified the original composition of the FS water.

Finally, neither the Na-HCO_3 water type, nor the fourth water type with Cl>20 mg/L are located closer to shale-gas wells (Online Supplement), which rules out the likelihood of salinization induced from shale gas exploitation and migration of fluids through the natural gas wells' annulus. Instead, we observed geographical distribution of the water types; the majority of Na-HCO_3 samples were identified in the southern portion of the study area (Figure 13) and at lower average elevations (Online Supplement), which could indicate increased Na and DIC to the southern portion of the study area, corresponding to a regional groundwater flow and increased water-rock interaction along regional flow paths (Imes and Emmett, 1994) and/or greater predominance of shale lithology in the low lying regions (Cordova, 1963).

2.4.4 The Fayetteville Shale flowback and produced waters

The FS flowback and produced water samples (Online Supplement) are saline (TDS ~ 20,000 mg/L), yet our data show that the salinity is substantially lower than

produced waters from other shale gas basins (e.g., Marcellus brine with TDS ~200,000 mg/L; Table 5). The FS saline water is composed of Na-Cl-HCO_3, with a linear correlation (r^2=0.39) between chloride and bromide and a high Br/Cl ratio (~$4x10^{-3}$ to $7x10^{-3}$; Figure 23a). This composition infers modified evaporated seawater (seawater evaporation, salt precipitation, followed by dilution with meteoric water) with Na, Sr, Mg, and Ca enrichments relative to the expected evaporated seawater curve (McCaffrey et al., 1987) (Figure 23a-23h). The $\delta^{18}O$ (-2.1‰ to -0.5‰) and $\delta^{2}H$ (-19.8‰ to -15.2‰) of the formation water samples plot to the right of the $\delta^{2}H/\delta^{18}O$ LMWL (Kendall and Coplan, 2001) (Figure 24).

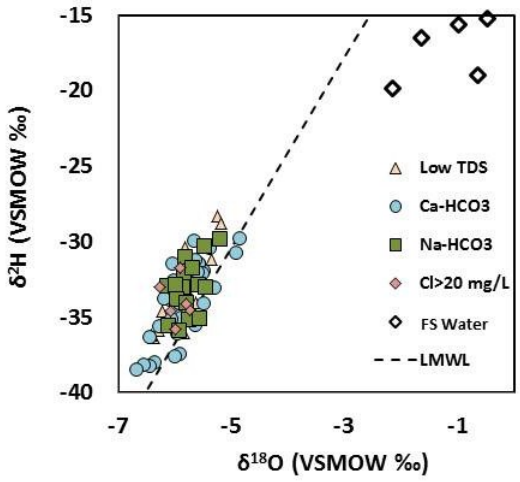

Figure 24: $\delta^{18}O$‰ versus $\delta^{2}H$‰ values in the study shallow groundwater and the Fayetteville brines. The relationship between $\delta^{18}O$ and $\delta^{2}H$ in shallow groundwater is consistent with the local meteoric water line (LMWL) while the Fayetteville brines plot to the right of the LMWL and could reflect mixing between depleted $\delta^{18}O$ and $\delta^{2}H$ low-saline water and $\delta^{18}O$ and $\delta^{2}H$-enriched brines.

DIC content was elevated (800-1800 mg/L) compared to many other produced waters in other shale basins in the US (Table 5), and had a distinctive elevated $\delta^{13}C_{DIC}$ (-12.7‰ to

+3.7‰), which may reflect the composition of the injected hydraulic fracturing fluid or methanogenesis. Boron ($\delta^{11}B$= 26-30‰; Online Supplement, Figure 17b) and strontium ($^{87}Sr/^{86}Sr$ = 0.7090-0.7111; Online Supplement, Figure 17a) isotopic fingerprints are different than would be expected for unaltered Mississippian-age evaporated seawater, which would generate $\delta^{11}B$>39‰ and a less radiogenic $^{87}Sr/^{86}Sr$ ratio for of ~0.7082 (Busch and Busch, 1997 ; Denison et al., 1998). The ^{226}Ra and ^{228}Ra concentrations (activities) were relatively low (20-260 pCi/L) (Online Supplement) compared to Appalachian brines (Rowan et al., 2011; USGS, 2013) with $^{228}Ra/^{226}Ra$ range of 0.1 to 0.5. This relatively low Ra level could have important implications for management strategies and evaluation of possible environmental effects, following disposal of the flowback and produced waters.

The chemical composition of the five flowback samples reflects mixing between the original formation water (represented by the produced water) and lower-saline water that was injected as fracturing fluids. Given the higher salinity of the formation water (relative to the injected water) its chemistry overwhelming controlled the composition of the flowback waters. Similar results were observed in the composition of flowback water from the Marcellus Formation (Haluszczak et al.). Overall, the combined geochemical data from five flowback and one produced water samples indicate that the FS water is likely the remnant of seawater that evaporated beyond the halite saturation stage (McCaffrey et al., 1987). Similar to the Appalachian brines (Dresel and Rose, 2010;

USGS, 2013) the evaporated seawater was modified by water-rock interactions that resulted in Na, Sr, Mg, and Ca enrichments and alterations of the original marine $\delta^{11}B$ and $^{87}Sr/^{86}Sr$ isotopic fingerprints. The brine was subsequently diluted by meteoric water with lower $\delta^{18}O$ and $\delta^{2}H$ values that reduced the original salinity to levels lower than seawater (TDS<32,000 mg/L).

Another unique characteristic of the FS is the substantial DIC enrichment that is inversely correlated (r^2=0.55) of chloride content (Figure 23b) with higher $\delta^{13}C\text{-}_{DIC}$ values (-12.7‰ to 3.7‰, Online Supplement). This suggests that the FS water is diluted with DIC-rich water. The elevated positive $\delta^{13}C_{DIC}$ could infer methanogenesis (Boschetti et al.) in the low-saline water that diluted the original FS brine. Alternatively, dissolution of the limestone matrix with a $\delta^{13}C$ of ~1.0‰ (Handford, 1986) coupled with reverse base-exchange reaction within the FS would generate Ca, Na (from base-exchange) and DIC with a positive $\delta^{13}C_{DIC}$ signature. This is confirmed by the correlation of Na/Cl and Ca/Cl ratios and inverse correlation of Cl with DIC (Figure 23b and 23c). Combined, the chemistry and isotopic results indicate a major modification and dilution of the original FS brine composition.

2.5 Conclusions and Implications

This study examined water quality and hydrogeochemistry in groundwater from shallow aquifers in an attempt to delineate possible groundwater contamination. We considered three types of contamination 1) stray gas contamination; 2) migration of

saline fluids from depth that were directly associated with drilling and exploration of the underlying Fayetteville Shale; and 3) natural migration of saline fluids from depth through leaky geological formations. The results of this study clearly show lack of saline fluid contamination (scenario #2) in wells located near shale gas sites, which is consistent with previous studies in shallow groundwater in the Marcellus in northeastern PA (Osborn et al., 2011a; Warner et al., 2012). However, the lack of apparent methane contamination with thermogenic carbon isotope composition in shallow groundwater near shale gas sites in the Fayetteville Shale differs from results reported for shallow groundwater aquifers overlying the Marcellus Formation (Osborn et al., 2011a). It has been proposed that the stray gas contamination likely resulted from poorly constructed and cemented natural gas well casings that allowed leakage and migration of methane to the shallow aquifers (Jackson et al., 2011; Osborn et al., 2011a, b). In this study we found no evidence for stray gas contamination in groundwater wells located near shale gas sites and most of the methane we identified (mostly low levels) had a biogenic composition that is different from the thermogenic fingerprint of the Fayetteville Shale gas.

Likewise, this study did not find evidence for natural hydraulic connectivity between deeper formations and shallow aquifers (Osborn et al., 2011a; USGS, 2013) that might provide conduits for flow of saline fluids from depth to the shallow groundwater. The spatial distribution of the slightly saline groundwater (Cl>20 mg/L) that could be

derived from dilution of the FS brine or another saline source is not associated with the location of the shale gas wells. Shallow groundwater samples for this study were collected from formations that are part of the Western Interior Confining System (Imes and Emmett, 1994). Previous investigation has shown that these formations impede the vertical flow of groundwater and restrict groundwater movement for domestic supply wells to only local near-surface flow systems (Imes and Emmett, 1994). The natural impermeability and perhaps lack of deformation of these formations seems to prevent hydraulic connectivity that might allow flow of saline fluids between deep saline formations and shallow drinking water aquifers in north-central Arkansas.

The lack of fracture systems that would enable hydraulic connectivity is very different from the geological formations overlying the Marcellus Shale in the Appalachian basin (USGS, 2013) and references therein). These differences could be explained by two structural deformation scenarios: 1) recent glaciation and isostatic rebound of shallow bedrock that was reported in the Appalachian and Michigan basins (Weaver et al., 1995); and 2) tectonic deformation that shaped particularly the Appalachian Basin (Lutz et al., 2013). These natural deformation events could explain the increased hydraulic connectivity and pathways that provide conduits for fluids and gas between the deeper production zones and shallow groundwater in the shallow geological formations overlying the Marcellus Shale in the Appalachian basin but apparently not in the study area in Arkansas.

Previous studies in the Marcellus Basin have suggested that the methane leakage to shallow drinking water wells is due to leakage and inadequate cement sealing in the shale gas wells(Osborn et al., 2011a). Such human factors could also explain the lack of methane contamination in Arkansas, particularly due to: 1) possibly better wellbore integrity; and/or 2) a lack of conventional oil and gas development in north-central Arkansas prior to the shale gas extraction from the Fayetteville Formation (Arkansas Oil and Gas Commission, 2012).

In conclusion, this study demonstrates the importance of basin- and site-specific investigations in an attempt to determine the possible effects of shale gas drilling and hydraulic fracturing on the quality of water resources. The study shows that possible groundwater impacts from shale-gas development differ between basins and variations in both local and regional geology could play major roles on hydraulic connectivity and subsurface contamination processes. Based on the results of this and previous studies (Osborn et al., 2011a; USGS, 2013), we conclude that systematic monitoring of multiple geochemical and isotopic tracers is necessary for assessing possible groundwater contamination in areas associated with shale gas exploration as well as the possible hydraulic connectivity between shallow aquifers and deeper production zones.

3. Impacts of Shale Gas Wastewater Disposal on Water Quality

3.1 Introduction

The safe disposal of large volumes of liquid waste associated with natural gas and oil production is a major challenge given that the waste fluids often contain high levels of salinity, toxic metals, and radioactivity (Kargbo, Wilhelm and Campbell 2010, Dresel and Rose 2010, Haluszczak, Rose and Kump 2013, Osborn and McIntosh 2010, Rowan et al. 2011). For example, in Pennsylvania the increase of oil and gas production from unconventional reservoirs through horizontal drilling and hydraulic fracturing has generated an increased volume of liquid wastes (Maloney and Yoxtheimer 2012, Lutz, Lewis and Doyle 2013) including (1) drilling fluids; (2) hydraulic fracturing flowback fluid; and (3) produced water. Here we collectively define all of these fluids as residual shale gas wastewater (wastewater).

In Pennsylvania, while the overall estimated volume of wastewater ($3.1x10^6$ to $3.8x10^6$ cubic meters per year) has increased during the last few years (Maloney and Yoxtheimer 2012, Lutz et al. 2013) an increasing fraction of the wastewater is also reused. In 2011, 70% of flowback and produced fluids were reused and current operations aim to reuse more of the wastewater (Maloney and Yoxtheimer 2012). However, options for the proper disposal and management of the wastewater that is not recycled are limited, due to the poor water quality of flowback and produced waters. In 2011, ~20% of drilling fluids, 8% of hydraulic fracturing flowback fluid, and 13.8% of produced water

(i.e., brine) from unconventional Marcellus Shale wells were treated at centralized waste treatment facilities (treatment facilities) and then discharged to rivers (Maloney and Yoxtheimer 2012). The salinity of shale gas waste fluids varies from 5,000 mg/L to >200,000 mg/L. This high-salinity water typically contains concentrated bromide, chloride, metals such as barium and strontium, and naturally occurring radioactive material (NORM), in the form of radium isotopes with activities of 185 to 592 Bq/L(Rowan et al. 2011). The elevated salinity and radioactivity in both flowback and produced waters reflect primarily the naturally occurring hypersaline brines that are present within the shale formations that are targeted for natural gas production (Haluszczak et al. 2013, Warner et al. 2012).

Pennsylvania has historically managed wastewater from conventional wells by hauling it to industrial brine treatment facilities, which then discharge to surface waters (Veil 2010). There are 74 facilities (including both brine treatment facilities and publicly owned treatment works (POTWs) permitted or awaiting permit approval to accept wastewater in Pennsylvania(Veil 2010) (Figure 25). Ferrar et al. (2013) (Ferrar et al. 2013) showed that treatment of wastewater by POTWs releases elevated concentrations of Cl, Br, Sr, and Ba to streams, at concentrations above US Environmental Protection Agency (USEPA) maximum contaminant levels, secondary maximum contaminant levels, criterion maximum concentrations, and criterion chronic concentrations (Ferrar et al. 2013). The disposal of Marcellus wastewater through treatment facilities was also

suggested to be linked to an overall increase of 5% in chloride concentrations at downstream surface water monitoring sites in western Pennsylvania (Olmstead et al. 2013 (in press)).

Ferrar et al. (2013) and Veil (2010) described in detail the treatment process of one facility, the Josephine Brine Treatment Facility, in western Pennsylvania that exclusively treats oil and gas wastewater. One key component involves the addition of Na_2SO_4 to remove salts and metals as a solid precipitate. The residual solid is then hauled to residual waste landfills (Ferrar et al. 2013). At the facility, treated wastewater is released at a rate of ~ 0.45 million liters per day [MLd] (Veil 2010) to a stream with an average flow of 756 MLd(U.S. Geological Survey accessed March 12 2013). During 2010 and 2011, a large portion (>50%) of wastewater treated in this facility was from unconventional wells (i.e., Marcellus) but by September 2011 the relative proportion was decreasing compared to conventional produced water (Ferrar et al. 2013).

In this study, we analyzed the effluent from the Josephine Brine Treatment Facility (facility) as well as river water and sediments both upstream and downstream from the effluent discharge site (Figure 26). The study aims to quantify the short- and long-term environmental impacts of shale gas wastewater disposal on surface water quality and stream sediments. We hypothesize that 1) the distinctive geochemical and isotopic fingerprints of the wastewater effluent would enable us to distinguish the unconventional Marcellus wastewater from conventional wastewaters, in spite of the

treatment process; 2) mass-balance calculations can quantify the relative contribution of salts in the effluent to the receiving stream; and 3) stream sediments could provide a record for the long-term impact that the disposal of treated wastewater has on the local environment.

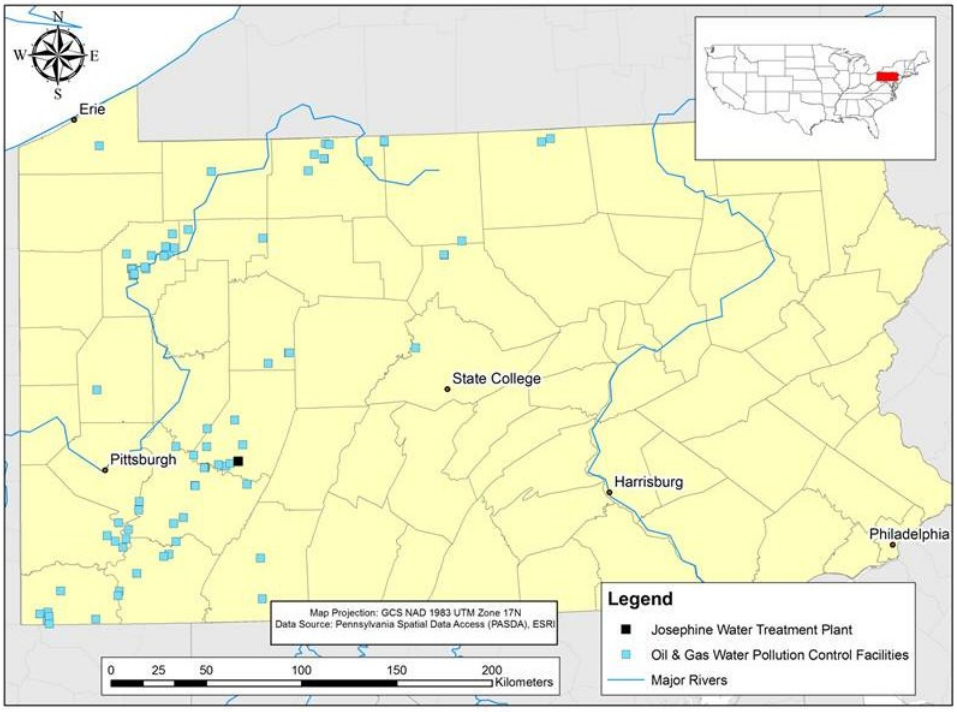

Figure 25: Map of Pennsylvania and the locations of 74 facilities permitted in 2010 to accept and treat produced and flowback waters (red squares). This investigation is at a centralized waste treatment facility in Indiana County where treated wastewater is discharged to a stream.

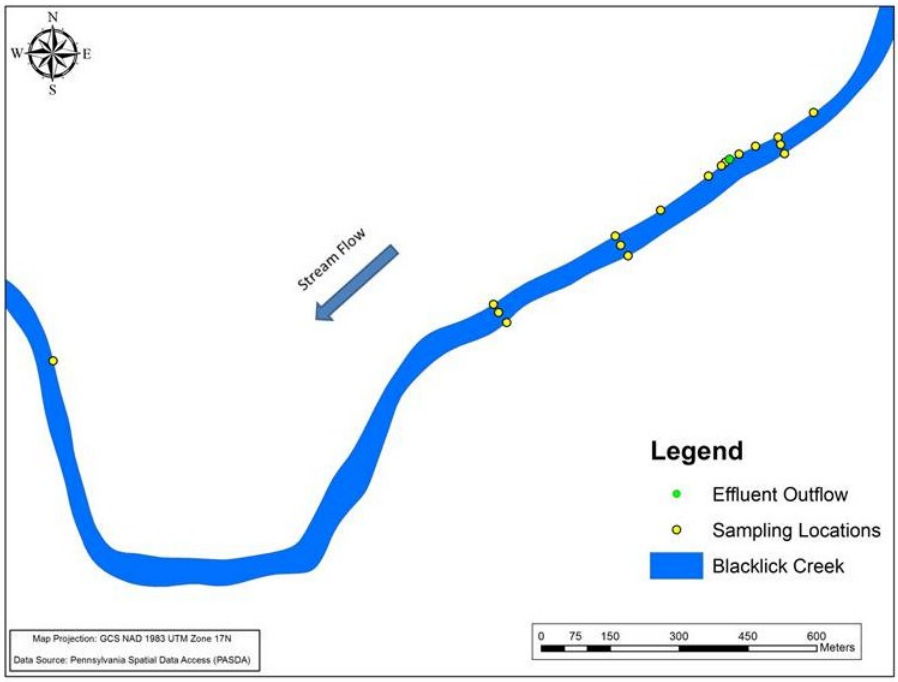

Figure 26. Josephine Brine Treatment Facility sample locations.

3.2 Methods

We analyzed the concentrations of major elements (Cl, Br, SO_4, Ca, Na, Mg, Ba, Sr) and isotopic ratios ($\delta^{18}O$, $\delta^{2}H$, $^{87}Sr/^{86}Sr$, and $^{228}Ra/^{226}Ra$) in effluents from Josephine Brine Treatment Facility as well as stream water and sediments upstream and at different distances downstream of the discharge site. Wastewater data was compared to background concentrations collected upstream of the facility, other streams in western PA, and published values for produced water and flowback of Appalachian Basin Brines.

3.2.1 Sample Collection

Samples from the treatment facility site were collected during five field campaigns across a 2-year period beginning in August 2010 and continuing through November 2012. Eighteen effluent and 32 surface water samples were collected. Surface water samples were collected from 200 meters upstream to 1780 meters downstream of the effluent discharge from the treatment facility. Seven samples were collected in 2011 from other streams/rivers in western PA, including the Conemaugh, Alleghany, and Monongahela Rivers, in an effort to establish background concentrations and variability. Sample collection began with the downstream locations and proceeded upstream to avoid mobilizing sediment. Following collection, all samples were stored on ice for transport to Duke University for analysis.

3.2.2 Analytical methods

Major anions were determined by ion chromatography on a Dionex IC DX-2100, major cations by direct current plasma optical emission spectrometry (DCP-OES) at Duke University. Additional information is available in Supplemental Information. Strontium isotopes were analyzed by thermal ionization mass spectrometer (TIMS) on a ThermoFisher Triton at Duke University. Oxygen and hydrogen isotopes were determined by thermochemical elemental analysis/continuous flow isotope ratio mass spectrometry (TCEA-CFIRMS), using a ThermoFinnigan TCEA and Delta+XL mass spectrometer at the Duke Environmental Isotope Laboratory (DEVIL).

3.2.3 Radium

A large volume (1-4 L) of treated wastewater was collected immediately before the discharge entered the stream during two of the sampling campaigns in 2011. The samples were filtered through a plastic column containing manganese-oxide covered acrylic fibers (Moore, 1984), which efficiently adsorbed the radium isotopes. The fibers were transported to the Laboratory of Environmental RadioNuclides (LEARN) at Duke University. The fibers were then incubated in a sealed glass cylinder for 3 weeks and measured for ^{226}Ra using a Radon-in-Air monitor (RAD7, Durridge Inc.), following the method of Kim et al. (2001). After determination of ^{226}Ra, the fibers were then crushed to achieve a uniform geometry and sealed in 90 mL tin cans. Their ^{228}Ra was then measured by a Canberra DSA2000 BEGe gamma detector at LEARN at Duke University following methods outlined in Vinson et al. (2009).

In addition to water samples, a total of 12 sediment samples were collected from the upper 5 cm interval over 3 separate sampling campaigns (2011-2012). Sediments were placed into 90 mL tin cans and then dried in an oven at 50°C for 24 hours. The dried sediments were crushed to a diameter < 5 mm using a mortar and pestle, weighed, and sealed in the can with electrical tape to prevent gas escape during incubations. The sealed cans were incubated for at least 3 weeks before each sample was counted on a Canberra DSA2000 broad energy germanium (BEGe) gamma detector at LEARN at Duke University. ^{226}Ra activities were obtained through the 609keV energy line of its

radioactive granddaughter, ^{214}Bi assuming secular equilibrium. ^{228}Ra activities were obtained through the 911keV energy line. The activities of all nuclides were calibrated using CCRMP U-Th ore standard DL-1a measured under similar physical conditions (e.g., can geometry).

3.3 Results

3.3.1 Characterization and sources of the wastewater effluent

The concentrations of major elements (Cl, Br, Ca, Na, and Sr) in the treated wastewater effluent varied throughout the two-year sampling period, with levels up to 6,700 times higher than the concentrations measured in the upstream river sites (Table 2). For example, chloride concentrations in upstream river water were low (15-21 mg/L) throughout the study 2010-2012, while chloride in wastewater effluent concentrations ranged between 55,000 and 98,000 mg/L.

Major element concentrations of wastewater effluent were similar to the concentrations reported for produced and flowback waters from the Appalachian Basin (Table 1)(Chapman et al. 2012, Dresel and Rose 2010, Warner et al. 2012, Osborn and McIntosh 2010, Haluszczak et al. 2013) . For example, wastewater effluents had high Br/Cl ratios (3-4x10^{3}), which characterize the Appalachian produced and flowback waters and behave conservatively (i.e., are not altered) throughout the treatment process. Other non-conservative elements (e.g., Na/Cl, Ca/Cl, Sr/Cl and Ba/Cl) varied on

both yearly and hourly time-scales, which is consistent with previous findings(Ferrar et al. 2013). Sulfate, which is reported in very low concentrations in produced and flowback water was enriched in the treated effluent by over 5000% relative to Marcellus flowback, likely due to the addition of Na_2SO_4 as part of the treatment process. In contrast, barium and radium contents in the effluents showed an average reduction of 99% (Table 1) relative to Marcellus flowback, indicating generally effective removal during the treatment process.

The total activity of radium (i.e., ^{226}Ra + ^{228}Ra) in wastewater effluent (0.11-0.29 Bq/L; Table 2) was well below the industrial discharge limit of 2.2 Bq/L (60 pCi/L in the USA). The total activities we measured were within the range of the radium values measured in May-June 2011 by the treatment facility and reported to the USEPA (^{228}Ra range of zero to 0.74 Bq/L and ^{226}Ra range 0.05 to 3.24 Bq/L)(USEPA 2011). The $^{228}Ra/^{226}Ra$ ratio of the effluent sample we collected in August 2011 was 0.39, consistent with ratios reported for Marcellus flowback and produced water(Rowan et al. 2011). In June 2012, the $^{228}Ra/^{226}Ra$ ratio was 0.69, which is closer to ratios reported for wastewaters from conventional oil and gas wells in the Appalachian Basin (0.79 to 1.61 range)(Rowan et al. 2011). The increase in $^{228}Ra/^{226}Ra$ ratio could reflect a change in the relative proportions of the different types of wastes treated at the treatment facility, with a decrease in the percentage of Marcellus flowback(Ferrar et al. 2013).

The $\delta^{18}O$ and $\delta^{2}H$ values of wastewater effluent ($\delta^{18}O$ = -3.85‰ to -4.39‰; $\delta^{2}H$ = -40.8‰ to -45.6‰) overlapped with the values reported for produced water(Dresel and Rose 2010, Osborn and McIntosh 2010) from western PA wells and were less negative than background surface streams in western PA ($\delta^{18}O$ = -6.4‰ to -9.4‰; $\delta^{2}H$ = -41.7‰ to -60.8‰; Figure 27). The wastewater effluent also had a different $\delta^{2}H$ - $\delta^{18}O$ slope relative to the local meteoric water line (LMWL)(Kendall and Coplen 2001). The $^{87}Sr/^{86}Sr$ ratios of the wastewater effluent ranged from 0.7101 to 0.7111, which is consistent with Marcellus produced waters specifically(Chapman et al. 2012) and Middle Devonian or older formations in the Appalachian Basin in general(Warner et al. 2012) (Figure 28). These values are distinct from the $^{87}Sr/^{86}Sr$ ratios of acid mine drainage (AMD; 0.7145-0.7146), surface water collected upstream of the facility (0.7130 – 0.7131), and background surface water (upstream from any disposal site) samples collected in western PA (0.7122-0.7145; Figure 28). We observed a slight increase in $^{87}Sr/^{86}Sr$ in effluent with time, from 0.7101 in 2010 to 0.7111 in 2012. The increase in $^{87}Sr/^{86}Sr$ from 2010 to 2012 is consistent with the changes we observed in the $^{228}Ra/^{226}Ra$ ratios. One possible explanation for this change is a decrease in the relative volume of Marcellus Shale wastewater treated at the investigated treatment facility during 2012. Overall, the use of multiple geochemical and isotopic tracers (Br/Cl, $^{87}Sr/^{86}Sr$, $^{228}Ra/^{226}Ra$, $\delta^{18}O$, and $\delta^{2}H$) confirms that the majority of the wastewater effluent from the investigated site originated from wastewater associated with shale gas development.

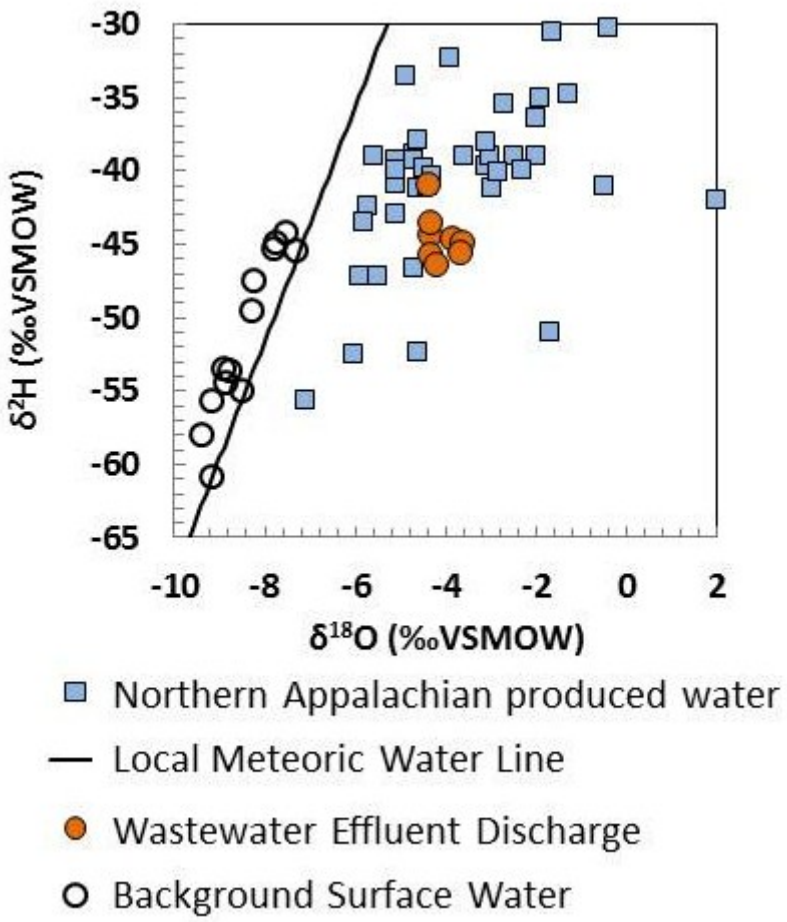

Figure 27: The values of δ2H versus δ18O in surface water samples collected from western PA streams (open black circles) and from wastewater discharged from the Josephine Brine Treatment Facility (orange circles), compared to the Local Meteoric Water Line (LMWL). The isotopic composition of the wastewater effluent is consistent with the isotopic range reported for produced and flowback waters from oil and gas wells drilled in the Appalachian Basin (blue squares).

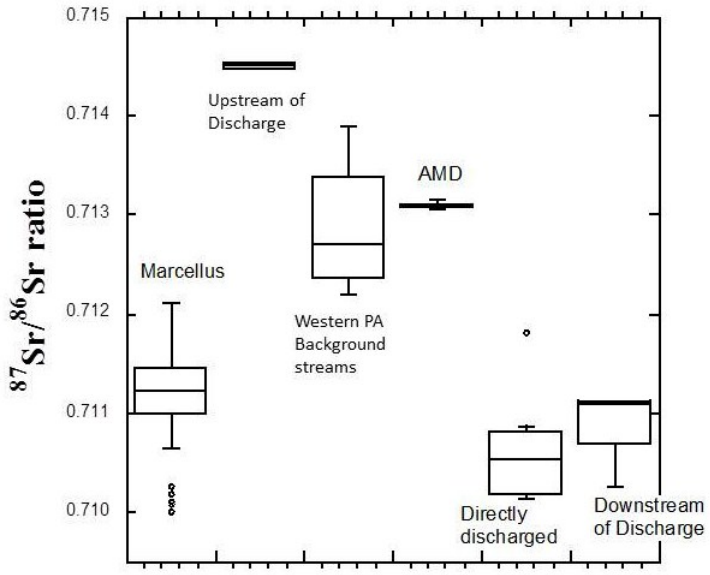

Figure 28: 87Sr/86Sr isotopic ratios in flowback fluids and produced waters from the Marcellus Shale, Acid Mine Drainage (AMD), treatment facility discharge, surface waters upstream of the treatment facility, river waters directly downstream of the facility, and background surface waters in western PA. The ranges in 87Sr/86Sr (0.7101 to 0.7108) of the discharge effluent and downstream river are consistent with Marcellus flowback waters and distinct from AMD (0.7145), background river values upstream of the facility (0.7131), and the range of background samples of surface water in western PA (0.7122-0.7145).

3.3.2 Salt Flux

We calculated the total flux of salts discharged by the facility to the stream by multiplying the mean concentrations of dissolved salts in the effluent by the total permitted volume of effluent. We assume the average concentrations of our data reflect the yearly average concentration and that the facility discharges its permitted volume,

0.45 ML/day. Our calculations show that the total annual chloride and bromide fluxes to the stream were $13.4x10^3$ and 105 metric tons/year, respectively. For comparison, the annual chloride flux of the upstream river was only $4.8\ x10^3$ metric tons/year. Therefore averaged over the year, the discharged effluent from the treatment facility contributes about 64% of the total downstream chloride flux from only 0.1% of the average flow volume.

Maloney and Yoxhiemer (2012) reported a total of 390 ML of Marcellus wastewater that were disposed to wastewater treatment plants during 2011. Lutz et al. (2013) reported larger volumes disposed at treatment facilities, 1,752.8 ML in 2010 and ~1,200 ML in 2011. Assuming that the studied site represents the Marcellus waste stream approximately, we estimate that in 2010-2011 the overall chloride flux to streams directly from Marcellus wastewater disposal were between $32x10^3$ and $143x10^3$ metric tons/year. Bromide fluxes were between 250 and 1,130 metric tons/year, respectively. For comparison, these estimates would represent between 4.5% and 20% of the total annual chloride flux ($714x10^3$ metric tons/year) in an Ohio River with "background" Cl concentration of 24 mg/L and an average flow rate of $28.5x10^6$ ML/year measured near Pittsburgh.

3.3.3 Effects on stream water quality

Samples collected downstream of the wastewater effluent discharge showed a significant dilution relative to the effluent for concentrations of all major elements (Table

2). To evaluate the impact of the wastewater discharge, we calculated the enrichment factors (EFs) for each sample, using the concentrations measured at downstream sites divided by the upstream concentrations. For a conservative element like chloride, the EF was >6,000 at the point of discharge. The EF substantially decreased downstream as the effluent mixed with the stream. However, an EF value of 16 for chloride was recorded 1.78 km downstream of the effluent discharge (Figure 29a). Likewise, bromide concentrations were very low in upstream samples (0.03-0.1 mg/L) and were enriched by 6,000-12,000 in the wastewater effluent. The downstream bromide EF values at distances of 300, 600, and 1,780 meters were 186, 33, and 37, respectively (Figure 29b). Our data show that in spite of a major dilution of the bromide-rich wastewater effluent, downstream river water had a significant bromide enrichment of almost 40 fold even at a distance of 1.78 km from the disposal site (a single sampling event during low ~5 m^3/s stream flow).

The EF data, calculated above, represent single sampling events. But a more robust estimate of yearly average EF in the stream can be determined by using the average concentrations of Br upstream of the facility (0.045 mg/L) and in the effluent (643 mg/L), combined with the average discharge of the stream (756 ML/d) and the treatment facility's permitted discharge (0.45 ML/d). Our calculations reveal an average yearly EF of 5 and 16 for Cl and Br, respectively (Fig. 4). It is important to note that this is an average EF, and seasonal fluctuations in stream flow can substantially alter the EF

on any given day. However, the overall Br enrichment in river water could be critical to downstream municipal water treatment plants given the risks of formation of carcinogenic trihalomethane compounds in chlorinated drinking water upon chlorination of water with even slightly enriched bromide(USEPA 2011).

More reactive constituents such as Sr, Ba, and Na showed somewhat lower EFs in the wastewater effluent discharge (200 to 20,000), which likely reflects the partial removal of these metals during the treatment process. Much lower EFs (1-3) were also recorded in the downstream river sites, inferring an additional uptake of these elements in the river sediments (Figure 30). The $^{87}Sr/^{86}Sr$ measured in downstream river waters (0.7102-0.7130) were in many cases identical to the wastewater effluents and significantly lower relative to the upstream values (0.71307-0.71309). The upstream section of the investigated stream was also influenced by AMD discharge with $^{87}Sr/^{86}Sr$ of 0.71455-0.71447, higher than values measured upstream (~0.713) and other reported values of AMD in western Pennsylvania (~0.712)(Sharma et al. 2013) and (0.712-0.718)(Chapman et al. 2013). Overall, our data show that in spite of the dilution of the wastewater effluent in the river system, different elements, in particular bromide, were elevated in downstream water compared to the upstream river.

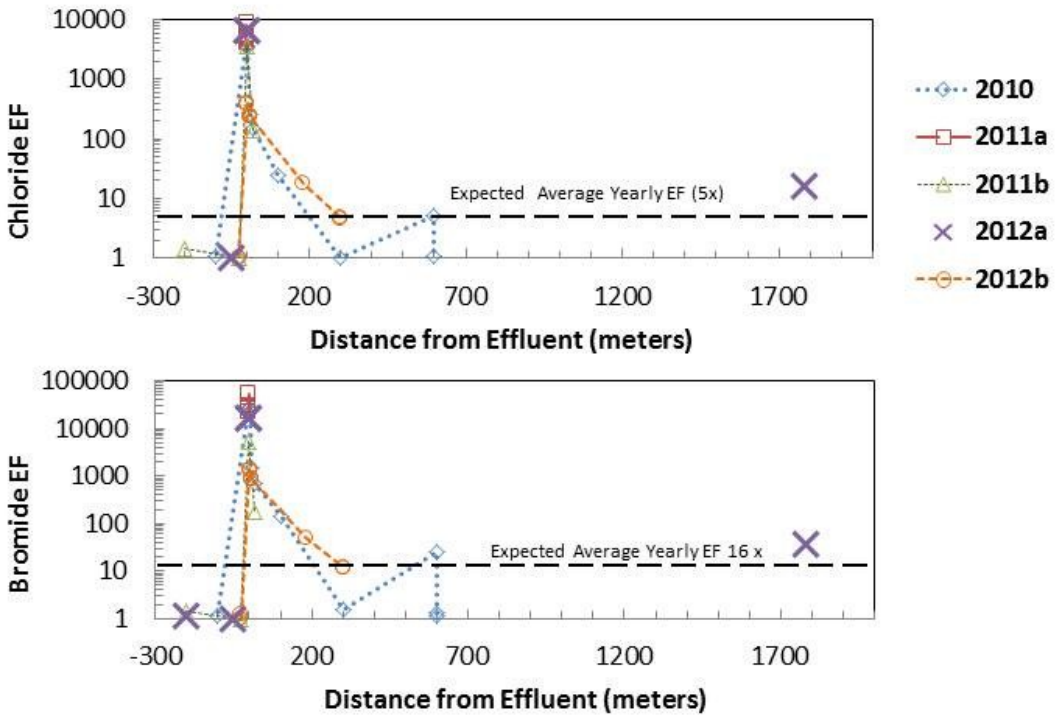

Figure 29: Enrichment factors (EFs) in logarithmic scale of Cl and Br plotted versus distance from the discharge site of the investigated treatment facility in western PA. EFs were calculated relative to upstream concentrations for each of 5 sampling events. Samples plotted upstream (negative values on the X-axis) include surface water samples collected directly upstream of the disposal site and acid mine drainage contribution to the stream near the facility. Concentrations in the discharged effluent were 1000-6000 times the upstream background concentrations, but concentrations decreased within 500 meters downstream because of dilution with the river water. The data show variability in concentrations during the same sampling event at the same distance downstream due to differential mixing of the effluents and river waters perpendicular to stream flow. Concentrations of conservative elements (Cl and Br) in river samples collected over 1,700 meters downstream remained at levels 16-37 times above background levels, respectively, during a period of moderate-low flow. Values of the estimated average yearly mass balance between effluent discharge and river flow rates are marked in dashed lines. These calculations assume that the annual discharge volume is mixed with the annual river flow.

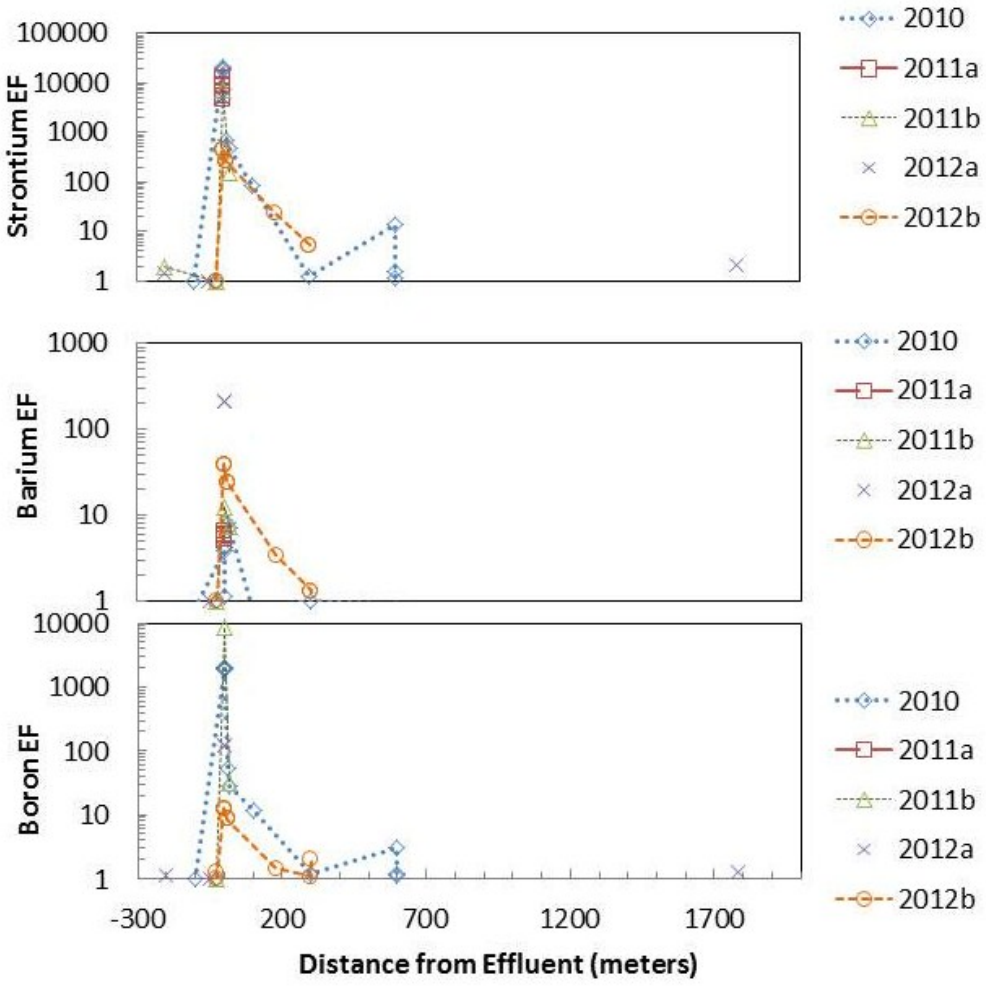

Figure 30. Enrichment factors of strontium, barium and boron, downstream of the effluent discharge.

3.3.4 Effects on stream sediments

The ^{226}Ra activities in the upstream river sediments were low (22.2 Bq/kg to 44.4 Bq/kg; Figure 31) with $^{228}Ra/^{226}Ra$ ratios of 0.56-0.97. These Ra activities are consistent with background Ra activities reported in soils of western New York (mean ^{226}Ra = 33.3

Bq/kg and ^{228}Ra =51.8 Bq/kg(NYDEC 1999)). Likewise, similar low levels of radium activities were reported for background river sediments (4 to 126 Bq/kg(Shahul Hameed et al. 1997) and 44 Bq/kg to 91 Bq/kg for suspended matter(Peterson et al. 2013)). In contrast, immediately adjacent to the treatment facility discharge site, we recorded much higher maximum activities of both ^{226}Ra (8732 Bq/kg) and ^{228}Ra (2072 Bq/kg) (Figure 31). These values were 200 times greater than any background sediment samples collected either upstream of the facility or from other western PA surface waters (Table 2). The mean values of all river sediment samples collected from within 10 meters of the discharge site (n=7) were 4255 Bq/kg and 1110 Bq/kg for ^{226}Ra and ^{228}Ra, respectively. These radioactivity levels are typical values for technologically enhanced naturally occurring radioactive material (TENORM), and are above management regulations in the USA that range from 5 to 50 pCi/gram (185-1850 Bq/kg; http://www.tenorm.com/regs2.htm). For example, in Michigan a radiation threshold that would require transportation of solid waste to a licensed radioactive waste disposal facility is 1850 Bq/kg or 50 pCi/g(Michigan Department of Environmental Quality 2007). Consequently, our data show that in spite of a significant reduction in Ra activities, the treated effluent discharged from the facility has an impact on the stream sediments because Ra has adsorbed and accumulated at the disposal site.

The ^{228}Ra/^{226}Ra ratio measured in the river sediments at the disposal site (0.22 - 0.27) is consistent with ratios reported for Marcellus flowback and produced

water(Rowan et al. 2011) and lower than the ratios recorded in all other background sediment samples we collected throughout western PA (0.56 to 0.97; Figure 31). The relatively low $^{228}Ra/^{226}Ra$ ratio in the sediments near the discharge site likely represents the influence of recent discharge of Marcellus flowback and produced waters. Because the decay of ^{228}Ra (5.76 years half-life) is faster than ^{226}Ra (1,600 year half-life), disposal of fluids with $^{228}Ra/^{226}Ra$ of ~0.9 would also result in $^{228}Ra/^{226}Ra$ ratios measured in the sediments of ~0.22-0.27 after 10 to 12 years of decay. Given the longer history (i.e., several decades) of conventional oil and gas wastewater disposal to streams in western PA, this would result in much lower $^{228}Ra/^{226}Ra$ ratios. The accumulation of Ra in the river sediments therefore appears to be primarily related to recent wastewater disposal that was dominated by unconventional shale gas wastes.

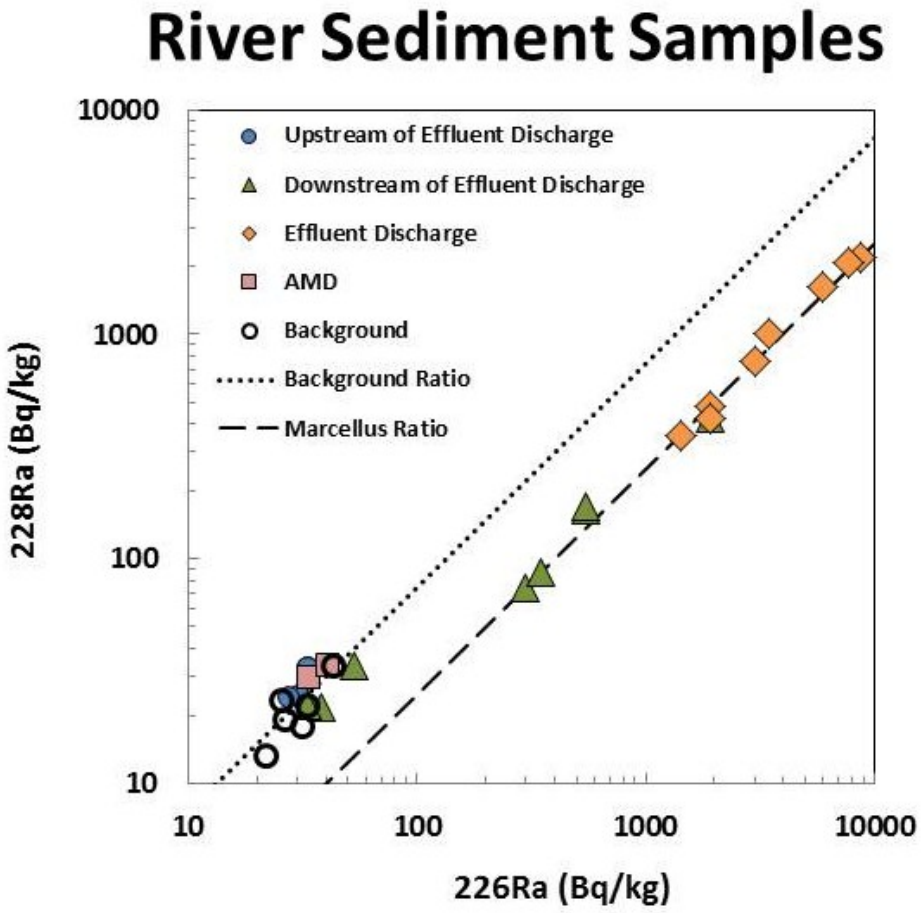

Figure 31: Activities of 228Ra versus 226Ra (Bq/kg) in river sediments collected upstream, adjacent, and downstream of the wastewater discharge site. Note that the maximum of both 226Ra (8732 Bq/kg) and 228Ra (2072 Bq/kg) activities were from samples collected in river sediments adjacent (<10 meters) to the effluent discharge point and are 200 times greater than any sediment sample collected upstream of the facility or any background sediment samples collected from other western PA surface waters. The 228Ra/226Ra ratio (0.22 - 0.27) in the sediments at the discharge point is consistent with Marcellus brine and flowback waters (dashed line; ratio =0.25). This isotopic signature measured in sediments from the disposal site is distinct from any background river sediment samples with higher 228Ra/226Ra ratios (0.56 to 0.97; dashed line ratio of 1).

3.4 Discussion

Our data show that the signature of Marcellus wastewater is apparent, even after treatment, in the effluent from the treatment facility and in the downstream water and sediments. The majority of elemental chemistry and isotopic ratios ($\delta^{18}O$, $\delta^{2}H$, $^{87}Sr/^{86}Sr$, $^{228}Ra/^{226}Ra$) in treated wastewater effluent during 2010 and 2011 were similar to the compositions of flowback and produced waters from the Marcellus shale gas operations. Therefore we conclude that despite treatment, the isotopic ratios in the effluent can still be used as tracers.

The disposal of wastewater effluent to surface water has a discernable impact on the water quality of the stream. The chloride concentrations 1.7 kilometers downstream of the treatment facility were 2-10 times higher than any Cl concentrations recorded in any background western PA streams that we examined. The average yearly EFs of Cl in the stream were calculated to be 5 times background concentrations. These data support recent models that suggest treatment facilities have an impact on concentrations of chloride throughout western PA(Olmstead et al. 2013 (in press)). These results also demonstrate that even a 500-3,000 dilution of the wastewater effluent is not sufficient to reduce bromide content to background levels; thus, discharge of wastewater could potentially increases the concentrations of Br in downstream drinking-water treatment facilities.

A large portion (>50%) of the brine treated by the facility in 2010 and 2011 was Marcellus Formation flowback(Ferrar et al. 2013), with an average reported activity of 185 Bq/L(Rowan et al. 2011). Assuming that the mean value of combined ^{226}Ra and ^{228}Ra reported for Marcellus flowback and produced waters by Rowan et al. (2011) represented the brine accepted and treated at the facility, then $^{226}Ra + ^{228}Ra$ was reduced by over 1000 times before the treated wastewater was discharged to the stream (Table 1). The wastewater treatment through the facility involves Na_2SO_4 addition that likely promotes radium co-precipitation with solid barium sulfate within the facility. The accumulation of Ra as this solid sludge that is then hauled to residual landfills represents a TENORM risk, common in oil and gas industry wastes such as scale and sludge, that could pose significant exposure risks if not properly managed(Smith 1992, U.S. Geological Survey 1999).

Based on the measurements of drastically reduced radium in the effluent, we calculated the total radium likely removed from the wastewater by the treatment facility. Assuming one-half of the 0.45ML/d treated in the facility in 2010 was Marcellus flowback or produced water with an estimated Ra activity of 180 Bq/L, and that for every liter of liquid wastewater, 100 g (10%) was precipitated as a solid during the wastewater treatment process, the solid product would contain roughly 900 Bq/kg of radium.

The estimated level of radiation in the waste treatment solids/sludge suggested in this study exceeds the U.S. regulations for ^{226}Ra disposal to soil of 5 to 15 pCi/g (185-555 Bq/kg) (http://www.tenorm.com/regs2.htm). These values could also exceed many of the typical municipal landfill limits for TENORM in the USA, which range from 5 to 50 pCi/gram (185-1850 Bq/kg; http://www.tenorm.com/regs2.htm). It should be noted that our calculations for the possible Ra content in the treatment residual solids assume that only wastewaters from shale gas contained Ra. Yet, produced waters from conventional oil and gas wells in Pennsylvania and New York also have elevated levels of radioactivity, similar to those from the Marcellus(Rowan et al. 2011).

Although the treatment facility substantially reduces the Ba and Ra in the treated discharge, there is also still a flux of Ra to the stream that we estimate to be 30×10^6 Bq/year (i.e., 0.45 ML/day x 0.185 Bq/L x 365 days). However, our data show that the Ra does not remain in the liquid phase and flow downstream; instead, most of the Ra appears to be adsorbed and retained in river sediments near the discharge site. Since Ra adsorption increases with decreasing salinity (Krishnaswami, Bhushan and Baskaran 1991, Webster, Hancock and Murray 1995, Sturchio et al. 2001) the mixing of the saline wastewater effluents and upstream low-saline water apparently enhances Ra adsorption onto the sediments.

The sediments we analyzed near the treatment facility are likely remobilized and transported downstream during storm events, but the impact of Ra appears to be

localized (<500 meters downstream; Table 2), creating a zone of concentrated Ra in the river bottom sediments. The accumulation of Ra in sediments could pose significant ecological risks. Bioaccumulation of Ra in known to occur in freshwater fish, invertebrates, mollusks, and shells with reported concentration factors (CF) of 100 to 1000(Iyengar and Nrayana Rao 1990, Jeffree 1990, Justyn and Havlik 1990, Shahul Hameed et al.). Radium also accumulates in freshwater plants with an apparent CF of 432 in algae(Williams 1990) and up to 1,000 in phytoplankton in rivers(Shahul Hameed et al.). Further investigations should focus on the possible bioaccumulation of radium in areas of wastewater discharge.

Overall we show that treatment in Josephine Brine Treatment Facility reduces the concentrations of many elements before releasing them into the stream, but in spite of the treatment, wastewater disposal deteriorates the quality of surface water and sediments. Disposal of conventional and unconventional shale gas wastewaters has generated a large flux of contaminants to surface water that created an extended mixing zone with high concentrations of contaminants above background levels. These fluxes include elevated Br concentrations in downstream river water and generation of TENORM contamination in river sediments at the disposal sites. Given the long decay rate of ^{226}Ra (i.e., half-life of 1600 years), Ra will remain in the environment generating radiation over a long time period. Future studies should explore Ra bioaccumulation and other ecological effects at wastewater disposal sites. Moreover, advanced treatment

technologies should be applied to prevent discharge of contaminants, including Ra and Br, to the environment in areas of shale gas development and hydraulic fracturing. Future studies should also examine the disposal options for residue solids generated during the treatment process and their suitability for disposal in "Subtitle D" and "C" landfills, given the expected high levels of radioactivity.

4. Synthesis

This thesis utilized novel geochemical and isotopic tracers (Br/Cl, $^{87}Sr/^{86}Sr$, $\delta^{11}B$, $^{228}Ra/^{226}Ra$) for the identification of hydraulic fracturing fluids by using the specific geochemical signatures of flowback and produced waters from the Marcellus, Utica, and Fayetteville Formations (Figure 13 and Figure 32). These tracers were applied to study possible contamination of private drinking water wells in shallow aquifers of both Pennsylvania and Arkansas. In both cases, the studies showed no direct evidence for groundwater contamination from HVHF (Warner et al., 2012; 2013). Nonetheless, the variability in shallow groundwater quality has demonstrated the need for basin-specific analyses in order to delineate natural salinity occurrence and areas of possible greater risk for contamination. The tracers were also applied to investigate the impact of shale gas wastewater disposal on a river in western Pennsylvania. The geochemical and isotopic signature of the treated effluent discharged from the Josephine Industrial Brine

Treatment facility resembled the original isotopic ratios of the Marcellus brines, demonstrating the isotopic tracers' fingerprints are preserved throughout the treatment and disposal process. A detailed summary of each project is below.

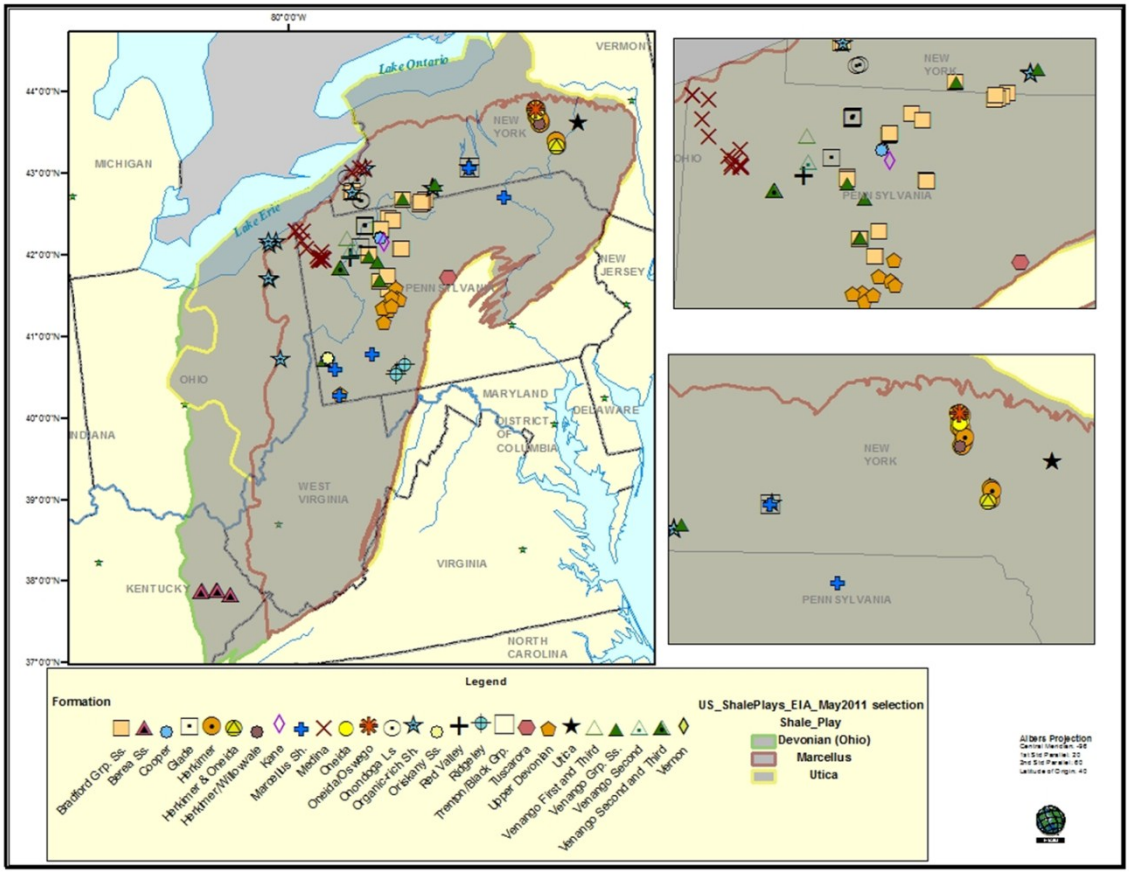

Figure 32: Map displaying the location of Appalachian Basin brine samples analyzed and/or evaluated during this study.

4.1 Shallow groundwater quality overlying the Marcellus Shale in northeastern Pennsylvania

The critical question common to many environmental risks associated with hydraulic fracturing is the hydraulic connectivity between the shale gas formations and the shallow drinking water aquifers. Geochemical evidence from northeastern Pennsylvania shows that pathways, unrelated to recent drilling activities, exist between deeper underlying formations and shallow drinking water aquifers in some locations. Integration of major element (Br, Cl, Na, Ba, and Sr) and trace element (Li) chemistry and isotopic ratios ($^{87}Sr/^{86}Sr$, $^{2}H/H$, $^{18}O/^{16}O$, $^{228}Ra/^{226}Ra$) in 95 newly-collected water samples suggest that mixing relationships between a fresh, shallow groundwater and Marcellus brine causes groundwater salinization. The strong geochemical fingerprint in the salinized (Cl>20 mg/L) groundwater sampled from the Alluvium, Catskill, and Lock Haven aquifers suggests possible migration of Marcellus brine through naturally-occurring pathways. The occurrences of saline water do not correlate with the location of shale-gas wells and are consistent with reported data before rapid shale-gas development in the region. However, the presence of these fluids suggests conductive pathways and specific geostructural and/or hydrodynamic regimes in northeastern Pennsylvania that are at increased risk for contamination of shallow drinking water resources, particularly by fugitive gases, because of natural hydraulic connections to deeper formations.

4.2 Shallow groundwater quality overlying the Fayetteville Shale in north-central Arkansas

Aquifers overlying the Fayetteville Shale in north-central Arkansas, where approximately 4,000 wells have been drilled since 2004 to extract unconventional natural gas, were investigated for indicators of contamination. The geochemistry of 127 drinking water wells was compared for major ions, trace metals, methane gas content and its carbon isotopes ($\delta^{13}C_{CH4}$), and select isotope tracers ($\delta^{11}B$, $^{87}Sr/^{86}Sr$, $\delta^{2}H$, $\delta^{18}O$, $\delta^{13}C_{DIC}$) to the composition of flowback-water samples directly from Fayetteville Shale gas wells. Dissolved methane was detected in 63% of the drinking-water wells (32 of 51 samples), but only six wells exceeded concentrations of 0.5 mg CH_4/L. The $\delta^{13}C_{CH4}$ of dissolved methane ranged from -42.3‰ to -74.7‰, with the most negative values characteristic of a biogenic source also associated with the highest observed methane concentrations, with possible minor contribution of trace values of thermogenic methane. The majority of these values are distinct from the reported thermogenic composition of the Fayetteville Shale gas ($\delta^{13}C_{CH4}$=-35.4‰ to -41.9‰).

Based on major element chemistry, we identified four shallow groundwater types: (1) low (<100 mg/L) total dissolved solids (TDS), (2) TDS>100 mg/L and Ca-HCO_3 dominated, (3) TDS> 100 mg/L and Na-HCO_3 dominated, and (4) slightly saline groundwater with TDS> 100 mg/L and Cl >20 mg/L with elevated Br/Cl ratios (>0.001). The strontium ($^{87}Sr/^{86}Sr$ = 0.7097 to 0.7166), carbon ($\delta^{13}C_{DIC}$ = -21.3 to -4.7‰), and boron ($\delta^{11}B$= 3.9 to 32.9‰) isotopes clearly reflect water-rock interactions within the aquifer

rocks, while the stable oxygen and hydrogen isotopic composition mimics the local meteoric water composition. Overall, a geochemical gradient from low-mineralized recharge water to more evolved Ca-HCO_3, and higher-mineralized Na-HCO_3 composition generated by a combination of carbonate dissolution, silicate weathering, and reverse base-exchange reactions was observed.

The chemical and isotopic compositions of the bulk shallow groundwater samples were distinct from the Na-Cl type Fayetteville flowback/produced waters (TDS ~10,000-20,000 mg/L). Yet, the high Br/Cl variations in a small subset of saline shallow groundwater suggest that they were derived from dilution of saline water similar to the brine in the Fayetteville Shale. Nonetheless, there was not an apparent spatial relationship between methane and salinity occurrences in shallow drinking water wells with proximity to shale-gas drilling sites. The integration of multiple geochemical and isotopic proxies shows no direct evidence of contamination in shallow drinking-water aquifers associated with natural gas extraction from the Fayetteville Shale.

4.3 Surface Water Disposal of Wastewater

The safe disposal of liquid wastes associated with oil and gas extraction in the United States is a major challenge given their large volumes and typically high levels of toxic and radioactive chemicals. In Pennsylvania, oil and gas operations in the Marcellus Shale generate ~3.8×10^6 cubic meters of wastewater a year, some of which is currently

treated at centralized waste treatment facilities and discharged to rivers. This study examined the water quality and isotopic compositions of discharged effluent, surface water, and river sediments at a treatment facility site in western Pennsylvania. The elevated levels of salinity (up to 180,000 mg/L total dissolved solids), chloride, and bromide, as well as the chemical and isotopic (boron, strontium, oxygen and hydrogen) compositions of the effluent reflect the composition of Marcellus Shale produced waters.

The discharge of the effluent from the treatment facility increased chloride and bromide concentrations in the downstream river. Based on water quality data measured in this study and the volumes of Marcellus wastewater disposed in 2011, we estimate a flux of ~$32x10^3$ tons of chloride were released from treatment facilities in 2011. Barium and radium were substantially (>90%) reduced in the treatment facility effluent compared to the original concentrations in shale gas wastewater. In spite of relatively low radium content in effluent (<2.2 Bq/L), elevated radium levels in stream sediments at the point of discharge were 1110-7400 Bq/kg, far exceeding background activities (33-41 Bq/kg) and posing potential environmental risks of radium bioaccumulation in ecological systems in localized areas of wastewater disposal.

4.4 Geochemical Signature of Unconventional Oil and Gas Produced Water

As part of this thesis, over 50 brine samples across thirteen producing formations were analyzed for major and minor elements coupled with $^{87}Sr/^{86}Sr$, $\delta^{11}B$, and $^{228}Ra/^{226}Ra$

ratios (Figure 32). This database provides, for the first time, a comprehensive characterization of variability and isotopic differences between produced waters from conventional reservoirs and unconventional organic-rich black shale deposits. The produced waters from the unconventional Marcellus, Utica, and Fayetteville Formations share similar geochemical characteristics including an evaporated seawater Br/Cl ratio ($3\text{-}7x10^{-3}$) and particularly narrow and specific ranges of $^{87}Sr/^{86}Sr$ ratios (0.709-0.712) (Figure 33a), $\delta^{11}B$ values (26-33‰) (Figure 33b), and $^{228}Ra/^{226}Ra$ ratios (0.1-0.6) (Figure 33c). These values appear distinct from the majority of produced waters collected from conventional oil and gas wells in a variety of geological formations (e.g., sandstone and siltstone) and ages (Silurian, Mississippian, and Upper Devonian).

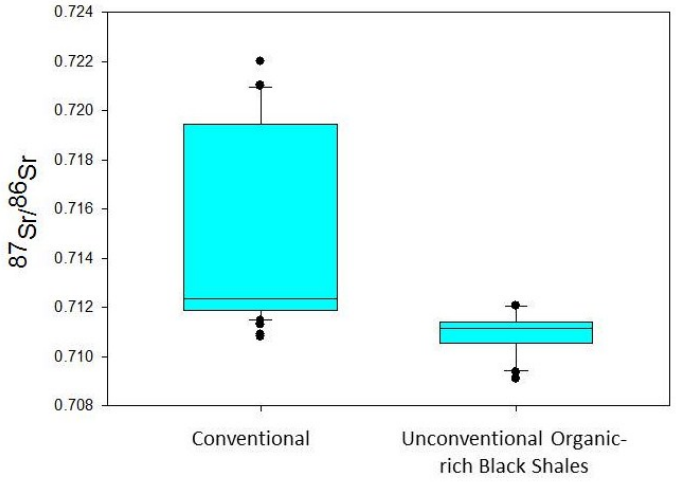
0.724
0.722
0.720
0.718
0.716
0.714
0.712
0.710
0.708
$^{87}Sr/^{86}Sr$
Conventional
Unconventional Organic-rich Black Shales

a

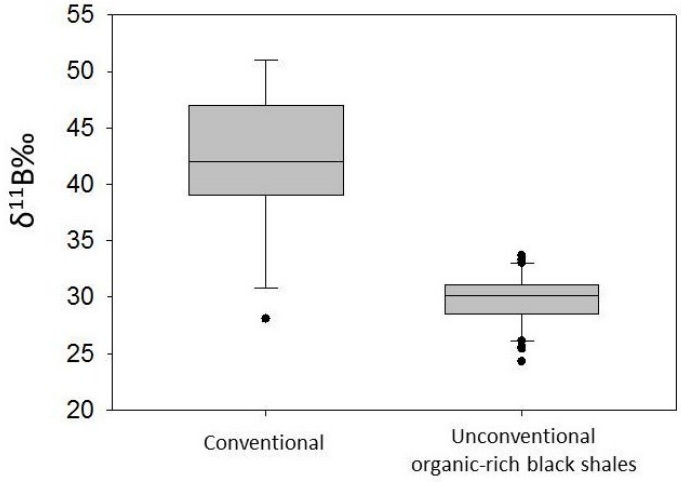
55
50
45
40
35
30
25
20
$\delta^{11}B‰$
Conventional
Unconventional organic-rich black shales

b

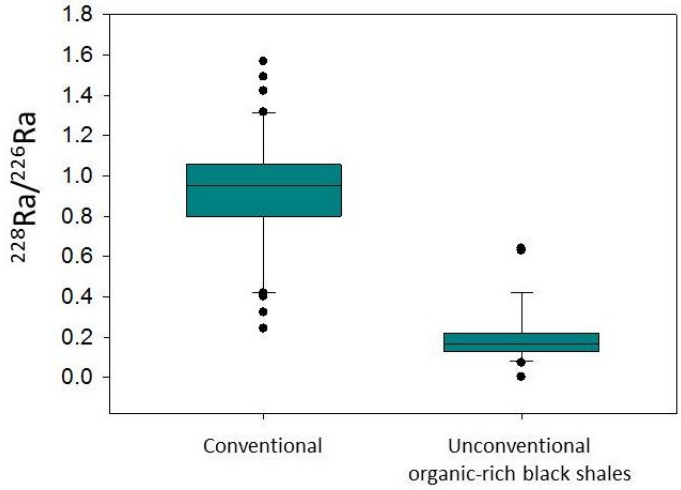
1.8
1.6
1.4
1.2
1.0
0.8
0.6
0.4
0.2
0.0
$^{228}Ra/^{226}Ra$
Conventional
Unconventional organic-rich black shales

c

Figures 33a, b and c: Box plots of $^{87}Sr/^{86}Sr$ (a) $\delta^{11}B$ (b) and $^{228}Ra/^{226}Ra$ (c) measured during this study from conventional oil and gas wells (Silurian, Mississippian, and Upper Devonian) compared to unconventional organic-rich shales (Marcellus, Fayetteville and Utica). The total numbers of conventional samples analyzed for $^{87}Sr/^{86}Sr$, $\delta^{11}B$, and $^{228}Ra/^{226}Ra$ during this study were 41, 36, and 12, respectively. For unconventional samples, the total numbers of samples were 34, 23, and 22 for $^{87}Sr/^{86}Sr$, $\delta^{11}B$, and $^{228}Ra/^{226}Ra$ respectively.

However, the data show some overlap in the isotopic ratios $^{87}Sr/^{86}Sr$ (Figure 33a), $\delta^{11}B$ values (Figure 33b) and $^{228}Ra/^{226}Ra$ (Figure 33c) across produced waters from both conventional and unconventional wells. Therefore, a single isotopic tracer may be misleading. Instead, integration of the isotopic tracers by plotting $\delta^{11}B$ versus $^{87}Sr/^{86}Sr$ (Figure 34) and $^{87}Sr/^{86}Sr$ versus $^{228}Ra/^{226}Ra$ (Figure 35) provides a more powerful and robust distinction between the different produced water sources compared to a lone isotopic tracer.

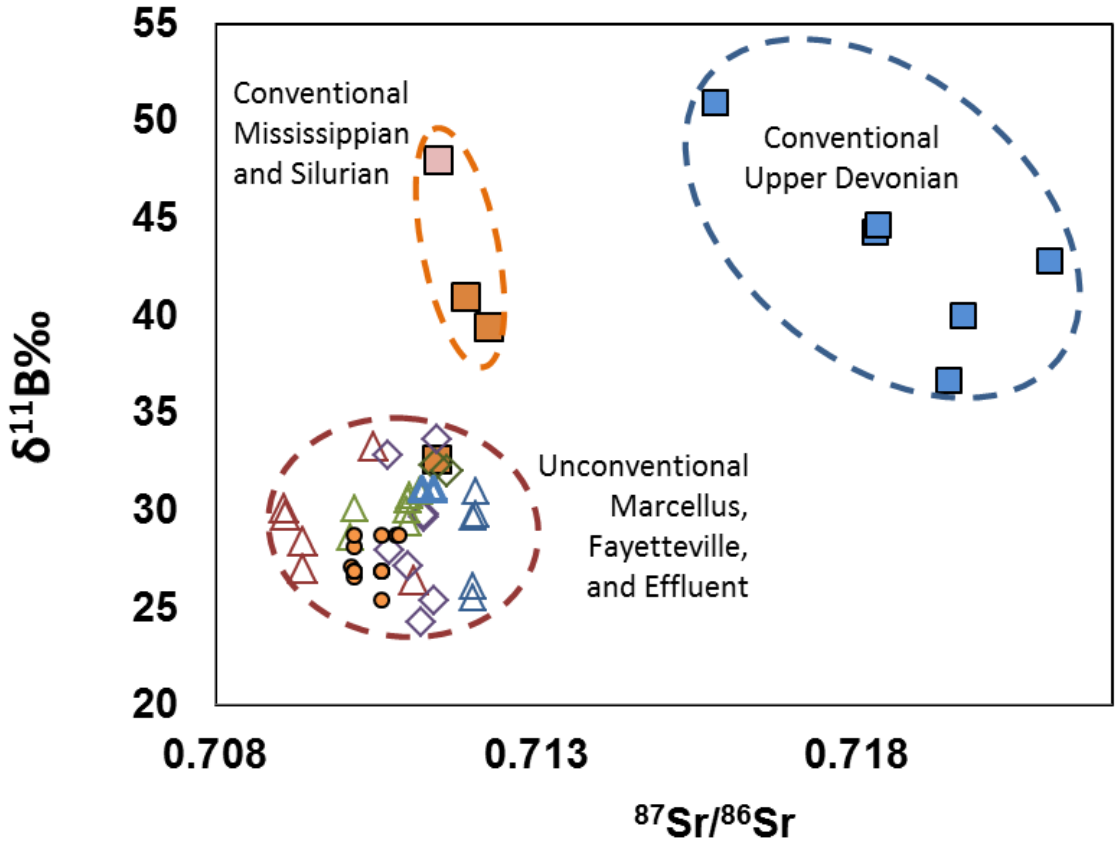

Figure 34: $\delta^{11}B‰$ versus $^{87}Sr/^{86}Sr$ for conventional oil and gas wells compared to unconventional shale-gas wells (Marcellus and Fayetteville). Note that the effluent discussed in Chapter 3 plots within a very narrow range of $\delta^{11}B$ (26-30‰) and $^{87}Sr/^{86}Sr$ (0.710-0.711). This range coincides with produced water and flowback from unconventional wells of both the Fayetteville and Marcellus. The narrow range of both isotopes is distinct from other conventional formations in the Appalachian Basin.

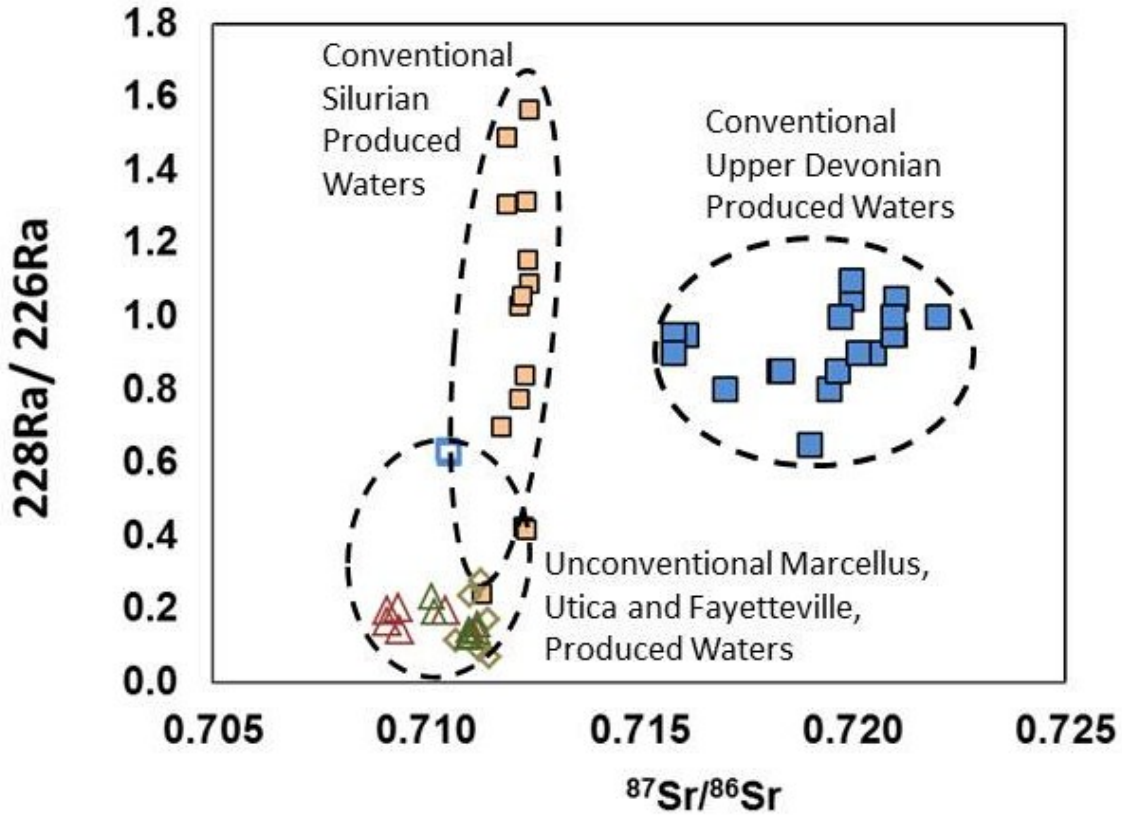

Figure 35: Radium 228/226 ratios versus $^{87}Sr/^{86}Sr$ ratios of conventional and unconventional produced waters. Upper Devonian $^{228}Ra/^{226}Ra$ ratios plotted based on the ranged presented by Rowan et al. (2011). All other values analyzed at Duke University.

The geochemical and isotopic data of produced waters consistently demonstrate that lower-saline fluids injected during HVHF mix with the remnants of brine present within (or immediately adjacent to) the organic-rich black shales. The resulting chemistry implies that there is fluid present within the black shales that is highly saline (TDS >200,000 mg/L) in the Marcellus Shale or less saline (TDS < 30,000 mg/L) in the

Fayetteville Shale. Despite the large range in TDS values, the narrow and consistent isotopic values within the unconventional formations implies these tracers are universal and could be applied in multiple basins for tracing groundwater and surface water contamination even after dilution with fresh water. The data also shows that combining $^{87}Sr/^{86}Sr$, $\delta^{11}B$, and $^{228}Ra/^{226}Ra$ isotope ratios enable the distinction between wastewaters from unconventional oil and gas development relative to conventional oil and gas production.

Table 1: Geochemical data for shallow groundwater samples in northeastern Pennsylvania

Sample Number	Sample Type	pH	DO (mg/L)	EC (µS/Cm)	TDS (mg/L)	Cl (mg/L)	Br (mg/L)	NO_3-N (mg/L)	SO_4 (mg/L)	Alkalinity as HCO3 (mg/L)	Ca (mg/L)	Mg (mg/L)	Sr (mg/L)	Na (mg/L)	Fe (mg/L)	Ba (mg/L)	Li (µg/L)	Ra-226 (pCi/L)	Ra-228 (pCi/L)	$^{87}Sr/^{86}Sr$	δ2H	δ18O	Reported Well Depth (feet)	Water Type	Distance to nearest NG well (km)	Distance to Valley Center Line[1] (km)	Distance to Valley Center Line[2] (km)	Digital Elevation model (m)	Aquifer Type
1	GW	6.93	na	195	127	2	0.01	0.25	9.17	142	27	7	0.37	12	0.00	0.11	24	0.14	0.15	0.71327	*-65.0*	*-10.3*	200	A	5.33	0.87	0.85	402	Dck
2	GW	6.81	na	181	101	1	0.01	1.42	8.80	108	22	5	0.34	10	0.00	0.10	20	na	na	0.71342	*-62.4*	*-9.7*	175	A	4.86	1.08	1.39	455	Dck
3	GW	6.78	na	191	133	2	0.02	1.98	9.12	143	32	7	0.32	9	0.02	0.16	20	na	na	0.71329	*-69.3*	*-10.9*		A	5.15	0.72	0.67	405	Dck
4	GW	7.08	6.05	293	169	2	0.02	0.03	7.10	192	36	10	0.49	20	0.18	0.22	35	na	na	0.71343	*-64.2*	*-10.1*	200	A	5.17	0.51	0.52	387	Dck
5	GW	6.53	na	313	178	13	0.04	3.64	11.31	169	37	9	0.31	21	0.00	0.15	29	na	na	0.71349	*-62.9*	*-9.9*		A	2.74	0.06	0.06	335	Dck
6	GW	6.72	na	270	150	6	0.02	1.61	12.04	154	35	7	0.44	13	0.01	0.15	26	na	na	0.71328	*-63.7*	*-9.9*		A	3.19	0.52	0.52	374	Dck
7	GW	6.61	na	211	116	2	0.02	1.74	7.18	129	27	7	0.22	8	0.01	0.15	15	na	na	0.71317	*-63.7*	*-9.8*	400	A	4.90	0.86	0.86	431	Dck
8	GW	6.78	na	208	115	6	0.04	0.38	12.73	112	23	7	0.44	10	0.00	0.14	17	na	na	0.71339	*-63.8*	*-9.9*	150	A	4.39	0.06	0.06	337	Dck
9	GW	6.09	8.65	122	76	6	0.01	1.65	7.12	69	17	5	0.05	5	0.00	0.05	3	na	na	0.71554	*-67.4*	*-10.5*	117	A	3.65	3.07	2.12	536	Dck
10	GW	6.43	na	323	180	8	0.03	0.22	14.73	185	38	10	0.11	18	0.02	0.05	5	na	na	0.714461	*-62.4*	*-9.8*	250	A	1.72	1.68	0.08	470	Dck
11	GW	5.09	na	241	130	9	0.04	2.66	18.54	113	29	8	0.53	6	0.00	0.15	14	0.22	0.13	0.71354	*-66.2*	*-10.3*	274	A	1.72	1.30	0.39	484	Dck
12	GW	5.72	na	200	111	6	0.02	1.79	14.07	102	26	6	0.06	7	0.03	0.03	4	na	na	0.71485	*-66.4*	*-10.1*	250	A	1.48	1.36	0.36	476	Dck
13	GW	5.75	na	310	176	13	0.03	31.08	20.62	116	36	11	0.08	7	0.00	0.10	7	na	na		*-58.8*	*-9.2*	390	A	0.27	0.57	0.54	465	Dck
14	GW	6.05	na	262	142	17	0.02	3.64	10.57	119	35	8	0.38	9	0.01	0.18	16	na	na		*-61.9*	*-10.1*	270	A	2.48	1.72	0.55	463	Dck
15	GW	6.13	na	245	136	8	0.02	2.72	18.51	121	38	4	0.08	5	0.01	0.04	5	na	na	0.71345	*-59.1*	*-9.6*		A	0.23	3.02	0.87	512	Dck
16	GW	6.25	na	204	115	1	0.01	2.47	12.52	116	35	3	0.18	3	0.01	0.12	10	na	na		*-62.7*	*-9.9*	430	A	1.98	2.90	0.51	502	Dck
17	GW	5.82	na	288	177	12	0.06	1.06	12.89	187	37	9	0.64	12	0.02	0.10	17	0.08	0.05	0.71318	*-64.5*	*-10.6*		A	0.20	1.97	0.51	430	Dck
18	GW	6.49	na	253	142	7	0.02	3.52	9.85	143	33	7	0.64	12	0.00	0.22	26	0.21	na	0.71299	*-67.0*	*-11.0*		A	0.22	0.91	0.07	343	Dck
19	GW	5.87	na	161	89	3	0.01	1.94	12.67	84	19	7	0.07	4	0.00	0.05	6	na	na	0.71444	*-64.7*	*-10.3*	375	A	1.57	2.10	1.11	496	Dck
20	GW	5.59	na	59	88	1	0.01	1.82	6.53	134	11	1	0.06	1	0.03	0.02	1	na	na		*-69.3*	*-11.3*	300	A	2.72	2.00	0.56	484	Dck
21	GW	6.87	7.50	210	118	2	0.08	1.31	19.94	111	31	6	0.04	3	0.09	0.08	7	0.14	0.11		*-64.1*	*-10.3*	150	A	2.20	1.83	0.38	471	Dck

22	GW	7.92	9.85	218	130	4	0.08	3.50	10.73	138.0	28	6	0.31	10	0.03	0.10	13	na	na		*-73.4*	*-11.4*	375	A	0.16	1.43	0.33	387	Dck
23	GW	6.96	2.91	230	126	15	0.12	2.19	12.45	105.0	30	7	0.21	7	0.00	0.06	8	na	na		*-72.7*	*-11.1*		A	0.13	2.12	0.50	439	Dck
24	GW	8.33	3.00	246	132	4	0.08	1.33	9.84	152.0	29	6	0.55	8	0.04	0.28	39	0.24	0.21	0.71306	*-69.1*	*-10.6*	300	A	0.32	1.30	0.05	360	Dck
25	GW	8.12	4.68	249	132	5	0.08	2.21	9.38	149.0	31	6	0.55	4	0.03	0.23	33	na	na	0.71304	*-69.2*	*-10.6*		A	0.16	1.14	0.07	355	Dck
26	GW	8.40	3.50	859	148	8	0.08	4.48	10.60	143.2	33	7	0.57	14	0.01	0.06	24	0.14			*-67.2*	*-10.4*	250	A	0.29	1.02	0.07	351	Dck
27	GW	6.92	3.94	250	132	11	0.09	7.38	17.53	111.9	35	7	0.20	0	0.05	0.08	7	na	na		*-64.7*	*-9.8*	225	A	0.05	1.92	0.93	406	Dck
28	GW	8.23	2.65	253	147	8	0.08	3.78	9.30	145.0	34	7	0.54	14	0.02	0.06	28	na	na	0.71304	*-65.0*	*-9.9*	250	A	0.28	0.91	0.02	343	Dck
29	GW	6.64	3.85	194	104	15	0.08	2.53	10.91	75.2	30	4	0.09	4	0.00	0.06	7	na	na		*-58.7*	*-9.7*	400	A	1.39	0.70	0.70	341	Dck
30	GW	7.73	0.52	284	153	13	0.07		4.44	156	33	6	1.45	18	0.05	1.59	41	0.66	0.28		-64.8	-9.8	260	A	0.65	0.20	0.20	277	Alluvium
31	GW	7.45	0.27	336	160	4	0.04	1.06	0.10	195	41	11	0.09	7	0.04	0.05	13			0.71725	-64.0	-10.0	195	A	1.46	1.24	1.24	419	Dlh
32	GW	7.18	0.14	620	364	8	0.06	0.54	108.85	278	62	26	0.29	22	0.82	0.04	15	0.14	0.17	0.71501	-62	-9.9	57	A	0.55	2.23	0.32	394	Dlh
33	GW	6.80	1.00	271	151	7	0.05	0.06	21.67	140	31	8	0.96	14	0.05	0.18	16			0.71190	-70.6	-10.4	375	A	2.49	0.85	0.85	397	Dlh
34	GW	6.86	1.50	161	86	2	0.04	3.13	8.70	84	18	7	0.36	6	0.02	0.15	10	0.14	0.16	0.71275	-65.2	-10.5	305	A	2.16	0.87	0.87	518	Dck
35	GW	7.51	0.16	350	190	19	0.06	1.92	14.68	171	46	9	0.10	15	0.01	0.17	6	0.13			-61.9	-9.5		A	1.98	2.78	1.14	471	Dck
36	GW	6.17	2.80	113	61	3	0.05	7.13	12.00	39	14	3	0.03	3	0.01	0.05	2	0.13	0.18		-62.3	-9.7	270	A	0.87	1.71	0.50	452	Dck
37	GW	6.75	1.80	268	132	19	0.03	1.52	13.05	106	30	8	0.17	9	0.01	0.13	8	0.19	0.20	0.71368				A	3.55	1.31	0.05	462	Dck
38	GW	6.84	2.20	163	87	3	0.05	4.11	9.43	80	22	5	0.03	4	0.01	0.01	5	na	na	0.71629	-63.5	-9.7		A	3.40	1.67	1.23	465	Dck
39	GW	6.57	na	228	122	7	0.02	0.93	12.89	112	28	4	0.23	13	0.07	0.16	17	na	na	0.71302	-58.0	-9.0	275	A	3.40	1.67	1.23	465	Dck
40	GW	7.73	na	390	101	5	0.09	1.14	16.47		41	14	0.84	22	0.00	0.12	32	na	na	0.71224	-66.8	-10.1	200	A	0.11	1.19	0.58	297	Dlh
41	GW	6.07	5.00	236	114	5	0.02	0.01	18.27	97	26	8	0.81	9	0.03	0.10	18	na	na	0.71091	-63.4	-10.0	438	A	1.77	0.54	0.54	448	Dlh
42	GW	7.30	0.29	280	134	2	0.07	0.05	12.55	134	31	9	0.32	13	0.27	0.05	15	na	na	0.71119	-66.5	-9.9		A	1.25	0.15	0.15	291	Dlh
43	GW	7.38	0.03	554	303	8	0.04	0.01	49.23	302	70	14	0.21	14	0.28	0.04	3	na	na	0.71405	-59.2	-9.3	330	A	0.69	0.14	0.14	330	Dck
44	GW	7.41	1.9	247	133	15	0.05	3.36	10.08	114	35	5	0.37	9	0.06	0.15	7	na	na	0.71360	-65.8	-10.0	180	A	1.99	1.09	0.38	526	Dck
45	GW	6.82	na	117	57	10	0.02	2.25	9.54	34	11	2	0.06	5	0.08	0.03	0	0.08	0.16	0.71348	-63.1	-9.1	45-50	A	1.20	0.11	0.11	292	Dck
46	GW	6.69	na	87	66	3	0.02	1.39	9.76	59	19	1	0.09	3	0.03	0.03	3	na	na		-57.3	-9.1		A	2.44	0.10	0.10	317	Dck

47	GW	5.91	2.54	282	141	18	0.02	13.87	14.89	98	30	3	0.09	12	0.03	0.08	0	na	na		-56.9	-8.9	20	A	2.07	0.07	0.07	310	Dck
48	GW	6.51	4.97	215	121	4	0.02	12.24	8.89	108	34	4	0.34	5	0.03	0.19	6	na	na	0.71166	-58.7	-8.9	240	A	0.43	0.62	0.34	471	Dck
49	GW	7.83	2.30	301	161	3	0.08	0.05	4.02	193	32	9	0.41	17	0.34	0.26	22	0.40	0.24	0.71393	-69.0	-10.6	260	A	0.27	2.31	1.06	457	Dck
50	GW	7.28	2.15	306	165	3	0.02	0.00	14.25	168	39	13	1.69	11	0.55	0.25	19	na	na		-64.6	-9.9	100	A	0.54	1.43	0.88	414	Dlh
51	GW	7.57	1.03	319	183	3	0.02	0.02	16.21	194	45	16	0.28	7	0.04	0.12	9	na	na	0.71175	-72.0	-10.3	195	A	1.14	1.95	1.24	392	Dlh
52	GW	7.31	1.02	849	411	1	0.02	0.01	0.10	465	102	26	0.54	52	1.08	0.16	13	na	na	0.71271	-68.6	-9.8		A	1.06	0.38	0.38	322	Alluvium
53	GW	7.47	4.81	393	218	7	0.02	0.84	22.24	227	45	15	0.89	15	0.01	0.16	32	na	na	0.71225	-67.8	-10.1		A	0.63	1.20	0.40	371	Dlh
54	GW	6.27	6	82	41	1	0.02	0.13	8.15	37	8	3	0.03	2	0.03	0.04	17	na	na		-64.8	-9.7	200	A	0.78	0.31	0.31	452	Dck
55	GW	6.76	8.05	160	79	7	0.02	1.52	12.32	66	15	6	0.05	5	0.00	0.05	20	na	na		-62.9	-9.9	500	A	1.52	1.89	0.64	531	Dck
56	GW	7.49	5.02	260	143	15	0.02	1.35	14.63	130	29	9	0.08	10	0.01	0.11	15	na	na	0.71503	-63.5	-10.1	400	A	4.52	1.09	0.48	492	Dck
57	GW	6.43	7.65	119	60	6	0.02	0.24	10.50	48	12	4	0.07	4	0.00	0.07	12	na	na	0.71369	-64.3	-10.2		A	2.96	0.10	0.10	414	Dck
58	GW	6.67	8.38	116	55	1	0.02	0.13	6.15	59	12	4	0.03	3	0.00	0.05	11	na	na	0.71448	-69.2	-10.3		A	3.29	0.41	0.02	429	Dck
59	GW	8.08	0.63	214	116	1	0.02	0.74	11.42	132	29	3	0.07	6	1.30	0.02	9	na	na	0.71661	-66.3	-9.9	150	A	4.35	0.41	0.08	257	Dck
60	GW	7.4	6.96	277	148	9	0.05	1.43	15.95	145	42	3	0.07	6	0.01	0.05	12	na	na	0.71104	-62.5	-9.6		A	4.06	0.16	0.16	299	Dck
61	GW	7.87	1.8	273	146	3	0.02	0.33	12.25	161	35	6	0.48	10	0.02	0.08	26	na	na	0.71218	-64.5	-9.7		A	0.19	0.97	0.59	303	Dck
62	GW	na	na	na	146	9	0.02	1.00	7.50	149	44	5	0.12	5	0.00	0.16	5	na	na	0.71212	-58.0	-9.0		A	0.18	1.78	1.78	445	Dck
63	GW	7.33	6.41	295	149	18	0.02	1.36	17.25	125	38	4	0.07	9	0.05	0.05	10	na	na	0.71441	-61.3	-9.3	300	A	1.24	0.41	0.41	351	Dck
64	GW	7.56	4.66	237	124	6	0.02	0.01	12.06	129	30	4	0.17	9	0.01	0.03	14	na	na	0.71320	-63.6	-9.4	200	A	0.48	0.26	0.26	340	Dck
65	GW	7.71	0.86	320	173	2	0.02	0.01	10.21	205	38	11	0.28	11	0.15	0.31	16	na	na	0.71182	-64.6	-9.7	138	A	0.54	0.15	0.15	218	Alluvium
66	GW	7.86	3.8	324	173	4	0.02	0.01	13.33	197	36	11	0.37	13	0.44	0.22	18	0.65	0.36	0.71172	-70.5	-10.0	100	A	0.52	0.15	0.15	217	Alluvium
67	GW	7.65	5.01	461	262	2	0.07	0.02	20.33	294	51	15	1.34	28	0.14	0.10	29	na	na	0.71120	-69.2	-10.1	104	A	2.15	0.69	0.30	252	Dlh
68	GW	7.27	1.71	305	159	3	0.02	0.70	15.93	176	36	10	0.44	7	0.04	0.20	24	na	na	0.71117	-66.2	-9.9		A	1.14	0.88	0.73	359	Dlh
69	GW	6.88	2.19	250	124	9	0.02	0.80	12.75	117	31	4	0.28	8	0.01	0.30	17	na	na	0.71433	-68.0	-9.7		A	2.19	1.25	0.56	414	Dck
70	GW	6.94	4.92	315	160	16	0.09	2.55	14.72	143	43	5	0.21	10	0.00	0.14	14	na	na	0.71365	-62.3	-9.2	175	A	0.29	0.77	0.77	370	Dck
71	GW	8.65	37.6	127	92	1	0.02	0.22	10.11	98	22	5	0.06	6	0.01	0.02	2	na	na		-62.6	-9.8	200	A	1.56	0.67	0.34	469	Dck

72	GW	8.65	65.4	64	44	1	0.02	0.74	7.58	42	11	2	0.03	2	0.02	0.02	2	na	na		-58.4	-9.0	100	A	1.04	1.29	0.22	472	Dck
73	GW	7.58	18	241	132	1	0.02	0.22	9.80	145	36	4	0.60	8	0.01	0.10	14	na	na		-63.4	-10.0	300	A	1.24	0.57	0.28	366	Dck
74	GW	6.77	4.25	158	79	3	0.02	0.39	9.24	83	19	3	0.05	4	0.02	0.09	4	na	na		-62.0	-9.3		A	2.00	0.81	0.81	432	Dck
75	GW	7.78	3.15	237	123	3	0.02	0.24	11.99	134	26	6	0.53	9	0.01	0.11	20	na	na				500	A	2.46	0.44	0.44	430	Dck
76	GW	6.71	5.9	153	85	3	0.02	1.02	12.23	83	17	4	0.19	7	0.01	0.09	12	na	na		-60.9	-9.1		A	1.07	0.28	0.28	367	Dck
77	GW	6.53	6.22	145	73	2	0.02	0.58	11.85	74	15	4	0.19	4	0.02	0.05	9	na	na		-63.9	-10.0	154	A	2.34	0.06	0.06	346	Dck
78	GW	6.09	8.14	133	65	1	0.02	1.32	9.36	66	17	2	0.10	3	0.03	0.06	3	na	na		-55.1	-8.4	485	A	0.71	0.79	0.41	382	Dck
79	GW	7.75	2.7	261	152	3	0.02	0.57	9.65	171	34	5	0.90	15	0.02	0.34	15	na	na		-64.8	-10.2	280	A	0.90	1.63	1.03	395	Dck
80	GW	7.25	16.2	305	172	19	0.02	2.73	16.30	156	40	5	1.06	12	0.02	0.33	14	na	na				100	A	1.02	1.45	0.90	359	Dck
81	GW	7.69	0.43	278	150	2	0.02	0.21	10.15	173	31	5	0.60	16	0.03	0.15	25	na	na		-63.9	-9.9	300	A	0.78	1.49	0.58	450	Dck
82	GW	6.3	4.91	148	74	3	0.02	1.07	13.62	67	16	3	0.10	4	0.02	0.07	7	na	na		-60.2	-9.2		A	1.00	0.44	0.44	372	Dck
83	GW	6.29	2.93	229	117	5	0.02	1.43	14.52	116	25	5	0.20	8	0.03	0.11	16	na	na		-64.1	-9.8	180	A	0.89	0.60	0.60	383	Dck
84	Spring	5.91	na	114	63	2	0.01	1.37	9.40	58	16	3	0.06	3	0.03	0.05	4	na	na	0.71337	*-62.2*	*-9.7*		A	4.58	0.10	0.10	341	Dck
85	Spring	5.97	9.00	66	30	1	0.04	0.43	5.86	26	7	1	0.02	1	0.02	0.03	1	na	na		-55.5	-9.0		A	1.34	0.87	0.85	402	Dck
86	Spring	5.96	6.16	155	78	6	0.05	5.51	10.19	62	20	2	0.04	3	0.01	0.03	3	na	na		-53.9	-8.9		A	0.65	0.20	0.20	277	Alluvium
87	Spring	5.55	2.94	140	86	18	0.05	6.22	9.78	46	17	2	0.05	11	0.01	0.05	2	na	na		-56.4	-9.2		A	1.43	0.14	0.14	290	Alluvium
88	spring	6.35	7.35	57	29	0	0.02	0.33	6.54	26	7	1	0.03	1	0.01	0.02	1	na	na		-60.0	-9.2		A	2.65	0.95	0.95	430	Dck
89	spring	5.97	9.38	54	26	1	0.02	0.08	7.79	17	7	1	0.03	1	0.04	0.02	1	na	na		-61.8	-9.2		A	0.72	1.49	0.58	450	Dck
90	GW	8.85		492	291	15	0.08	0.06	5.84	304	8	2	0.12	112	0.79	0.06	173	0.35	0.25	0.71245			380	B	0.71	0.43	0.43	431	Dlh
91	GW	6.95		354	246	4	0.02	0.69	7.89	284	22	6	1.19	66	0.04	0.30	82	na	na	0.71202				B	0.71	0.43	0.43	431	Dlh
92	GW	8.30		450	269	15	0.14	0.02	1.60	300	4	1	0.08	101	0.06	0.04	348	0.09	0.10	0.71321			280	B	1.79	1.50	0.85	418	Dck
93	GW	6.58		315	177	17	0.04	7.57	16.71	143	34	7	0.20	24	0.02	0.18	50	0.14	0.16	0.71296	*-60.1*	*-9.6*		B	0.32	1.91	0.83	437	Dck
94	GW	9.32		529	297	8	0.08	0.03	3.11	335	2	0	0.15	119	0.34	0.07	380	0.21	0.18					B	0.22	1.30	0.29	376	Dck
95	GW	6.59		243	141	2	0.02	0.06	18.44	120	34	5	0.12	23	0.16	0.03	7	na	na		*-58.6*	*-9.5*		B	1.05	1.55	1.00	383	Dck
96	GW	6.45	4.90	473	285	18	0.14	1.31	9.98	290.1	8	2	0.43	103	0.07	0.06	149	0.28	0.21	0.71226	*-61.9*	*-9.9*	180	B	0.67	0.39	0.39	422	Dlh

97	GW	8.24	3.45	240	142	4	0.08	1.43	8.33	148	30	6	0.52	19	0.08	0.06	33	0.18	0.22	0.71289	*-74.0*	*-11.5*	250	B	0.21	1.27	0.04	357	Dck
98	GW	8.04	3.80	320	266	4	0.10	1.31	3.72	293.6	21	7	0.83	84	0.06	0.32	65	0.33	na	0.7103	*-65.4*	*-9.9*	280	B	0.84	1.92	0.41	402	Dlh
99	GW	7.23	2.20	176	89	2	0.05	0.03	2.94	106	12	4	0.25	15	0.70	0.10	615	0.23	0.18	0.712256	-66.6	-10.2	180	B	3.51	0.18	0.18	272	Dck
100	GW	8.08	0.17	456	303	17	0.04	0.01	12.88	320	26	6	1.09	83	0.09	0.26	66	na	na	0.71206	-67.1	-10.1	210	B	2.88	0.43	0.43	329	Dlh
101	GW	7.76	0.52	335	195	8	0.09	0.04	15.06	191	26	9	0.22	43	0.10	0.14	53	na	na		-65.6	-10.3	175	B	0.12	1.05	0.06	441	Dck
102	GW	8.89	0.40	308	166	2	0.05	0.32	5.80	188	7	2	0.24	57	0.02	0.45	84	0.37	0.34		-68.2	-10.5	700	B	2.46	0.44	0.44	508	Dck
103	GW	7.29	1.32	275	149	3	0.07	2.10	10.51	160	27	11	0.22	17	0.05	0.12	11	0.30	0.27	0.71253	-65.1	-10.3	160	B	2.61	0.11	0.11	448	Dck
104	GW	7.81		406	198	2	0.03	0.02	7.82	202	39	12	0.91	37	0.19	0.12	48	0.56	0.41	0.71286	-65.4	-10.1	200	B	0.11	1.19	0.58	297	Dlh
105	GW	9.07		520	307	13	0.06	0.00	9.85	319	13	5	0.85	109	0.05	0.32	208	0.10	0.10	0.71291	-66.6	-9.7	250	B	0.45	0.84	0.84	304	Dlh
106	GW	8.14	0.72	294	180	2	0.04	0.01	8.48	203	27	7	0.84	35	0.05	0.50	36	0.51	0.47	0.713856	-73.1	-10.4	30	B	2.10	0.44	0.22	399	Dck
107	GW	8.3	0.75	389	239	10	0.08	0.02	1.09	252	25	7	0.42	72	0.00	0.74	80	0.31	0.33	0.71443	-75.4	-10.8	125	B	0.56	1.96	0.67	430	Dck
108	GW	8.28	1.27	335	190	3	0.08	0.05	4.02	224	20	6	0.40	46	0.10	0.47	62	0.76	0.75	0.71391	-71.8	-10.4	127	B	0.27	2.31	1.06	457	Dck
109	GW	7.6	2.05	513	145	3	0.04	0.02	30.25		51	16	0.41	45	0.31	0.07	43	0.33	0.22	0.71500	-63.0	-9.9	180	B	1.37	3.85	0.85	382	Dlh
110	GW	7.94		348	202	18	0.10	0.05	8.45	188	37	8	1.82	36	0.00	0.26	46	na	na	0.71157	-71.9	-10.5	80	B	2.47	0.58	0.58	356	Dlh
111	GW	7.48	3.33	272	158	2	0.02	0.01	19.56	153	19	4	0.63	38	0.03	0.09	37	na	na	0.71089	-71.3	-10.0	140	B	1.89	0.95	0.14	305	Dlh
112	GW	7.44		515	298	3	0.02	0.10	23.79	326	46	16	2.13	47	0.02	0.45	66	na	na	0.71180	-68.4	-10.3	390	B	0.80	0.44	0.44	414	Dlh
113	GW	7.62	0.62	380	215	3	0.02	0.01	23.26	230	30	11	0.28	35	0.39	0.08	36	na	na	0.71401	-64.3	-9.9		B	1.02	1.27	0.03	388	Dlh
114	GW	7.38	0.7	372	211	1	0.02	0.01	39.18	206	36	13	0.17	22	0.25	0.03	8	na	na	0.71437	-67.5	-10.2	275	B	0.34	1.91	0.24	422	Dck
115	GW	7.9	5.69	252	136	8	0.02	0.28	13.20	135	25	9	0.39	14	0.00	0.18	28	na	na	0.713416	-68.9	-10.3		B	2.96	0.10	0.10	414	Dck
116	GW	8.07	0.6	351	198	6	0.02	0.01	8.16	219	27	7	1.94	41	0.20	0.66	76	na	na	0.711084	-65.8	-9.5	186	B	0.55	0.11	0.11	215	Alluvium
117	GW	7.68	0.44	463	263	2	0.03	0.01	22.32	293	50	14	0.65	31	0.19	0.09	30	na	na	0.71175	-62.6	-9.8	100	B	2.15	0.59	0.59	249	Dlh
118	GW	7.93	1.3	475	291	4	0.02	1.72	13.19	339	19	4	2.09	82	0.07	0.75	164	na	na		-64.9	-9.9		B	0.37	1.99	0.31	316	Dck
119	GW	6.01		298	159	40	0.04	4.67	13.99	89	35	8	0.27	13	0.01	0.20	10	na	na	0.71346	*-63.3*	*-9.8*	300	C	5.50	1.96	0.06	496	Dck
120	GW	6.69		439	238	59	0.04	5.20	19.47	134	68	6	0.10	14	0.01	0.07	6	na	na		*-60.7*	*-9.7*		C	0.35	2.96	0.89	508	Dck
121	GW	6.88	0.39	516	258	63	0.08	1.36	15.46	170	38	12	0.20	44	0.36	0.07	50	0.24	0.26	0.71473	-64.6	-9.9		C	0.53	0.04	0.04	274	Dlh

122	GW	6.35	1.80	274	139	36	0.05	0.81	14.36	82	29	7	0.16	12	0.04	0.08	3	0.12	0.17	0.71446	-62.6	-9.6	260	C	1.60	1.31	1.31	409	Dlh
123	GW	8.58	0.79	688	403	69	0.15	3.82	18.76	329	25	8	0.17	117	0.05	0.08	122	0.20	0.13	0.71443	-63.9	-9.8	265	C	1.55	0.88	0.88	424	Dck
124	GW	7.66	0.62	293	150	24	0.05	4.39	10.80	123	31	11	0.23	8	0.01	0.17	13	0.12	0.17		-66.1	-10.3	360	C	4.34	1.80	0.47	513	Dck
125	GW	6.06	1.47	386	198	73	0.04	6.35	9.65	78	28	6	0.28	36	0.03	0.14	7	na	na	0.71136	-61.7	-9.4	351	C	1.25	0.27	0.12	348	Dlh
126	GW	6.01	1.46	349	196	46	0.09	0.63	15.12	111	27	6	0.11	47	0.06	0.07	1	na	na	0.71325	-53.4	-8.3	305	C	0.31	0.04	0.04	307	Dlh
127	GW	7.02	2.50	296	157	31	0.05	5.29	12.98	121	35	3	0.12	11	0.01	0.06	5	na	na		-64.3	-9.8		C	1.92	1.16	0.32	521	Dck
128	GW	6.74	6.50	627	345	112	0.08	30.96	21.05	134	56	9	0.15	50	0.31	0.19	19	na	na	0.71353	-70.7	-9.9	40	C	1.11	0.44	0.20	408	Dlh
129	GW	6.95	6.62	473	251	79	0.04	13.01	18.65	110	48	6	0.10	31	0.00	0.11	15	na	na		-66.4	-10.0	65	C	1.02	0.59	0.19	410	Dlh
130	GW	6.31	2.7	280	143	23	0.02	0.70	15.06	114	31	5	0.12	13	0.02	0.05	8	na	na		-65.5	-9.5	375	C	1.30	1.52	0.80	424	Dck
131	Spring	5.98	1.04	175	87	27	0.05	3.95	9.56	35	13	6	0.02	10	0.06	0.01	140	na	na	0.71446	-58.6	-9.3		C	1.60	1.31	1.31	409	Dlh
132	GW	8.04		418	220	59	0.56	0.02	2.48	153	27	9	0.68	47	0.02	2.12	144	na	na	0.71346	*-65.3*	*-10.3*	150	D	4.25	0.18	0.11	343	Dck
133	GW	6.27		290	175	21	0.09	2.27	11.47	171	41	8	0.45	7	0.00	0.09	13	na	na	0.71343	*-64.5*	*-10.6*	340	D	0.39	3.15	0.74	522	Dck
134	GW	6.94		800	327	197	1.75	0.03	0.31	31	21	6	0.94	84	0.12	1.44	514	0.47	0.28	0.71201	*-69.4*	*-11.5*	220	D	3.37	0.05	0.05	270	Dck
135	GW	7.11	4.50	497	301	29	0.26	1.30	0.58	293.0	28	6	2.35	90	0.15	0.06	64	0.49	0.31	0.71037	*-64.0*	*-10.1*	250	D	0.16	0.64	0.64	386	Dlh
136	GW	6.62	4.40	604	335	57	0.50	1.32	0.01	299.0	18	3	1.45	107	0.07	0.78	95	na	na	0.71034	*-65.2*	*-10.0*	200	D	0.21	0.69	0.69	388	Dlh
137	GW	7.06	8.30	524	312	30	0.28	1.30	1.28	319	36	9	1.13	77	0.10	0.55	64	0.95	0.52	0.71453	*-62.1*	*-9.8*	240	D	0.51	0.16	0.16	280	Dlh
138	GW	8.53	6.12	417	245	22	0.18	11.86	11.02	208.0	36	8	1.51	52	0.01	0.06	83	0.46	na	0.71258	*-72.3*	*-10.9*	200	D	0.63	1.57	0.62	290	Dck
139	GW	6.99	2.80	275	146	21	0.13	1.78	13.91	116.0	35	8	0.28	9	0.60	0.06	8	0.19	0.19		*-65.1*	*-10.1*	475	D	0.13	1.80	0.56	442	Dck
140	GW	8.38	2.50	324	204	45	0.42	0.02	0.69	185	22	7	0.68	37	0.10	0.69	16	0.32	0.22		-64.6	-10.2	300	D	3.64	0.04	0.03	265	Dck
141	GW	9.34	1.10	525	316	54	0.48	0.01	0.60	272	4	1	0.34	122	0.07	0.19	678	na	na	0.71232	-65.2	-10.4	220	D	2.71	0.43	0.15	278	Dck
142	GW	7.46	0.47	469	228	60	0.32	0.01	12.49	148	48	8	0.95	26	0.03	0.43	67	1.18	0.29		-61.5	-9.5		D	0.26	0.07	0.07	278	Alluvium
143	GW	7.65	0.39	441	243	59	0.43	0.01	4.19	161	23	3	0.43	73	0.27	0.40	216	na	na		-60.9	-9.3		D	1.43	0.14	0.14	290	Alluvium
144	GW	7.30	0.57	474	241	33	0.09	0.02	10.21	236	59	11	0.88	11	0.19	1.18	24	na	na	0.71015	-64.1	-9.8	303	D	0.50	0.05	0.05	302	Dlh
145	GW	7.56	1.08	1088	558	183	1.19	0.02	2.69	365	85	18	3.50	85	0.28	2.42	237	1.26	0.47	0.70991	-60.9	-9.4	305	D	0.47	0.06	0.06	308	Dlh
146	GW	7.80	0.33	628	330	71	0.50	0.01	0.10	232	41	14	3.00	87	0.10	1.25	127	na	na	0.70983	-63.1	-9.6	307	D	0.82	0.02	0.02	304	Dlh

147	GW	7.23	0.05	4700	2385	1412	9.51	7.23	0.10	399	254	47	23.11	437	1.85	13.97	1701	3.54	1.63	0.70962	-63.6	-9.8	293	D	1.51	0.08	0.08	293	Dlh
148	GW	7.72	1.58	1080	547	191	1.51	0.01	1.69	319	33	9	2.40	152	0.34	3.35	212	2.03	0.77	0.711986	-65.0	-10.0	75	D	0.15	0.61	0.12	292	Dlh
149	GW	8.37	3.95	1180	570	292	2.26	0.02	0.00	179	22	4	2.74	160	0.10	1.50	302	na	na	0.71183	-68.5	-10.6	212	D	3.22	0.12	0.12	337	Dck
150	GW	8.2	2.35	3568	2058	1003	9.99	5.40	30.82	266	105	20	1.80	752	1.17	1.82	853	1.54	1.10	0.71173	-71.8	-10.3		D	0.67	2.11	0.14	321	Dlh
151	GW	8.13	3.54	808	644	143	1.13	0.11	0.11	276	42	9	4.10	310	0.12	2.12	488	na	na	0.71175	-69.6	-10.5	90	D	0.73	1.16	0.09	272	Dlh
152	GW	7.84		1951	919	425	3.00	0.02	1.59	252	66	12	9.79	278	0.12	5.24	692	na	na	0.70960	-65.5	-9.6	37	D	0.40	0.01	0.01	298	Dlh
153	GW	8.52	2.25	1452	789	368	2.55	0.01	2.37	199	26	5	1.92	285	0.10	1.50	42	na	na	0.71187	-68.0	-9.9	250	D	1.13	0.12	0.12	219	Dlh
154	GW	7.64	1.08	695	355	108	0.73	0.01	18.16	187	48	11	1.18	76	0.17	0.55	233	na	na	0.71287	-64.3	-9.6		D	3.88	0.28	0.28	232	Alluvium
155	GW	8.15	1.34	688	391	178	1.25	0.01	0.08	175	52	9	0.86	64	0.08	0.35	38	na	na	0.71277			130	D	0.24	0.07	0.07	278	Alluvium
156	Salt Spring	7.59	0.10	11950	6418	4014	37.89	1.69	0.65	169	370	61	48.52	1800	1.90	84.44	4345	18.42	9.27	0.71115	-63.7	-9.8	800	D	2.21	0.31	0.31	426	Dck
157	GW	7.85	1.01	1791	1151	623	5.10	0.01	5.30	163	58	11	4.10	364	0.36	6.22	663	na	na	0.71155	-65.2	-10.3	100	D	1.60	0.01	0.01	358	Dlh
158	GW	8.08	8.50	2050	328	141	1.08	0.01	0.10		40	9	3.01	134	0.18	2.99	142	na	na		-71.6	-10.6	125	D	0.78	1.15	0.02	271	Dlh

Table 2: Geochemical data for Appalachian Basin Brines.

Formation	Source Supp. Info. Ref	Sample Name	Age	Cl ppm	Br ppm	SO4 ppm	Ca ppm	Mg ppm	Sr ppm	Na ppm	Ba ppm	Ra-226 pCi/L	Ra-228 pCi/L	$^{87}Sr/^{86}Sr$	$\delta^{2}H$ ‰	$\delta^{18}O$ ‰	TDS ppm
Berea Ss.	5	M1	L. Miss.	32,579	228	88	4,520	972	221	11,381				0.710800	-33.5	-4.9	109,500
Berea Ss.	5	M4	L. Miss.	87,881	894	412	15,320	3,281	609	30,457					-35.4	-2.7	109,503
Berea Ss.	this study [1]	M1	L. Miss.	32,579	228	88	4,548	1,092	173	12,279	12			0.710886			
Berea Ss.	this study [1]	M4	L. Miss.	87,881	894	412	16,078	3,293	476	32,101	8			0.711479			
Organic-rich Sh.	5	D6	U. Dev.	60,903	602	194	9,560	1,604	123	25,327				0.718300	-42.4	-5.7	109,505
Organic-rich Sh.	5	D7	U. Dev.	80,542	783	127	12,360	2,066	180	30,503					-38.9	-4.7	109,506
Organic-rich Sh.	5	D14	U. Dev.	60,655	675	184	10,000	1,920	104	23,289				0.715800	-37.9	-4.6	109,513
Organic-rich Sh.	5	D17	U. Dev.	60,655	675	184	10,000	1,920	104	23,289					-47.2	-5.5	109,516
Venango Grp. Ss.	5	D24	U. Dev.	70,581	642	483	10,920	1,798	171	27,457							109,523

Venango Grp. Ss.	5	D33	U. Dev.	99,792	918	564	18,720	2,333	128	34,510				-39.7	-3.1	109,532
Bradford Grp. Ss.	5	D10	U. Dev.	61,399	653	-	8,640	1,823	85	23,198			0.719000	-39.3	-5.1	109,509
Bradford Grp. Ss.	5	D27	U. Dev.	62,108	631	119	11,160	1,458	84	24,411				-41.2	-4.6	109,526
Bradford Grp. Ss.	5	D29	U. Dev.	131,697	944	62	24,760	2,430	2,317	44,586				-43.5	-5.8	109,528
Bradford Grp. Ss.	5	D30	U. Dev.	148,784	1,037	-	30,760	2,965	3,601	57,548				-39.2	-4.7	109,529
Bradford Grp. Ss.	5	D31	U. Dev.	81,003	692	706	12,680	1,823	74	29,770				-40.9	-5.1	109,530
Bradford Grp. Ss.	5	D32	U. Dev.	83,095	734	314	12,760	1,944	77	32,701				-46.7	-4.7	109,531
Bradford Grp. Ss.	5	D34	U. Dev.	91,213	804	110	15,800	2,138	325	30,114				-39.8	-4.5	109,533
Bradford Grp. Ss.	5	D37	U. Dev.	45,376	463	1,182	8,440	1,191	47	19,305				-55.6	-7.1	109,536
Bradford Grp. Ss.	5	D38	U. Dev.	96,424	984	657	16,080	2,430	126	34,739				-40.4	-4.3	109,537
Bradford Grp. Ss.	5	D39	U. Dev.	72,070	723	286	10,880	1,774	62	29,060			0.720500	-42.9	-5.1	109,538
Bradford Grp. Ss.	5	D40	U. Dev.	72,566	730	249	10,960	1,677	52	27,343			0.721000	-40.0	-5.1	109,539
Upper Devonian	6	ED-82-01	U. Dev.	122,000	1,170	4	18,000	2,520	691	56,700	171			-39.0	-2.5	201,470
Upper Devonian	6	ED-82-02	U. Dev.	123,000	1,180	1	18,800	2,500	1,490	58,300	843					206,345
Upper Devonian	6	ED-82-03	U. Dev.	123,000	1,100		19,000	2,520	1,470	58,500	815					206,585
Upper Devonian	6	ED-82-04	U. Dev.	111,000	1,070	8	17,100	2,410	1,290	52,100	1020					186,182
Upper Devonian	6	ED-82-05	U. Dev.	151,000	1,340	2	24,700	2,880	2,340	63,500	1840					247,787
Upper Devonian	6	ED-82-06	U. Dev.	155,000	1,350	11	25,100	2,850	2,420	63,700	2010	1900				252,563
Upper Devonian	6	ED-82-07	U. Dev.	181,000	1,250	18	34,400	3,140	6,080	71,900	698					298,993
Upper Devonian	6	ED-82-08	U. Dev.	70,600	622	5	11,000	1,650	404	30,600	174					115,427
Upper Devonian	6	ED-82-09	U. Dev.	151,000	1,210	140	24,500	2,970	1,420	61,900	7	200		-35.0	-1.9	243,307
Upper Devonian	6	ED-82-10	U. Dev.	105,000	983	50	14,900	2,150	578	47,400	623			-39.0	-3.0	171,912
Upper Devonian	6	ED-82-11	U. Dev.	123,000	1,190	1	17,700	2,600	936	58,900	668			-39.0	-2.0	205,166
Venango Second	6	ED-82-13	U. Dev.	57,400	586	270	8,150	1,570	129	25,000	2					93,155
Venango First and Third	6	ED-82-15	U. Dev.	35,400	365	8	3,930	910	124	15,200	355					56,408
Venango Second and Third	6	ED-82-23	U. Dev.	50,000	472	17	6,490	1,400	137	21,800	52			-39.0	-5.6	80,571
Red Valley	6	ED-82-12	U. Dev.	6,780	94	2	1,580	195	22	3,400	17					12,348
Glade	6	ED-82-14	U. Dev.	80,500	800	570	12,700	2,110	117	35,000	1					132,799
Glade	6	ED-82-16	U. Dev.	63,200	792	390	11,800	2,050	152	30,000	3					108,462
Glade	6	ED-82-17	U. Dev.	55,800	609	350	8,680	1,510	141	24,000	ND	0				
Glade	6	ED-82-18	U. Dev.	67,800	835	850	12,600	2,180	151	31,000	ND			-41.0	-4.4	
Cooper	6	ED-82-19	U. Dev.	5,760	99	4	920	100	5	3,000	7					9,936
Kane	6	ED-82-20	U. Dev.	44,000	436	14	5,780	1,150	191	19,800	ND					

Cooper	6	ED-82-21	U. Dev.	41,200	437	310	6,110	1,040	39	17,400	ND			
Upper Devonian SS	this study	PAGB-3a	U. Dev.	87,000	780	93	13,677	1,740	160	37,054	69			
Upper Devonian SS	this study	PAGB-4a	U. Dev.	90,000	826	36	14,786	1,777	216	36,350	165			
Organic-rich Sh.	this study [1]	D6	U. Dev.	60,903	602	194	9,419	1,692	107	27,883	10	0.718347		
Organic-rich Sh.	this study [1]	D14	U. Dev.	60,655	675	184	10,375	2,050	96	25,402	13	0.715800		
Bradford Grp. Ss.	this study [1]	D27	U. Dev.	62,108	631	119	10,693	1,535	82	26,187	22	0.719459		
Bradford Grp. Ss.	this study [1]	D31	U. Dev.	81,003	692	706	12,639	1,912	72	31,107	7	0.719670		
Bradford Grp. Ss.	this study [1]	D32	U. Dev.	83,095	734	314	13,098	2,004	72	32,771	8	0.720131		
Venango Grp. Ss.	this study [1]	D33	U. Dev.	99,792	918	564	18,243	2,504	115	39,383	8	0.719725		
Bradford Grp. Ss.	this study [1]	D34	U. Dev.	91,213	804	110	14,707	2,083	266	35,642	13	0.716113		
Bradford Grp. Ss.	this study [1]	D37	U. Dev.	45,376	463	1,182	7,937	1,308	47	20,517	7	0.722000		
Bradford Grp. Ss.	this study [1]	D40	U. Dev.	72,566	730	249	10,770	1,718	61	28,950	10	0.721026		
Marcellus Sh.	4	BR-A1	M. Dev.	77,000			6,120	538	1,970	30,400	5490	0.710653		109,500
Marcellus Sh.	4	BR-A2	M. Dev.	159,000			20,800	1,750	5,230	49,400	12000	0.710270		211,400
Marcellus Sh.	4	BR-A3	M. Dev.	68,000			11,300	1,110	3,340	41,900	7820	0.710742		154,100
Marcellus Sh.	4	BR-A4	M. Dev.	77,000			7,930	840	2,870	34,000	6470	0.710757		136,600
Marcellus Sh.	4	BR-A5	M. Dev.	73,000			7,050	726	2,600	27,600	5860	0.710733		120,900
Marcellus Sh.	4	WE-A1.5	M. Dev.				349		46		70	0.711992		14,800
Marcellus Sh.	4	WE-A2	M. Dev.	10,300			624	43	88	2,792	179	0.712013		21,400
Marcellus Sh.	4	WE-A4	M. Dev.	29,000			2,278	217	381	11,747	740	0.712036		44,800
Marcellus Sh.	4	WE-A5	M. Dev.	32,200			2,880	254	450	14,216	888	0.712027		51,100
Marcellus Sh.	4	WE-A7	M. Dev.	42,000			3,938	381	651	18,288	1405	0.712044		65,700
Marcellus Sh.	4	WE-A12	M. Dev.	47,900			5,603	518	934	23,928	2193	0.712013		81,200
Marcellus Sh.	4	WE-A15	M. Dev.	53,500			6,292	629	1,127	24,820	2687	0.712019		89,500
Marcellus Sh.	4	WE-A29	M. Dev.	76,600			6,236	671	1,215	26,297	2987	0.712091		99,000
Marcellus Sh.	4	WE-B3	M. Dev.	19,000			1,239	694	214	9,901	333	0.712076		33,300
Marcellus Sh.	4	WE-B5	M. Dev.	30,600			2,782	376	533	16,704	1058	0.712108		55,600
Marcellus Sh.	4	WE-B7	M. Dev.	40,700			3,900	490	738	18,288	1490	0.712088		69,400
Marcellus Sh.	4	WE-B9	M. Dev.	46,800			4,627	559	900	18,510	1892	0.712108		78,400
Marcellus Sh.	4	WE-B13	M. Dev.	71,100			5,749	211	1,063	22,437	2306	0.712117		89,300
Marcellus Sh.	4	WE-B18	M. Dev.				6,278		1,380		2700	0.712113		98,100
Marcellus Sh.	4	WA-A11	M. Dev.	88,500			12,278	1,267	1,393	32,500	151	0.711129		136,200
Marcellus Sh.	4	WA-A13	M.	102,100			14,028	1,47	1,694	35,07	194	0.71098		146,70

			Dev.					8		0				8			0		
Marcellus Sh.	4	WA-A15	M. Dev.	107,300			15,269	1,632	1,832	37,100	253						153,400		
Marcellus Sh.	4	WA-A17	M. Dev.	102,600			15,875	1,671	1,872	38,530	296			0.711056			156,700		
Marcellus Sh.	4	WA-A20	M. Dev.	115,300			16,509	1,820	1,888	40,350	328			0.711088			167,800		
Marcellus Sh.	4	WA-A25	M. Dev.	116,100			17,612	1,896	2,045	46,260	349			0.711021			168,400		
Marcellus Sh.	4	WA-A30	M. Dev.				18,080	1,992	2,151	47,881	379			0.711076			169,400		
Marcellus Sh.	4	WA-B1-8	M. Dev.	59,600			8,682	880	1,192	20,310	176			0.710880			108,000		
Marcellus Sh.	4	WA-B1-4	M. Dev.	65,300			8,796	890	1,205	20,440	191			0.710905			117,000		
Marcellus Sh.	4	WA-B2-9	M. Dev.	59,400			8,779	859	1,277	20,510	389			0.710969			110,700		
Marcellus Sh.	4	WA-B2-6	M. Dev.	58,700			8,818	866	1,296	20,910	339			0.710954			108,000		
Marcellus Sh.	4	WA-B3-10	M. Dev.	36,700			5,674	570	795	12,890	11			0.710737			71,400		
Marcellus Sh.	4	WA-B3-5	M. Dev.	36,800			5,733	589	803	12,940	10			0.710722			71,400		
Marcellus Sh.	4	GR-AF	M. Dev.	41,900			4,377	567	1,389	20,923	393			0.710084			88,700		
Marcellus Sh.	4	GR-A1	M. Dev.	63,700			6,532	776	1,397	26,020	1108			0.710988			127,200		
Marcellus Sh.	4	GR-A2	M. Dev.	65,000			7,903	828	1,823	30,100	1560			0.710976			138,800		
Marcellus Sh.	4	GR-A3	M. Dev.	67,300			7,372	866	1,721	26,840	1487			0.710957			137,800		
Marcellus Sh.	4	GR-A4	M. Dev.	70,200			8,874	755	2,009	30,910	1756			0.710961			146,200		
Marcellus Sh.	4	GR-A5	M. Dev.	71,200			7,952	762	1,868	28,270	1638			0.710975			143,100		
Marcellus Sh.	4	GR-A7	M. Dev.	81,900			8,786	841	2,415	32,800	962			0.710148			157,000		
Marcellus Sh.	4	GR-A15	M. Dev.	86,500			9,634	953	2,275	32,380	2273			0.711160			161,500		
Marcellus Sh.	4	GR-A20	M. Dev.	87,700			10,390	976	2,484	34,520	2525			0.711173			188,200		
Marcellus Sh.	5	D60	M. Dev.	132,087	1,213	-	22,840	3,038	4,788	41,335				0.710000	-47.2	-5.9	109,559		
Marcellus Sh.	5	D61	M. Dev.	105,854	1,081	-	21,160	2,187	1,975	37,785					-30.2	-0.4	109,560		
Marcellus Sh.	5	D62	M. Dev.	112,377	1,142	-	22,720	2,819	1,844	37,304							109,561		
Marcellus Sh.	this study	PAGB-1a	M. Dev.	88,000	815	5	13,215	1,342	2,305	34,371	2655								
Marcellus Sh.	this study[2]	PAGB-2a	M. Dev.	94,000	819	3	13,625	1,333	2,421	36,019	3100								
Marcellus Sh.	this study[1]	D61	M. Dev.	105,854	1,081	-	21,741	2,183	1,624	36,222	240			0.711432					
Marcellus Sh.	this study[1]	D62	M. Dev.	112,377	1,142	-	22,334	2,261	1,532	38,407	268			0.711605					
Marcellus Sh.	7	127	M. Dev.									2,653	318				122,527		
Marcellus Sh.	7	128	M. Dev.									3,082	935				250,112		
Marcellus Sh.	7	129	M. Dev.									1,958	572				134,880		
Marcellus Sh.	7	130	M. Dev.									1,486	472				222,681		
Marcellus Sh.	7	131	M. Dev.									1,756	377				117,259		

Marcellus Sh.	7	3	M. Dev.									50	37					333,000
Marcellus Sh.	this study[2]	4-0	M. Dev.	46,000	451	55	6,522	660	1,229	21,300	472	1277		0.710115				77,208
Marcellus Sh.	this study[2]	4-1	M. Dev.	59,000	583	18	7,898	972	1,047	26,224	899	2780						97,211
Marcellus Sh.	this study[2]	4-2	M. Dev.	59,000	581	30	8,390	1,023	1,198	27,246	1104	4044		0.711016				98,929
Marcellus Sh.	this study[2]	4-3	M. Dev.	56,000	543	26	7,956	965	1,170	25,175	1073	4835		0.710998				92,756
Marcellus Sh.	this study[2]	4-4	M. Dev.	54,000	531	37	8,186	983	1,236	25,993	1135	4988		0.710995				91,789
Marcellus Sh.	this study[2]	4-5	M. Dev.	62,000	608	27	8,310	1,009	1,256	26,703	1199	4769		0.710997				101,240
Marcellus Sh.	this study[2]	4-7	M. Dev.	75,000	733	34	10,308	1,134	1,732	32,622	771	3548		0.710185				122,282
Marcellus Sh.	this study[2]	4-15	M. Dev.	68,000	668	29	10,884	1,235	1,611	31,628	1746	5863		0.711197				115,748
Marcellus Sh.	this study[2]	4-20	M. Dev.	66,000	655	32	9,138	1,178	1,321	24,735	1388	5383		0.711220				104,859
Ridgeley	6	ED-82-37	L. Dev.	58,900	349	2	8,930	797	4,400	24,400	1510					-41.0	-0.5	99,746
Ridgeley	6	ED-82-38	L. Dev.	133,000	763		17,600	1,580	8,930	61,300	3890					-51.0	-1.7	227,497
Ridgeley	6	ED-82-39	L. Dev.	174,000	1,010	1	23,800	2,050	13,100	79,900	4370	5000						298,560
Ridgeley	6	ED-82-40	L. Dev.	207,000	1,130		28,400	2,390	12,800	83,300	3680					-42.0	2.0	339,024
Medina Ss.	6	ED-82-22	L Sil.	93,000	943	400	16,600	2,050	477	37,600	ND							
Medina Ss.	6	ED-82-27	L Sil.	159,000	2,240	280	41,600	4,150	1,610	42,400		500						251,712
Medina Ss.	6	ED-82-28	L Sil.	151,000	1,860	360	26,900	2,750	1,030	59,900	4							244,292
Medina Ss.	6	ED-82-29	L Sil.	187,000		270	36,300	3,790	1,430	78,900	4					-38.0	-3.1	308,158
Medina Ss.	6	ED-82-30	L Sil.	130,000	1,490	260	22,000	2,160	893	51,100	3					-39.0	-3.6	208,083
Medina Ss.	6	ED-82-31	L Sil.	159,000	1,990	300	30,100	3,120	1,160	65,300	4							261,468
Tuscarora	6	ED-82-36	L Sil.	152,000	1,540	3	25,500	1,370	3,810	70,700	919	5300				-40.0	-2.3	256,191
Medina Ss.	5	S70	L Sil.	159,383	1,609	262	27,800	2,989	747	60,639								109,569
Medina Ss.	5	S73	L Sil.	141,623	1,311	164	25,040	3,353	705	54,571				0.711900		-32.3	-3.9	109,572
Medina Ss.	this study[1]	S73	L Sil.	141,623	1,311	164	22,201	2,836	520	45,253	7			0.711954				
Utica	this study	RW-1	Ord.	43,866	440	363	3,717	516	747	19,113	578	157		0.710505				69,864

Table 3. Statistical analysis of shallow groundwater types.

Descriptive Statistics for Each Water Type								
					95% Confidence Interval for Mean			
	N	Mean	Std. Deviation	Std. Error	Lower Bound	Upper Bound	Minimum	Maximum

pH	A	88	6.92	.77	.08	6.76	7.08	5.09	8.65
	B	29	7.89	.73	.13	7.61	8.16	6.45	9.32
	C	13	6.71	.75	.21	6.26	7.17	5.98	8.58
	D	27	7.72	.66	.13	7.46	7.98	6.27	9.34
	Total	157	7.22	.86	.07	7.08	7.35	5.09	9.34
Cl (mg/L)	A	89	6.25	5.30	.56	5.14	7.37	.49	19.35
	B	29	6.49	5.91	1.10	4.24	8.74	1.64	18.22
	C	13	52.35	26.38	7.32	36.41	68.29	22.79	111.73
	D	26	224.06	328.85	64.49	91.23	356.88	20.75	4014.00
	Total	157	46.18	154.55	12.33	21.82	70.55	.49	4014.00
Br (mg/L)	A	89	.04	.02	.00	.03	.04	.01	.12
	B	29	.07	.04	.01	.05	.08	.02	.14
	C	13	.06	.03	.01	.04	.08	.02	.15
	D	27	3.08	7.41	1.43	.15	6.01	.09	37.89
	Total	158	.56	3.23	.26	.06	1.07	.01	37.89
Ca(mg/L)	A	89	30.02	14.00	1.48	27.07	32.97	6.56	102.34
	B	29	23.65	11.94	2.22	19.11	28.20	2.38	51.06
	C	13	35.63	14.54	4.03	26.85	44.42	12.96	68.47
	D	27	60.78	77.17	14.85	30.25	91.31	4.24	370.47
	Total	158	34.57	35.91	2.86	28.93	40.21	2.38	370.47
Mg(mg/L)	A	89	6.64	4.50	.48	5.69	7.59	.95	26.37
	B	29	6.45	3.86	.72	4.98	7.92	.31	15.84
	C	13	7.19	2.45	.68	5.71	8.67	3.29	11.76
	D	27	12.15	12.98	2.50	7.02	17.28	1.33	61.23
	Total	158	7.59	6.83	.54	6.52	8.66	.31	61.23
Sr(mg/L)	A	89	.32	.33	.04	.25	.39	.02	1.69
	B	29	.56	.50	.09	.37	.74	.08	2.13
	C	13	.16	.07	.02	.11	.20	.02	.28
	D	27	4.52	9.87	1.90	.62	8.43	.28	48.52
	Total	158	1.07	4.33	.34	.39	1.75	.02	48.52
Na(mg/L)	A	89	9.31	7.20	.76	7.80	10.83	.00	52.24
	B	29	55.07	31.31	5.81	43.16	66.98	15.45	118.84
	C	13	31.42	30.14	8.36	13.21	49.64	7.86	117.29
	D	27	212.10	357.35	68.77	70.74	353.46	7.20	1800.16
	Total	158	54.18	163.99	13.05	28.41	79.95	.00	1800.16

Ba (mg/L)	A	89	.127	.175	.019	.090	.164	.014	1.592
	B	29	.195	.180	.033	.127	.264	.032	.745
	C	13	.100	.059	.016	.064	.136	.006	.199
	D	27	5.028	16.123	3.103	-1.350	11.406	.064	84.439
	Total	158	.975	6.818	.542	-.096	2.046	.006	84.439

Descriptive Statistics for Each Water Type

						95% Confidence Interval for Mean			
		N	Mean	Std. Deviation	Std. Error	Lower Bound	Upper Bound	Minimum	Maximum
Br/Cl (molar)	A	89	4.3E-03	4.1E-03	4.4E-04	3.5E-03	5.2E-03	4.7E-04	2.0E-02
	B	29	7.9E-03	6.5E-03	1.2E-03	5.5E-03	1.0E-02	9.4E-04	2.3E-02
	C	13	5.8E-04	2.7E-04	7.4E-05	4.2E-04	7.4E-04	2.4E-04	9.6E-04
	D	27	3.4E-03	7.6E-04	1.5E-04	3.1E-03	3.7E-03	1.1E-03	4.4E-03
	Total	158	4.5E-03	4.6E-03	3.6E-04	3.8E-03	5.2E-03	2.4E-04	2.3E-02
Sr/Ca	A	89	4.61E-03	4.11E-03	4.36E-04	3.74E-03	5.47E-03	5.58E-04	2.02E-02
	B	29	1.20E-02	8.38E-03	1.56E-03	8.85E-03	1.52E-02	1.65E-03	3.08E-02
	C	13	2.19E-03	1.21E-03	3.36E-04	1.46E-03	2.92E-03	6.88E-04	4.63E-03
	D	27	2.62E-02	1.81E-02	3.49E-03	1.91E-02	3.34E-02	3.64E-03	6.74E-02
	Total	158	9.47E-03	1.20E-02	9.54E-04	7.58E-03	1.14E-02	5.58E-04	6.74E-02
$^{87}Sr/^{86}Sr$	A	53	.71332	.00138	.00019	.71294	.71370	.71091	.71725
	B	25	.71283	.00107	.00021	.71239	.71327	.71030	.71500
	C	8	.71371	.00110	.00039	.71279	.71463	.71136	.71473
	D	22	.71162	.00138	.00029	.71101	.71223	.70960	.71453
	Total	108	.71289	.00145	.00014	.71261	.71317	.70960	.71725
$^{228}Ra/^{226}Ra$	A	13	.967	.467	.129	.685	1.249	.422	2.160
	B	15	.920	.164	.042	.829	1.011	.683	1.212
	C	4	1.113	.329	.165	.589	1.636	.666	1.368
	D	11	.556	.201	.061	.421	.691	.247	.978
	Total	43	.859	.352	.054	.751	.967	.247	2.160

Distance to nearest Natural Gas Well (km)	A	89	1.73	1.42	.15	1.43	2.03	.05	5.33
	B	24	1.21	1.00	.20	.79	1.64	.11	3.51
	C	13	1.72	1.52	.42	.80	2.64	.31	5.50
	D	27	1.33	1.31	.25	.82	1.85	.13	4.25
	Total	153	1.58	1.36	.11	1.36	1.79	.05	5.50
Distance to Valley[1](km)	A	89	1.03	.75	.08	.87	1.18	.06	3.07
	B	24	1.11	.86	.17	.75	1.48	.11	3.85
	C	13	1.10	.85	.24	.59	1.61	.04	2.96
	D	27	.56	.79	.15	.25	.87	.01	3.15
	Total	153	.96	.80	.06	.84	1.09	.01	3.85
Distance to Valley[2](km)	A	89	.52	.41	.04	.43	.61	.02	2.12
	B	24	.47	.31	.06	.34	.60	.03	1.06
	C	13	.51	.47	.13	.22	.80	.04	1.31
	D	27	.20	.23	.04	.11	.29	.01	.74
	Total	153	.46	.39	.03	.39	.52	.01	2.12
DEM (m)	A	89	397	74	8	382	413	217	536
	B	24	391	58	12	366	416	272	508
	C	13	419	78	22	372	466	274	521
	D	27	316	67	13	290	343	219	522
	Total	153	384	77	6	372	396	217	536

Multiple Comparisons - Dunnett T3

Dependent Variable	(I) Type	(J) Type	Mean Difference (I-J)	Std. Error	Sig.	95% Confidence Interval	
						Lower Bound	Upper Bound
pH	A	B	-.968*	.158	.000	-1.399	-.537
		C	0.209	.224	.917	-.457	.876
		D	-.797*	.152	.000	-1.212	-.382
	B	A	.968*	.158	.000	.537	1.399
		C	1.177*	.249	.001	.464	1.890
		D	0.171	.186	.927	-.335	.676
	C	A	-0.209	.224	.917	-.876	.457
		B	-1.177*	.249	.001	-1.890	-.464
		D	-1.007*	.245	.003	-1.712	-.301
	D	A	.797*	.152	.000	.382	1.212
		B	-0.171	.186	.927	-.676	.335
		C	1.007*	.245	.003	.301	1.712

Cl (mg/L)	A	B	-0.237	1.233	1.000	-3.627	3.152
		C	-46.0968346*	7.339	.000	-68.764	-23.430
		D	-217.805	64.495	.014	-401.061	-34.549
	B	A	0.237	1.233	1.000	-3.152	3.627
		C	-45.8594774*	7.399	.000	-68.593	-23.126
		D	-217.568	64.502	.014	-400.837	-34.298
	C	A	46.0968346*	7.339	.000	23.430	68.764
		B	45.8594774*	7.399	.000	23.126	68.593
		D	-171.708	64.906	.077	-355.778	12.361
	D	A	217.8051472*	64.495	.014	34.549	401.061
		B	217.5677900*	64.502	.014	34.298	400.837
		C	171.708	64.906	.077	-12.361	355.778
Br (mg/L)	A	B	-.0318427*	.007	.000	-.051	-.012
		C	-0.026	.009	.084	-.054	.003
		D	-3.045	1.427	.218	-7.088	.997
	B	A	.0318427*	.007	.000	.012	.051
		C	0.006	.011	.994	-.026	.038
		D	-3.013	1.427	.228	-7.056	1.029
	C	A	0.026	.009	.084	-.003	.054
		B	-0.006	.011	.994	-.038	.026
		D	-3.019	1.427	.226	-7.062	1.023
	D	A	3.045	1.427	.218	-.997	7.088
		B	3.013	1.427	.228	-1.029	7.056
		C	3.019	1.427	.226	-1.023	7.062

Multiple Comparisons - Dunnett T3

Dependent Variable	(I) Type	(J) Type	Mean Difference	Std. Error	Sig.	95% Confidence Interval	

			(I-J)				
Ca(mg/L)	A	B	6.364	2.668	.115	-.902	13.630
		C	-5.612	4.297	.721	-18.428	7.205
		D	-30.762	14.925	.249	-72.980	11.457
	B	A	-6.364	2.668	.115	-13.630	.902
		C	-11.976	4.601	.094	-25.336	1.384
		D	-37.125	15.015	.110	-79.527	5.276
	C	A	5.612	4.297	.721	-7.205	18.428
		B	11.976	4.601	.094	-1.384	25.336
		D	-25.150	15.388	.493	-68.347	18.048
	D	A	30.762	14.925	.249	-11.457	72.980
		B	37.125	15.015	.110	-5.276	79.527
		C	25.150	15.388	.493	-18.048	68.347
Mg(mg/L)	A	B	0.189	.862	1.000	-2.159	2.537
		C	-0.548	.830	.984	-2.900	1.805
		D	-5.511	2.542	.203	-12.677	1.654
	B	A	-0.189	.862	1.000	-2.537	2.159
		C	-0.737	.988	.972	-3.483	2.009
		D	-5.700	2.598	.190	-12.983	1.583
	C	A	0.548	.830	.984	-1.805	2.900
		B	0.737	.988	.972	-2.009	3.483
		D	-4.963	2.588	.317	-12.228	2.301
	D	A	5.511	2.542	.203	-1.654	12.677
		B	5.700	2.598	.190	-1.583	12.983
		C	4.963	2.588	.317	-2.301	12.228
Sr(mg/L)	A	B	-0.236	.098	.121	-.509	.037
		C	.1646630*	.041	.001	.055	.274
		D	-4.202	1.900	.189	-9.584	1.180
	B	A	0.236	.098	.121	-.037	.509
		C	.4003334*	.094	.001	.137	.664
		D	-3.966	1.902	.239	-9.352	1.420
	C	A	-.1646630*	.041	.001	-.274	-.055
		B	-.4003334*	.094	.001	-.664	-.137

		D	-4.366	1.900	.159	-9.748	1.015
	D	A	4.202	1.900	.189	-1.180	9.584
		B	3.966	1.902	.239	-1.420	9.352
		C	4.366	1.900	.159	-1.015	9.748

Multiple Comparisons - Dunnett T3

Dependent Variable	(I) Type	(J) Type	Mean Difference (I-J)	Std. Error	Sig.	95% Confidence Interval	
Na(mg/L)	A	B	-45.7581696*	5.865	.000	-62.246	-29.270
		C	-22.112	8.394	.111	-48.017	3.793
		D	-202.785	68.776	.038	-397.618	-7.951
	B	A	45.7581696*	5.865	.000	29.270	62.246
		C	23.647	10.183	.154	-5.380	52.674
		D	-157.027	69.017	.166	-352.341	38.288
	C	A	22.112	8.394	.111	-3.793	48.017
		B	-23.647	10.183	.154	-52.674	5.380
		D	-180.673	69.278	.082	-376.515	15.169
	D	A	202.7848115*	68.776	.038	7.951	397.618
		B	157.027	69.017	.166	-38.288	352.341
		C	180.673	69.278	.082	-15.169	376.515
Ba (mg/L)	A	B	-0.068	.038	.388	-.173	.037
		C	0.027	.025	.855	-.041	.095
		D	-4.901	3.103	.532	-13.691	3.889
	B	A	0.068	.038	.388	-.037	.173
		C	0.095	.037	.084	-.008	.198

		D	-4.833	3.103	.547	-13.624	3.958
	C	A	-0.027	.025	.855	-.095	.041
		B	-0.095	.037	.084	-.198	.008
		D	-4.928	3.103	.526	-13.718	3.862
	D	A	4.901	3.103	.532	-3.889	13.691
		B	4.833	3.103	.547	-3.958	13.624
		C	4.928	3.103	.526	-3.862	13.718
Br/Cl (molar)	A	B	-.0036013*	.001	.045	-.007	.000
		C	.0037570*	.000	.000	.003	.005
		D	0.001	.000	.193	.000	.002
	B	A	.0036013*	.001	.045	.000	.007
		C	.0073583*	.001	.000	.004	.011
		D	.0045809*	.001	.004	.001	.008
	C	A	-.0037570*	.000	.000	-.005	-.003
		B	-.0073583*	.001	.000	-.011	-.004
		D	-.0027774*	.000	.000	-.003	-.002
	D	A	-0.001	.000	.193	-.002	.000
		B	-.0045809*	.001	.004	-.008	-.001
		C	.0027774*	.000	.000	.002	.003

Multiple Comparisons - Dunnett T3

Dependent Variable	(I) Type	(J) Type	Mean Difference (I-J)	Std. Error	Sig.	95% Confidence Interval	
Sr/Ca	A	B	-.0074262*	.002	.000	-.012	-.003
		C	.0024202*	.001	.000	.001	.004
		D	-.0216215*	.004	.000	-.032	-.012
	B	A	.0074262*	.002	.000	.003	.012
		C	.0098464*	.002	.000	.005	.014
		D	-.0141953*	.004	.004	-.025	-.004
	C	A	-.0024202*	.001	.000	-.004	-.001

		B	-.0098464*	.002	.000	-.014	-.005
		D	-.0240417*	.004	.000	-.034	-.014
	D	A	.0216215*	.004	.000	.012	.032
		B	.0141953*	.004	.004	.004	.025
		C	.0240417*	.004	.000	.014	.034
$^{87}Sr/^{86}Sr$	A	B	0.000	.000	.432	.000	.001
		C	0.000	.000	.926	-.002	.001
		D	.001700109*	.000	.000	.001	.003
	B	A	0.000	.000	.432	-.001	.000
		C	-0.001	.000	.328	-.002	.001
		D	.001211504*	.000	.011	.000	.002
	C	A	0.000	.000	.926	-.001	.002
		B	0.001	.000	.328	-.001	.002
		D	.002088614*	.000	.004	.001	.004
	D	A	-.001700109*	.000	.000	-.003	-.001
		B	-.001211504*	.000	.011	-.002	.000
		C	-.002088614*	.000	.004	-.004	-.001
$^{228}Ra/^{226}Ra$	A	B	0.047	.136	.999	-.362	.456
		C	-0.146	.209	.973	-.871	.580
		D	0.411	.143	.058	-.011	.833
	B	A	-0.047	.136	.999	-.456	.362
		C	-0.193	.170	.811	-1.008	.622
		D	.3639082*	.074	.001	.149	.579
	C	A	0.146	.209	.973	-.580	.871
		B	0.193	.170	.811	-.622	1.008
		D	0.557	.175	.139	-.226	1.339
	D	A	-0.411	.143	.058	-.833	.011
		B	-.3639082*	.074	.001	-.579	-.149
		C	-0.557	.175	.139	-1.339	.226

Multiple Comparisons - Dunnett T3							
Dependent Variable	(I) Type	(J) Type	Mean Difference (I-J)	Std. Error	Sig.	95% Confidence Interval	
Distance to nearest Natural Gas Well (km)	A	B	0.514	.254	.249	-.179	1.208
		C	0.006	.448	1.000	-1.333	1.345
		D	0.395	.293	.693	-.409	1.199
	B	A	-0.514	.254	.249	-1.208	.179
		C	-0.509	.469	.850	-1.884	.867
		D	-0.120	.324	.999	-1.007	.767
	C	A	-0.006	.448	1.000	-1.345	1.333
		B	0.509	.469	.850	-.867	1.884
		D	0.389	.491	.961	-1.029	1.807
	D	A	-0.395	.293	.693	-1.199	.409
		B	0.120	.324	.999	-.767	1.007
		C	-0.389	.491	.961	-1.807	1.029
Distance to Valley Center[1](km)	A	B	-0.086	.192	.998	-.622	.449
		C	-0.072	.248	1.000	-.815	.672
		D	0.468	.171	.052	-.002	.939
	B	A	0.086	.192	.998	-.449	.622
		C	0.014	.293	1.000	-.818	.847
		D	0.555	.231	.115	-.079	1.188
	C	A	0.072	.248	1.000	-.672	.815
		B	-0.014	.293	1.000	-.847	.818
		D	0.540	.280	.318	-.262	1.342
	D	A	-0.468	.171	.052	-.939	.002
		B	-0.555	.231	.115	-1.188	.079
		C	-0.540	.280	.318	-1.342	.262
Distance to Valley[2](km)	A	B	0.051	.077	.985	-.161	.263
		C	0.012	.138	1.000	-.403	.426
		D	.3187538*	.062	.000	.151	.486
	B	A	-0.051	.077	.985	-.263	.161
		C	-0.039	.146	1.000	-.467	.388
		D	.2676800*	.077	.008	.054	.481
	C	A	-0.012	.138	1.000	-.426	.403
		B	0.039	.146	1.000	-.388	.467
		D	0.307	.138	.211	-.108	.722
	D	A	-.3187538*	.062	.000	-.486	-.151

		B	-.2676800*	.077	.008	-.481	-.054
		C	-0.307	.138	.211	-.722	.108

Multiple Comparisons - Dunnett T3

Dependent Variable	(I) Type	(J) Type	Mean Difference (I-J)	Std. Error	Sig.	95% Confidence Interval	
DEM (m)	A	B	6.204	14.226	.998	-32.840	45.249
		C	-22.130	22.902	.903	-90.478	46.218
		D	80.7953782*	15.129	.000	39.330	122.261
	B	A	-6.204	14.226	.998	-45.249	32.840
		C	-28.334	24.568	.814	-99.710	43.041
		D	74.5913087*	17.550	.001	26.577	122.605
	C	A	22.130	22.902	.903	-46.218	90.478
		B	28.334	24.568	.814	-43.041	99.710
		D	102.9254139*	25.102	.003	30.524	175.327
	D	A	-80.7953782*	15.129	.000	-122.261	-39.330
		B	-74.5913087*	17.550	.001	-122.605	-26.577
		C	-102.925	25.102	.003	-175.327	-30.524

Table 4: Comparison of Historical data and this study.

Historical and 2010-2011 Groundwater Comparison				
Constituent	Type A p-value	Type B p-value	Type C p-value	Type D p-value
Ca	0.06	0.78	0.97	0.79
Cl	0.96	0.93	0.15	0.18
Na	0.11	0.68	0.55	0.38
Ba	0.89	0.68	N/A	0.12
Sr	0.38	0.66	N/A	0.89

Table 5: Comparison of total dissolved solids in produced water of various unconventional formations.

	TDS (mg/L)	DIC (mg/L)
Fayetteville Shale	**25,000**	1300[a]
Barnett Shale	60,000	610*
Woodford Shale	110,000	
Haynesville Shale	120,000	
Permian Basin	140,000	
Marcellus Shale	180,000	140*

a - this study

* EPA workshop on hydraulic fracturing -http://www.epa.gov/hfstudy/12_Hayes_-_Marcellus_Flowback_Reuse_508.pdf
Source, Kimball, 2012 citation of USGS produced water database- available at http://energy.cr.usgs.gov/prov/prodwat/data.htm

Table 6: Comparison of the mean values of major and trace elements reported for Upper Devonian Brines, Marcellus flowback waters, and the wastewater effluent from the Josephine Brine Treatment Facility in western PA. Also shown is the relative

percent of each constituent in the wastewater discharge effluent relative to Marcellus flowback waters.

Mean values of produced water and flowback compared to discharge	TDS	Cl	Br	SO4	Ca	Mg	Sr	Na	Ba	Ra-226 (pCi/L)	Ra-226 (Bq/L)	Ra-228 (pCi/L)	Ra-228 (Bq/L)	$^{87}Sr/^{86}Sr$	δ^2H	$\delta^{18}O$
	ppm	ppm	ppm	ppm	ppm	ppm	ppm	ppm	ppm	pCi/L		pCi/L				
[#]Upper Devonian	120,791	84,861	787	214	13,495	1,920	586	34,150	332	700	26			0.71906	-41.25	-4.50
[#]Marcellus	93,170	69,516	744	21	9,634	1,056	1,594	28,050	1,692	3,231	120	452	17	0.71119		
[#] Lower Devonian or Older	216,482	139,198	1,283	222	23,766	2,393	3,491	55,625	1,361	2,739	101			0.71145	-40.47	-1.87
Effluent 2010-2012 (Treated Discharge)	98,899	81,771	643	1,092	12,710	830	1,363	27,670	13	2	0.09	4		0.71047	-44.14	-4.33
Treated Discharge Percentage of Marcellus	***106***	***118***	***86***	***5186***	***132***	***79***	***86***	***99***	***0.8***	***0.1***		***0.9***				
NOTES:																
* - Only 2 measurements available																
[#] Includes data from Dresel and Rose (2010), Chapman et al. (2012), Osborn and McIntosh (2010)																

Table 7: Chemical and isotopic data for surface waters and effluent from the Josephine Brine Treatment Facility disposal site in western Pennsylvania.

Location Number	Location Type	Sample Type	Distance Downstream	Date Sampled	TDS calculated (mg/L)	Cl (mg/L)	Br (mg/L)	SO4 (mg/L)	Alkalinity (mg/L)	Ca(mg/L)	Mg(mg/L)	Sr(mg/L)	Na(mg/L)	Ba (mg/L)	$^{87}Sr/^{86}Sr$	δ^2H	$\delta_{18}O$
AMD-1	AMD	SW		2011	659	26	0.14	441		114	28	0.6	14	0.1	0.714474	-59.4	-9.2
AMD-2	AMD	SW		2012	164	17	0.07			80	24	0.5	11	0.0	0.714549		
AMD-3	AMD	SW		2012	539	15	0.05	377		73	23	0.4	9	0.0			
US-1	Upstream	SW	-25	2011	403	17	0.10	244	22	59	14	0.3	43	0.1	0.713120	-49.9	-8.1
US-2	Upstream	SW	-25	2010	194	17	0.02	118		25	7	0.1	16	3.4			
US-3	Upstream	SW	-50	2012	240	15	0.04	161	4	34	10	0.2	12	0.1	0.713096		
US-4	Upstream	SW	-100	2010	189	17	0.02	115		25	7	0.1	15	2.8			
US-5	Upstream	SW	-100	2010	197	17	0.03	119		26	8	0.1	16	2.8			
US-6	Upstream	SW	-25	2012	117	20	0.05		3	52	13	0.3	22	0.0	0.713155		
US-7	Upstream	SW	-25	2012	119	21	0.06		3	53	14	0.3	23	0.0	0.713000		
EFF-1	Effluent	Brine Discharge	0	2011	94079	61260	522	585	241	16837	653	2230	11702	1	0.710124	-40.9	-4.4
EFF-2	Effluent	Brine Discharge	0	2010	131362	74309	602	1013	250	16957	1087	2326	34727	13	0.710185	-44.3	-4.3
EFF-3	Effluent	Brine Discharge	0	2010					250	13996	919	1871	29520	7			
EFF-4	Effluent	Brine Discharge	0	2010					250	10245	682	1340	22601	6		-44.6	-3.8
EFF-5	Effluent	Brine Discharge	0	2010					250	12693	832	1686	27143	6		-44.9	-3.7
EFF-6	Effluent	Brine Discharge	0	2010	86438	60751	474	1118	250	6663	455	856	15682	4	0.710183	-45.7	-4.4
EFF-7	Effluent	Brine Discharge	0	2010	108412	55077	477	200	250	16127	1050	2197	32980	14	0.710597	-45.6	-3.7
EFF-8	Effluent	Brine Discharge	0	2010	126829	74026	605	746	250	15490	1016	2120	32485	14	0.710831	-43.5	-4.3
EFF-9	Effluent	Brine Discharge	0	2010					250	16330	1063	2296	34718	14	0.710883	-46.4	-4.2
EFF-10	Effluent	Brine Discharge	0	2011	144559	85656	674	1136	272	15813	961	1419	38495	21	0.710500	-44.3	-4.3
EFF-11	Effluent	Brine Discharge	0	2011					257	13420	860	1155	33523	21		-39.1	-3.8
EFF-12	Effluent	Brine Discharge	0	2011	135909	89299	738	1010	269	12233	689	976	30584	19	0.710800	-40.8	-4.2
EFF-13	Effluent	Brine Discharge	0	2011	120290	78827	609	928	241	10276	612	777	27907	19		-39.8	-3.9
EFF-14	Effluent	Brine Discharge	0	2011	127026	75277	622	1103	252	13619	783	1031	34234	20	0.710800	-45.7	-4.4
EFF-15	Effluent	Brine Discharge	0	2011	183648	150153	1266	2911	249	7611	624	612	20134	17		-39.7	-3.9
EFF-16	Effluent	Brine Discharge	0	2011	104919	76877	605	1116	268	7003	565	632	17743	17	0.710579	-43.5	-4.3
EFF-17	Effluent	Brine Discharge	0	2011	90406	67773	543	1405	273	5509	517	542	13752	17	0.710197	-46.4	-4.2
EFF-18	Effluent	Brine Discharge	0	2011	151009	97756	632	1012	249	15336	1200	912	33900	12	0.711100		
DS-1	Downstream	SW	1	2012	13343	8193	69	194	27	1421	106	114.2	3216	1.9	0.711000		
DS-2	Downstream	SW	10	2012	8131	5000	42	208	17	890	70	69.6	1832	1.1			
DS-3	Downstream	SW	20	2011	4409	2403	18	260	33	555	39	49.4	1048	0.6	0.710258	-47.0	-8.0
DS-4	Downstream	SW	180	2012	900	367	2.42	153	5	123	19	6.3	219	0.2			
DS-5	Downstream	SW	300	2012	248	97	0.58		2	71	15	1.4	53	0.1			
DS-6	Downstream	SW	300	2012	240	95	0.58		2	69	15	1.3	51	0.1			
DS-7	Downstream	SW	1	2010		75085	650	397									
DS-8	Downstream	SW	10	2010	7076	4191	36	199		837	92	78.0	1584	27.3			
DS-9	Downstream	SW	20	2010	4375	2411	17			664	82	55.8	1100	23.4			
DS-10	Downstream	SW	100	2010	810	401	3.32	112		100	13	9.7	160	2.8			
DS-11	Downstream	SW	600	2010	52					27	8	0.1	14	0.0			
DS-12	Downstream	SW	300	2010	78					35	9	1.2	30	0.1	0.711181		
DS-13	Downstream	SW	300	2010	52					27	8	0.2	14	0.0	0.713004		
DS-14	Downstream	SW	300	2010	206	17	0.04	118		32	9	0.1	18	3.4	0.710207		
DS-15	Downstream	SW	600	2010	304	85	0.58	110		40	9	1.6	46	3.1	0.710362		
DS-16	Downstream	SW	600	2010	189	18	0.03	105		29	8	0.2	18	3.0	0.712109		
DS-17	Downstream	SW	600	2010	197	16	0.03	114		29	9	0.1	17	3.1	0.713002		
DS-18	Downstream	SW	1780	2012	543	233	1.43	157	3	73	23	0.4	9	0.0			
BG-1	Background	SW		2011	360	32	0.12	144	79	48	11	0.3	43	0.0	0.714500	-41.7	-6.4
BG-2	Background	SW		2011	127	24	0.02	10	59	18	3	0.1	12	0.0	0.712545	-55.0	-8.5
BG-3	Background	SW		2011	184	28	0.11	11	93	29	5	0.1	16	0.1	0.712880	-60.8	-9.2
BG-4	Background	SW		2011	91	13	0.02	9	44	13	3	0.0	8	0.0	0.713900	-45.4	-7.3
BG-5	Background	SW		2011	376	37	0.21	189	44	57	17	0.3	29	0.1	0.712200	-45.3	-7.8

Table 8. Radium isotope data of effluents from Josephine Brine Treatment Facility and river sediments collected upstream, adjacent to, and downstream of the discharge site of the treated effluent. Also included are measurements from background streams throughout western Pennsylvania (Figure 1).

Location Number	Location Type	Sample Type	Distance Downstream	Year Sampled	Effluent 228Ra (Bq/L)	Effluent 226Ra (Bq/L)	Sediment 226Ra (Bq/kg)	Sediment 228Ra (Bq/kg)	228Ra/226Ra
EFF-1	Effluent	Discharge	0	2011	1.19	3.09			0.39
EFF-18	Effluent	Discharge	0	2011	3.5	5.1			0.7
BG-1	Background	Sediment	-300	2011			26	24	0.92
BG-2	Background	Sediment	-300	2011			32	18	0.56
BG-3	Background	Sediment	-300	2011			22	13	0.61
BG-4	Background	Sediment	-300	2011			27	19	0.73
BG-5	Background	Sediment	-300	2011			44	33	0.77
US-1	Upstream	Sediment	-25	2011			34	22	0.66
US-3	Upstream	Sediment	-50	2012			31	25	0.82
USS-1	Upstream	Sediment	-50	2012			34	33	0.98
US-7	Upstream	Sediment	-25	2012			27	24	0.89
AMD-1	AMD	Sediment	-200	2011			34	30	0.88
AMD-3	AMD	Sediment	-200	2012			41	33	0.82
EFF-1	Effluent	Sediment	0	2011			8759	2187	0.25
EFF-18	Effluent	Sediment	0	2011			3497	1016	0.29
EFFS-2	Effluent	Sediment	0	2011			3497	1016	0.29
EFFS-3	Effluent	Sediment	1	2011			1419	355	0.25
EFFS-4	Effluent	Sediment	5	2011			3036	757	0.25
EFFS-5	Effluent	Sediment	0	2012			7708	2083	0.27
EFFS-6	Effluent	Sediment	10	2012			1908	426	0.22
EFFS-1	Effluent	Sediment	50	2011			544	164	0.30
DS-1	Downstream	Sediment	1	2012			5967	1617	0.27
DS-2	Downstream	Sediment	10	2012			1923	478	0.25
DS-3	Downstream	Sediment	20	2011			299	75	0.25
DS-4	Downstream	Sediment	180	2012			348	87	0.25
DS-5	Downstream	Sediment	300	2012			38	22	0.57
DS-6	Downstream	Sediment	300	2012			53	34	0.63
DS-18	Downstream	Sediment	1780	2012			33	22	0.67

References

Alexander S, Cakir, R, Doden, AG, Gold, DP, Root, SI (2005) Basement depth and related geospatial database for Pennsylvania. in 4th (Pennsylvania Geological Survey), pp Open-File General Geology Report 05-01.00.

Aravena, R., Wassenaar, L.I., 1993. Dissolved organic carbon and methane in a regional confined aquifer, southern Ontario, Canada: Carbon isotope evidence for associated subsurface sources. Appl. Geochem. 8, 483-493.

Aravena, R., Wassenaar, L.I., Barker, J.F., 1995. Distribution and isotopic characterization of methane in a confined aquifer in southern Ontario, Canada. J Hydrol. 173, 51-70.

Arkansas Oil and Gas Commission, 2012. Arkansas online data system. http://www.aogc.state.ar.us/JDesignerPro/JDPArkansas/AR_Welcome.html.

Baird, G., Staeten, C.v., 1999. The first great Devonian flooding episodes in Western New York: Reexamination of Union Springs, Oatka Creek, and Skaneateles formation successionss (Latest Eifelian-Lower Givetian) in the Buffalo-Seneca lake Region: Field Trip Guidebook. New York State Geological Association 71st meeting.

Boschetti, T., Etiope, G., Pennisi, M., Romain, M., Toscani, L., Boron, lithium and methane isotope composition of hyperalkaline waters (Northern Apennines, Italy): Terrestrial serpentinization or mixing with brine? Applied Geochemistry.

Brett, C., Baird, G., 1996. Middle Devonian sedimentary cycles and sequences in the northern Appalachian Basin., in: Witzke, B.J., Ladvigson, G.A., Day, J. (Eds.), Paleozoic Sequence Stratigraphy: Views from the Northern American Craton:. Geological Society of America Special Paper Boulder, Colorado.

Brett, C.E., Baird, G.C., Bartholomew, A.J., DeSantis, M.K., Straeten, C.A.V., 2011. Sequence stratigraphy and a revised sea-level curve for the Middle Devonian of eastern North America. Palaeogeography Palaeoclimatology Palaeoecology 304, 21-53.

Brett, C.E., Goodman, W.M., LoDuca, S.T., Lehmann, D.F., 1996. Upper Ordovician and Silurian strata in western New York: sequences, cycles and basin dynamics, in: Brett, C.E. (Ed.), New York State Geological Association Field Trip Guide, 1996. University of Rochester, Rochester, NY, pp. 71-120.

Burke, W.H., Denison, R.E., Hetherington, E.A., Koepnick, R.B., Nelson, H.F., Otto, J.B., 1982. Variation of seawater 87Sr/86Sr throughout Phanerozoic time. Geology 10, 516-519.

Busch, K., Busch, M., 1997 Cavity ring-down spectroscopy: An ultratrace absorption measurement technique. ACS Symposium Series, Oxford.

Chapman, E.C., Capo, R.C., Stewart, B.W., Hedin, R.S., Weaver, T.J., Edenborn, H.M., 2013. Strontium isotope quantification of siderite, brine and acid mine drainage contributions to abandoned gas well discharges in the Appalachian Plateau. Applied Geochemistry 31, 109-118.

Chapman, E.C., Capo, R.C., Stewart, B.W., Kirby, C.S., Hammack, R.W., Schroeder, K.T., Edenborn, H.M., 2012. Geochemical and Strontium Isotope Characterization of Produced Waters from Marcellus Shale Natural Gas Extraction. Environmental Science & Technology 46, 3545-3553.

Clement, G.P., Holser, W.T., 1988. Geochemistry of Moroccan evaporites in the setting of the North Atlantic Rift. Journal of African Earth Sciences (and the Middle East) 7, 375-383.

Cheung, K., Klassen, P., Mayer, B., Goodarzi, F., Aravena, R., 2010. Major ion and isotope geochemistry of fluids and gases from coalbed methane and shallow groundwater wells in Alberta, Canada. Appl. Geochem. 25, 1307-1329.

Coleman, D.D., Risatti, J.B., Schoell, M., 1981. Fractionation of carbon and hydrogen isotopes by methane-oxidizing bacteria. Geochim Cosmochim Acta 45, 1033-1037.

Cordova, R., 1963. Water Resources of the Arkansas Valley Region, Arkansas. US Geological Survey, Washington DC.

Darrah, T.H., Prutsman-Pfeiffer, J.J., Poreda, R.J., Campbell, M.E., Hauschka, P.V., Hannigan, R.E., 2009. Incorporation of excess gadolinium into human bone from medical contrast agents. Metallomics 1, 479-488.

Davis, D.M., Engelder, T., 1985. The role of salt in fold-and-thrust belts. Tectonophysics 119, 67-88.

Denison, R.E., Kirkland, D.W., Evans, R., 1998. Using Strontium Isotopes to Determine the Age and Origin of Gypsum and Anhydrite Beds. The Journal of Geology 106, 1-18.

Dresel, P., Rose, A., 2010. Chemistry and origin of oil and gas well brines in western Pennsylvania: Pennsylvania Geological Survey, 4th series Open-File Report OFOG 10–01.0. Pennsylvania Department of Conservation and Natural Resources, p. 48.

Eltschlager, K., Hawkins, J., Ehler, W., Baldassare, F., 2001. Technical measures for the investigation and mitigation of fugitive methane hazards in areas of coal mining: U.S. Department of the Interior, Office of Surface Mining Reclamation and Enforcement, p. 125.

Engelder, T., 1979. Mechanism for strain within the Upper Devonian Clastic Sequence of the Appalachian Plateau, Western New York. American Journal of Science 279, 527-542.

Engelder, T., Engelder, R., 1977. Fossil Distortion and Decollement Tectonics of Appalachian Plateau. Geology 5, 457-460.

Engelder, T., Geiser, P., 1980. On the Use Of Regional Joint Sets as Trajectories of Paleostress Fields During the Development of the Appalachian Plateau, New York. Journal of Geophysical Research 85, 6319-6341.

Engelder, T., Lash, G.G., Uzcategui, R.S., 2009. Joint sets that enhance production from Middle and Upper Devonian gas shales of the Appalachian Basin. American Association Petroleum Geologists Bulletin 93, 857-889.

Engelder, T., Whitaker, A., 2006. Early jointing in coal and black shale: Evidence for an Appalachian-wide stress field as a prelude to the Alleghanian orogeny. Geology 34, 581-584.

Etiope, G., Klusman, R.W., 2002. Geologic emissions of methane to the atmosphere. Chemosphere 49, 777-789.

Evans, M.A., 1995. Fluid Inclusions in Veins From the Middle Devonian Shales - A Record of Deformation Conditions and Fluid Evolution in the Appalachian Plateau. Geological Society of America Bulletin 107, 327-339.

Faill, R., 1985. The Acadian Orogeny and the Catskill Delta. Geological Society of America Special Paper 201, 15-38.

Faill, R., Nickelsen, R., 1999. Chapter 9: Appalachian Mountains Section of the Valley and Ridge Province, in: Shultz, C. (Ed.), The Geology of Pennsylvania. Pennsylvania Geological Survey, Harrisburg, PA.

Faill, R.T., 1997a. A geologic history of the north-central Appalachians .1. Orogenesis from the mesoproterozoic through the taconic orogeny. American Journal of Science 297, 551-619.

Faill, R.T., 1997b. A geologic history of the north-central Appalachians .2. The Appalachian basin from the Silurian through the Carboniferous. American Journal of Science 297, 729-761.

Farber, E., Vengosh, A., Gavrieli, I., Marie, A., Bullen, T.D., Mayer, B., Holtzman, R., Segal, M., Shavit, U., 2004. The origin and mechanisms of salinization of the lower Jordan river. Geochimica et Cosmochimica Acta 68, 1989-2006.

Ferrar, K.J., Michanowicz, D.R., Christen, C.L., Mulcahy, N., Malone, S.L., Sharma, R.K., 2013. Assessments of effluent contaminants from three wastewater treatment plants discharging Marcellus Shale wastewater to surface waters in Pennsylvania. Environmental Science & Technology.

Fisher, L., (2010) Data confirm safety of well fracturing. Reporter, Available at: http://www.fidelityepco.com/Documents/OilGasRept_072010.pdf .

Frey, M.G., 1973. Influence of Salina salt on structure in New York-Pennsylvania part of the Appalachian Plateau. American Association of Petroleum Geologists Bulletin 57, 1027-1037.

Geyer, A., and Wilshusen, JP 1982 Engineering Characteristics of the rocks of Pennsylvania; environmental geology supplement to the state geologic map, 2nd ed. Pennsylvania Geological Survey, p. 300

Gray, M.B., Mitra, G., 1999. Ramifications of four-dimensional progressive deformation in contractional mountain belts. Journal of Structural Geology 21, 1151-1160.

Gregory, K.B., Vidic, R.D., Dzombak, D.A., 2011. Water Management Challenges Associated with the Production of Shale Gas by Hydraulic Fracturing. Elements 7, 181-186.

Haluszczak, L.O., Rose, A.W., Kump, L.R., 2013. Geochemical evaluation of flowback brine from Marcellus gas wells in Pennsylvania, USA. Applied Geochemistry 28, 55-61.

Handford, C., 1986. Facies and bedding sequences in shelf-storm deposited carbonates—Fayetteville Shale and Pitkin Limestone (Mississippian), Arkansas. Jour. Sed. Petrol. 56, 123-137.

Harrison, S.S., 1983. Evaluating System for Ground-Water Contamination Hazards Due to Gas-Well Drilling on the Glaciated Appalachian Plateau. Ground Water 21, 689-700.

Harrison, S.S., 1985. Contamination of Aquifers by Overpressuring the Annulus of Oil and Gas Wells. Ground Water 23, 317-324.

Hayes, T., 2009. Sampling and Analysis of Water Streams Associated with the Development of Marcellus Shale Gas. Marcellus Shale Coalition.

Hogan, J.F., Phillips, F.M., Mills, S.K., Hendrickx, J.M.H., Ruiz, J., Chesley, J.T., Asmerom, Y., 2007. Geologic origins of salinization in a semi-arid river: The role of sedimentary basin brines. Geology 35, 1063-1066.

Howarth, R.W., Ingraffea, A., Engelder, T., 2011. Natural gas: Should fracking stop? Nature 477, 271-275.

Imes, J., Emmett, L., 1994. Geohydrology of the Ozark Plateaus aquifer system in parts of Missouri, Arkansas, Oklahoma, and Kansas: U.S. Geological Survey Professional Paper 1414D, 127 p.

Iyengar, M., Nrayana Rao, K., 1990. Uptake of radium by marine animals, in: The Environmental Behaviour of Radium Vol 1. IAEA.

Jackson, R.B., Osborn, S.G., Vengosh, A., Warner, N.R., 2011. Reply to Davies: Hydraulic fracturing remains a possible mechanism for observed methane contamination of drinking water. Proceedings of the National Academy of Sciences 108, E872.

Jacobi, R.D., 2002. Basement faults and seismicity in the Appalachian Basin of New York State. Tectonophysics 353, 75-113.

Jeffree, R., 1990. Radium uptake by freshwater invertibrates, in The Environmental Behaviour of Radium Vol 1. IAEA.

Jenden, P.D., Drazan, D.J., Kaplan, I.R., 1993. Mixing of Thermogenic Natural Gasas in Northern Appalachian Basin. American Association of Petroleum Geologists Bulletin 77, 980-998.

Jiang, M., Griffin, W.M., Hendrickson, C., Jaramillo, P., VanBriesen, J., Venkatesh, A., 2011. Life cycle greenhouse gas emissions of Marcellus shale gas. Environmental Research Letters 6, 034014.

Justyn, J., Havlik, B., 1990. Radium uptake by freshwater fish, in The Environmental Behaviour of Radium Vol 1. IAEA.

Kampbell, D.H., Vandegrift, S.A., 1998. Analysis of dissolved methane, ethane, and ethylene in ground water by a standard gas chromatographic technique. J Chromatog. Sci. 36, 253-256.

Kargbo, D.M., Wilhelm, R.G., Campbell, D.J., 2010. Natural Gas Plays in the Marcellus Shale: Challenges and Potential Opportunities. Environmental Science & Technology 44, 5679-5684.

Kendall, C., Coplen, T., 2001. Distribution of oxygen-18 and deuterium in river waters across the United States. Hydrological Processes 15, 1363-1393.

Kerr, R.A., 2010. Natural Gas From Shale Bursts Onto the Scene. Science 328, 1624-1626.

Kesler, S.E., Gruber, P.W., Medina, P.A., Keoleian, G.A., Everson, M.P., Wallington, T.J., 2012. Global lithium resources: Relative importance of pegmatite, brine and other deposits. Ore Geology Reviews 48, 55-69.

Kim G, Burnett WC, Dulaiova H, Swarzenski PW, & Moore WS (2001) Measurement of 224Ra and 226Ra Activities in Natural Waters Using a Radon-in-Air Monitor. Environmental Science & Technology 35(23):4680-4683.

Kloppmann, W., Négrel, P., Casanova, J., Klinge, H., Schelkes, K., Guerrot, C., 2001. Halite dissolution derived brines in the vicinity of a Permian salt dome (N German Basin). Evidence from boron, strontium, oxygen, and hydrogen isotopes. Geochimica et Cosmochimica Acta 65, 4087-4101.

Kresse, T., Hays, P., 2009. Geochemistry, comparative analysis, and physical and chemical characteristics of the thermal waters east of Hot Springs National Park, Arkansas, 2006-09: U.S. Geological Survey Scientific Investigations Report 2009-5263, 48 p.

Krishnaswami, S., Bhushan, R., Baskaran, M., 1991. Radium isotopes and 222Rn in shallow brines, Kharaghoda (India). Chemical Geology: Isotope Geoscience section 87, 125-136.

Kumar, M.B., Martinez, J.D., 1982. Character of Brines from the Belle Isle and Weeks Island Salt Mines, Louisiana, U.S.A, in: William, B., René, L. (Eds.), Developments in Water Science. Elsevier, pp. 107-140.

Lash, G., Blood, D.R., 2007. Origin of Early Overpressure in the Upper Devonian Catskill Delta Complex, western New York State. Basin Research 19.

Lash, G., Loewy, S., Engelder, T., 2004. Preferential jointing of Upper Devonian black shale, Appalachian Plateau, USA: evidence supporting hydrocarbon generation as a joint-driving mechanims. Geological Society of London, Special Publications 231, 129-151.

Lash, G.G., Engelder, T., 2009. Tracking the burial and tectonic history of Devonian shale of the Appalachian Basin by analysis of joint intersection style. Geological Society of America Bulletin 121, 265-277.

Lash, G.G., Engelder, T., 2011. Thickness trends and sequence stratigraphy of the Middle Devonian Marcellus Formation, Appalachian Basin: Implications for Acadian foreland basin evolution. Aapg Bulletin 95, 61-103.

Lavoie, D., 1994. Diachronous tectonic collapse of the Ordovician continental-margin, eastern Canada- Comparison between the Quebec reentrant and St. Lawrence promontory. Canadian Journal of Earth Sciences 31, 1309-1319.

LaZerte, B.D., 1981. The relationship between total dissolved carbon dioxide and its stable carbon isotope ratio in aquatic sediments. Geochim. Cosmochim. Acta 45, 647-656.

Lehmann, D., Brett, C.E., Cole, R., Baird, G., 1995. Distal sedimentation in a peripheral foreland basin- Ordovician black shales and associated flysch of the western taconic foreland, New York State and Ontario Geological Society of America Bulletin 107, 708-724.

Lemarchand, D., Gaillardet, J., 2006. Transient features of the erosion of shales in the Mackenzie basin (Canada), evidences from boron isotopes. Earth and Planetary Science Letters 245, 174-189.

Llewellyn, G., 2011. Structural and topographic assessment of shallow bedrock permeability variations throughout Susquehanna County PA: a focus area of Marcellus Shale Gas Development Geological Society of America Abstracts with Programs, p. 567.

Lohman, S.W., 1957. Ground water in northeastern Pennsylvania, 2nd ed. Pennsylvania Department of Conservation and Natural Resources, p. 312

Lohman, S.W., 1973. Ground water in north-central Pennsylvania, 3rd ed. Pennsylvania Department of Conservation and Natural Resources, p. 219.

Long, D.T., Wilson, T.P., Takacs, M.J., Rezabek, D.H., 1988. Stable-isotope geochemistry of saline near-surface ground water: East-central Michigan basin. Geological Society of America Bulletin 100, 1568-1577.

Lutz, B.D., Lewis, A.N., Doyle, M.W., 2013. Generation, transport, and disposal of wastewater associated with Marcellus Shale gas development. Water Resources Research 49, 647-656.

Maloney, K., Yoxtheimer, D., 2012. Production and disposal of waste materials from gas and oil extraction from the Marcellus Shale play in Pennsylvania. Environmental Practice 14, 278-287.

McCaffrey, M.A., Lazar, B., Holland, H.D., 1987. The evaporation path of seawater and the coprecipitation of Br- and K+ with halite. J Sediment Petrol 57, 928-938.

Mehta, S., Fryar, A.E., Banner, J.L., 2000a. Controls on the regional-scale salinization of the Ogallala aquifer, Southern High Plains, Texas, USA. Applied Geochemistry 15, 849-864.

Mehta, S., Fryar, A.E., Brady, R.M., Morin, R.H., 2000b. Modeling regional salinization of the Ogallala aquifer, Southern High Plains, TX, USA. Journal of Hydrology 238, 44-64.

Michigan Department of Environmental Quality, 2007. Cleanup and disposal guidelines for site contaminated with radium-226, in: Waste and Hazardous Materials Division (Ed.).

Milici, R.C., W. de Witt, J., 1988. The Appalachian Basin, in: Sloss, L.L. (Ed.), Sedimentary cover-North American craton: U.S.:. Geological Society of America, pp. 427-469.

Molofsky, L.J., Connor, J.A., Farhat, S.K., Jr., A.S.W., Wagner, T., 2011. Methane in Pennsylvania water wells unrelated to Marcellus shale fracturing. Oil and Gas Journal 109.

Moore, W., 1984. Radium isotope measurements using germanium detectors. Nuclear Instruments and Methods in Physics Research 407-411.

NYDEC, 1999. An Investigation of Naturally Occurring Radioactive Materials (NORM) in Oil and Gas Wells in New York State, in: Division of Solid & Hazardous Materials Bureau of Radiation and Hazardous Site Management (Ed.), Albany, New York.

Olmstead, S.M., Muehlenbachs, L.A., Shih, J.-S., Chu, Z., Krupnick, A.J., 2013. Shale gas development impacts on surface water quality in Pennsylvania. Proceedings of the National Academy of Sciences.

Osborn, S.G., McIntosh, J.C., 2010. Chemical and isotopic tracers of the contribution of microbial gas in Devonian organic-rich shales and reservoir sandstones, northern Appalachian Basin. Applied Geochemistry 25, 456-471.

Osborn, S.G., McIntosh, J.C., Hanor, J.S., Biddulph, D., 2012. Iodine-129, 87Sr/86Sr, and trace elemental geochemistry of northern Appalachian Basin brines: Evidence for basinal-scale fluid migration and clay mineral diagenesis. American Journal of Science 312, 263-287.

Osborn, S.G., Vengosh, A., Warner, N.R., Jackson, R.B., 2011a. Methane contamination of drinking water accompanying gas-well drilling and hydraulic fracturing. Proceedings of the National Academy of Sciences 108, 8172-8176.

Osborn, S.G., Vengosh, A., Warner, N.R., Jackson, R.B., 2011b. Reply to Saba and Orzechowski and Schon: Methane contamination of drinking water accompanying gas-well drilling and hydraulic fracturing. Proceedings of the National Academy of Sciences 108, E665-E666.

Palmer, M.R., Spivack, A.J., Edmond, J.M., 1987. Temperature and pH controls over isotopic fractionation during adsorption of boron on marine clay. Geochimica et Cosmochimica Acta 51, 2319-2323.

Peterson, R.N., Burnett, W.C., Opsahl, S.P., Santos, I.R., Misra, S., Froelich, P.N., 2013. Tracking suspended particle transport via radium isotopes (226Ra and 228Ra) through the Apalachicola–Chattahoochee–Flint River system. Journal of Environmental Radioactivity 116, 65-75.

Pohn, H., 2000. Lateral ramps in the folded Appalachians and in overthrust beltsworldwide - A fundamental element of thrust-belt architecture: U.S. Geological Survey Bulletin, in: Survey, U.G. (Ed.), p. 63.

Rast, N., 1989. The evolution of the Appalachian chain, in: Bally, A.W., Palmer, A.R. (Eds.), The geology of North America-an overview. Geological Society of America, pp. p.347-358.

Renner, R., 2009. Spate of gas drilling leaks raises Marcellus concerns. Environmental Science & Technology 43, 7599-7599.

Rowan, E., Engle, M., Kirby, C., Kraemer, T., 2011. Radium content of oil- and gas-field produced waters in the northern Appalachian Basin (USA)—Summary and discussion of data: U.S. Geological Survey Scientific Investigations Report 2011–5135. U.S. Geological Survey p. 31.

Ryder, R.T., Aggen, K.L., Hettinger, R.D., Law, B.E., Miller, J.J., Nuccio, V.F., Perry, W.J., Prensky, S.E., SanFilipo, J.R., Wandry, C.J., 1996. Possible continuous-type (unconventional) gas accumulation in the Lower Silurian "Clinton" sands, Medina Group, and Tuscarora Sandstone in the Appalachian basin: A progress report of 1995 activities. United States Geological Survey USGS Open-File Report 96-42. .

Ryder, T.T., 1998. Characteristics of Discrete and Basin-Centered Parts of the Lower Silurian Regional Oil and Gas Accumulation, Appalachian Basin: Preliminary results from data set of 25 Oil and Gas Fields. U.S. Geological Survey Open-File Report 98-216.

Sass, E., Starinsky, A., 1979. Behaviour of strontium in subsurface calcium chloride brines: Southern Israel and Dead Sea rift valley. Geochimica et Cosmochimica Acta 43, 885-895.

Saunders, J.A., Swann, C.T., 1990. Trace-metal content of Mississippi oil field brines. Journal of Geochemical Exploration 37, 171-183.

Scanlin, M.A., Engelder, T., 2003. The basement versus the no-basement hypotheses for folding within the Appalachian plateau detachment sheet. American Journal of Science 303, 519-563.

Schoell, M., 1980. The hydrogen and carbon isotopic composition of methane from natural gases of various origins. Geochimica et Cosmochimica Acta 44, 649-661.

Shahul Hameed, P., Shaheed, K., Somasundaram, S.S.N., Iyengar, M.A.R., 1997. Radium-226 levels in the Cauvery river ecosystem, India. Journal of Biosciences 22, 225–231.

Sharma, S., Sack, A., Adams, J.P., Vesper, D.J., Capo, R.C., Hartsock, A., Edenborn, H.M., 2013. Isotopic evidence of enhanced carbonate dissolution at a coal mine drainage site in Allegheny County, Pennsylvania, USA. Applied Geochemistry 29, 32-42.

Smith, K., 1992. An overview of naturally occuring radioactive material (NORM) in the Petroleum Industry. Environmental Assessment and Information Sciences Division, Argonne National Laboratory.

Spivack, A.J., Edmond, J.M., 1987. Boron isotope exchange between seawater and the oceanic crust. Geochimica et Cosmochimica Acta 51, 1033-1043.

Straeten, C.A.V., Brett, C.E., Sageman, B.B., 2011. Mudrock sequence stratigraphy: A multi-proxy (sedimentological, paleobiological and geochemical) approach, Devonian Appalachian Basin. Palaeogeography Palaeoclimatology Palaeoecology 304, 54-73.

Straeten, C.A.V., Griffing, D.H., Brett, C.E., 1994. The lower part of the Middle Devonian Marcellus "shale', central to western New York State: stratigraphy and depositional history. New York State Geological Association.

Stueber, A.M., Pushkar, P., Hetherington, E.A., 1984. A strontium isotopic study of Smackover brines and associated solids, southern Arkansas. Geochimica et Cosmochimica Acta 48, 1637-1649.

Sturchio, N.C., Banner, J.L., Binz, C.M., Heraty, L.B., Musgrove, M., 2001. Radium geochemistry of ground waters in Paleozoic carbonate aquifers, midcontinent, USA. Applied Geochemistry 16, 109-122.

Taylor, L., 1984. Groundwater Resources of the Upper Susquehanna River Basin, Pennsylvania: Water Resources Report 58. Pennsylvania Department of Environmental Resources-Office of Parks and Forestry - Bureau of Topographic and Geologic Survey, p. 136.

Tóth, J., 1970. A conceptual model of the groundwater regime and the hydrogeologic environment. Journal of Hydrology 10, 164-176.

Trenton, Black, River, Research, Consortium, 2006. A geologic play book for Trenton-Black River Appalachian Basin Exploration: U. S. Dept. of Energy Final Report Award No. DE-FC26-03NT41865 p. 543.

U.S. Geological Survey, 1999. Naturally Occurring Radioactive Materials (NORM) in Produced Water and Oil-Field Equipment-An Issue for the Energy Industry. Fact Sheet 0142-99.

U.S. Geological Survey, 2013. National Water Information System Database (http://waterdata.usgs.gov/pa/nwis/uv?site_no=03042000).

USEIA, 2011. Review of Emerging Resources: U.S. Shale Gas and Shale Oil Plays. US Dept of Energy.

USEPA, 2011. Voluntary sampling Data from Oil and Gas Wastewater Treatment Facilities, available at http://www.epa.gov/region3/marcellus_shale/#epawpadep.

Veil, J., 2010. Water Management Technologies Used by Marcellus Shale Gas Producers. prepared for US Department of Energy Office of Fossil Fuel Energy, National Energy Technology Laboratory.

Veil, J., 2011. White Paper on SPE Summit on Hydraulic Fracturing Society of Petroleum Engineers (Society of Petroleum Engineers, Houston) Houston TX.

Vengosh, A., 2003. Salinization and Saline Environments, in: Editors-in-Chief: Heinrich, D.H., Karl, K.T. (Eds.), Treatise on Geochemistry. Pergamon, Oxford, pp. 1-35.

Vengosh, A., Kolodny, Y., Starinsky, A., Chivas, A.R., Mcculloch, M.T., 1991. Coprecipitation and Isotopic Fractionation of Boron in Modern Biogenic Carbonates. Geochimica et Cosmochimica Acta 55, 2901-2910.

Vinson, D.S., Lundy, J.R., Dwyer, G.S., Vengosh, A., 2009a. Coupled use of Sr and Ra isotopes to assess Ra mobility and water-rock interaction in sandstone aquifers. Geochimica et Cosmochimica Acta 73, A1387-A1387.

Vinson, D.S., Vengosh, A., Hirschfeld, D., Dwyer, G.S., 2009b. Relationships between radium and radon occurrence and hydrochemistry in fresh groundwater from fractured crystalline rocks, North Carolina (USA). Chemical Geology 260, 159-171.

Warner, N.R., Jackson, R.B., Darrah, T.H., Osborn, S.G., Down, A., Zhao, K., White, A., Vengosh, A., 2012. Geochemical evidence for possible natural migration of Marcellus Formation brine to shallow aquifers in Pennsylvania. Proceedings of the National Academy of Sciences.

Warner, N.R., Kresse, T., Hays, P., Jackson, R.B., Down, A., Vengosh, A., 2013. Geochemical and isotopic variations in shallow groundwater in areas of Fayetteville Shale development, north-central Arkansas. Applied Geochemistry Available online May 15, 2013.

Weaver, T.R., Frape, S.K., Cherry, J.A., 1995. Recent cross-formational fluid flow and mixing in the shallow Michigan Basin. Geol Soc Am Bull 107, 697-707.

Webster, I.T., Hancock, G.J., Murray, A.S., 1995. Modeling the effect of salinity on radium desorption from sediments. Geochimica et Cosmochimica Acta 59, 2469-2476.

Whiticar, M.J., Faber, E., Schoell, M., 1986. Biogenic methane formation in marine and freshwater environments: CO2 reduction vs. acetate fermentation—Isotope evidence. Geochim. Cosmochim. Acta 50, 693-709.

Wilde, F., 2006 Collection of water samples (ver. 2.0): U.S. Geological Survey Techniques of Water-Resources Investigations, book 9, chap A4.

Williams, A., 1990. Radium uptake by Freshwater Plants, in The Environmental Behaviour of Radium Vol 1. IAEA.

Williams, J., Taylor, L., Low, D., 1998. Hydrogeology and Groundwater Quality of the Glaciated Valleys of Bradford, Tioga, and Potter Counties, Pennsylvania: Water Resources Report 68. Commonwealth of Pennsylvania Department of Conservation and Natural Resources, p. 89.

Williams, L.B., Hervig, R.L., Holloway, J.R., Hutcheon, I., 2001a. Boron isotope geochemistry during diagenesis. Part I. Experimental determination of fractionation during illitization of smectite. Geochimica et Cosmochimica Acta 65, 1769-1782.

Williams, L.B., Hervig, R.L., Hutcheon, I., 2001b. Boron isotope geochemistry during diagenesis. Part II. Applications to organic-rich sediments. Geochimica et Cosmochimica Acta 65, 1783-1794.

Williams, L.B., Hervig, R.L., Wieser, M.E., Hutcheon, I., 2001c. The influence of organic matter on the boron isotope geochemistry of the gulf coast sedimentary basin, USA. Chemical Geology 174, 445-461.

Zumberge, J., Ferworn, K., Brown, S., 2012. Isotopic reversal ('rollover') in shale gases produced from the Mississippian Barnett and Fayetteville formations. Marine Petrol. Geol. 31, 43-52.

Biography

Nathaniel Warner was born February 8, 1978 and graduated from Hamilton College with a BA in Geology and a minor in Physics in 2000 followed in 2002 with a MS in Geology from Miami University. He has received the following awards; Nicholas School of the Environment-Dean's Award for Best Student Manuscript, 2nd Place (2013), Geological Society of America- Student Research Grant Award in Hydrogeology (2001), Graduate School of Miami University-Graduate Achievement Award (2001). Nathaniel has authored or coauthored the following; Geochemical and isotopic variations in shallow groundwater in areas of Fayetteville Shale Development, North Central Arkansas (2013), Integration of geochemical and isotopic tracers for elucidating water sources and salinization of shallow aquifers in the sub-Saharan Drâa Basin, Morocco (2013), Geochemical evidence for possible natural migration of Marcellus Formation brine to shallow aquifers in Pennsylvania (2012); Geochemical and isotopic (oxygen, hydrogen, carbon, strontium) constraints for the origin, salinity, and residence time of groundwater from a carbonate aquifer in the Western Anti-Atlas Mountains, Morocco (2012); Methane contamination of drinking water accompanying gas-well drilling and hydraulic fracturing (2011); Drinking water quality in Nepal's Kathmandu Valley: a survey and assessment of selected controlling site characteristics (2008); Millennial- to decadal-scale paleoenvironmental change during the Holocene in the Palmer Deep, Antarctica, as recorded by particle size analysis (2002).